University of Évora

ARCHMAT
(ERASMUS MUNDUS MASTER IN ARCHaeological MATerials Science)

Mestrado em Arqueologia e Ambiente (Erasmus Mundus – ARCHMAT)

Interdisciplinary study of the dental calculus in skeleton remains from the cemetery of Santa Maria do Olival (Tomar, Portugal) - 15th to 16th century A.D.

Roshan Paladugu
m38416

Anne-France Maurer
(Supervisor - Universidade de Évora)

Cristina Maria Barrocas Dias
(Co-supervisor– Universidade de Évora)

Évora, September 2018

A tese inclui as criticas e sugestões do Júri

University of Évora

ARCHMAT
(ERASMUS MUNDUS MASTER IN ARCHaeological MATerials Science)

Mestrado em Arqueologia e Ambiente (Erasmus Mundus – ARCHMAT)

O estudo interdisciplinar do cálculo dentário no esqueleto é feito no cemitério de Santa Maria do Olival (Tomar, Portugal) - 15th to 16th século A.D.

Roshan Paladugu
m38416

Anne-France Maurer
(Supervisor - Universidade de Évora)
Cristina Maria Barrocas Dias
(Co-supervisor– Universidade de Évora)

Évora, September 2018
A tese inclui as criticas e sugestões do Júri

Panel of Jury

Dr.Nicola Schiavon (Presidente)

Dr. Ana Cristina Cabaça Manhita (Arguente)

Dr. Anne-France Maurer (Orientadora)

Contents

List of Abbreviations and Terms

AD: Anno Domini
AIR: Ambient Inhalable Reservoir
Am/P: Amide I to phosphate ratio (relative collagen content)
ATR-FTIR: Attenuated Total Reflection- Fourier Transmission Infrared Spectroscopy
Ba/Ca: Barium to calcium ratio
Ba/Sr: Barium to strontium ratio
BCE: Before Common Era
C/P: Carbonate to phosphate ratio
Ca/P: Calcium to phosphorus index
CAM: Crassulacean Acid Metabolism
EA-IRMS: Elemental Analyser- Isotope Ratio Mass Spectrometry
IAEA: International Atomic Energy Agency
ICP-MS: Inductively Coupled Plasma- Mass Spectrometry
IR-SF: Infrared Splitting Factor
I1**:** First incisor
LA-ICP-MS: Laser Ablation – Inductively Coupled Plasma- Mass Spectrometry
M1: First permanent molar
M2: Second permanent molar
mL: Milliliters
NIST: National Institute of Standards and Technology
Nm: Nanometer
Ppm: Parts per million
REE: Rare earth elements
Rpm: Revolutions per minute
Sr/Ca: Strontium to calcium ratio
SRM: Standard reference materials
VPDB: Vienna Pee Dee Belemnite
XRD: X-ray Diffraction
µg/g: Microgram per gram

List of Figures

List of Tables

Abstract

14 humans and 6 faunal dental calculus samples from the medieval necropolis of Santa Maria do Olival, Tomar were selected for microdebris, isotopes, trace elements and organic residues analyses. The major aim of the study was to setup methods for analysis of dental calculus to complement information from bones and teeth. The isotopic values from dental calculi of humans and fauna were comparable to those from bone collagen and led to similar conclusions on dietary practices. Trace element values from human and faunal calculi followed similar trends to their respective bones. Microscopy yielded stray phytoliths from the Poaceae family and no silica skeletons or starch grains. Organic residues analysis indicated a diet based on protein and carbohydrates. Evidences of poor air quality due to char substances from incomplete combustion of wood and biomass were found. Since this is a pilot study, sample size is restricted. The direction of future research on dental calculus is to analyse a large quantity of samples to generate standard range of values for isotopes and trace element concentrations.

Keywords: dental calculus, phytoliths, starch grains, microscopy, trace elements, organic residues, Optical Microscope (OM), Scanning Electron Microscope (SEM), EA-IRMS, LA-ICP-MS, Py-GC-MS, Tomar.

Resumo

O estudo interdisciplinar do cálculo dentário no esqueleto é feito no cemitério de Santa Maria do Olival (Tomar, Portugal) - 15th to 16th século A.D.

Foram selecionadas 14 amostras de humanos e 6 amostras de cálculo dentário da fauna da necrópole medieval de Santa Maria do Olival, Tomar, para análises de microdíbris, isótopos, oligoelementos e resíduos orgânicos. O principal objetivo do estudo foi configurar métodos para análise de cálculo dentário para complementar informações de ossos e dentes. Os valores isotópicos dos cálculos dentários de humanos e fauna foram comparáveis aos do colágeno ósseo e levaram a conclusões semelhantes sobre práticas alimentares. Os valores dos elementos de traço dos cálculos humanos e faunísticos seguiram tendências semelhantes aos seus respectivos ossos. A microscopia produziu fitólitos dispersos da família Poaceae e nenhum esqueleto de sílica ou grãos de amido. A análise de resíduos orgânicos indicou uma dieta baseada em proteínas e carboidratos. Evidências de baixa qualidade do ar devido a substâncias carbonatadas de combustão incompleta de madeira e biomassa foram encontradas. Como este é um estudo piloto, o tamanho da amostra é restrito. A direção de pesquisas futuras sobre cálculo dentário é analisar uma grande quantidade de amostras para gerar uma faixa padrão de valores para isótopos e concentrações de elementos traços.

Acknowledgements

I have enjoyed the challenging and innovative nature of thesis especially during the interpretation of the results. I have had the great fortune of working with many dedicated and experienced people. I would like to express my heartfelt gratitude to my supervisor Anne France-Maurer and co-supervisor Prof. Cristina Barrocas Dias for all the support and guidance they have provided during the period of this study. I would like to thank Ana Margarida Cardoso for her help with FTIR, Pedro Barrulas for all his chemistry pointers and help in trace element analysis, Ana Manhita for helping me run pyrolysis gas chromatography mass spectrometry, Nicasio Tomás Jiménez-Morillo for his help with stable isotope analysis and Tania Rosado for her kind help with microscopy. A special mention to Guillermo Marin Garcia for sparing his time to help me with phytolith identification.

I would like to dedicate a big thank you to Silvia Irene Russo for her constant constructive criticism and company during the entire duration of this thesis. I would also like to thank Sergio Lins, my dear friend for helping me with the Portuguese translation of the abstract. Finally, I would like to thank my parents for providing me with the great opportunity of studying in this masters.

1. Introduction

Dental calculus is an emerging source of ancient diet and environment information. The aim of the study was to setup method and to gauge the scope of dental calculus as a complement for teeth and bones in dietary reconstruction. Comparing the isotopic values from dental calculus to the already established values from bones will help in evaluation of the reliability of calculus. The skeletal remains from the necropolis of Santa Maria do Olival gave an excellent opportunity to investigate the potential of calculus. The city of Tomar has constantly evolved through time evolving from one cultural period to another right from Romans, followed by Visigothic and Paleochristian periods and then the brief Islamic period, culminating with the Reconquista establishing Christianity as the major religion. Each cultural period had its own distinctive dietary patterns due to economic and political situations as well as climatic conditions. This provides an excellent testing grounds to see if dental calculus can be relied upon to reconstruct the past diets.

The buried remains from the necropolis showed a relatively large frequency of dental calculi in individuals. Microscopy was carried out to identify biogenic silica such as phytoliths and diatoms as well as starch grains. Phytoliths and starch grains can be utilised to uniquely identify the plant of origin. Trace element studies are also carried out as there are no standard published values for the concentration ranges. Finally, pyrolysis-chromatography mass spectrometry was utilised to understand the organic constituents of the dental calculus.

2. Historical Context

To the north of Lisbon and just below Coimbra, lies Tomar where the church of Santa Maria do Olival is located. The Nabão River, passing in the west, has played the role of a lifeline throughout the human settlement history in the area. There have been neolithic and Iron Age remains discovered in previous excavations (Santos, 2009). The location of the settlement is not based on strategy of military defense or natural resources. Instead, there have been two hypothesis proposed for explaining this fact. The first one is that the Roman city of Sellium was based on the existence of an earlier settlement and the second being that Sellium was built in the beginning of the Empire, as a part of Romanization of Lusitânia where modern day Tomar stands (Figure 1) (Pereira et al., 2009).

Figure 1. Map of the Iberian Peninsula showing the location of Tomar. (Mary Ames Michell®)

2.1 Tomar as Sellium

During the Roman period, Tomar was known as Sellium. It was a part of urbanization reforms carried out by Emperor Augustus leading to establishment and elevation of cities to *civitates*. Sellium was amongst the ranks of others such as Ammaia, Aritium Vetus, and Eburobritium which were located non-strategically along waterbodies, in this case Nabão River. However what puts Sellium apart from the others is that it served as *caput viarium* of the route of via Olissipo-Bracara Augusta. The movement of goods was primarily to the north of Sellium on this route. The city further developed due to its centrality with respect to land trade routes and proximity to the Tagus River. In all possible scenarios, the demography was indigenous and homogenous with cultural practices rooted in Lusitânia. In a stark contrast, very little was recorded in historical records about Sellium from the Roman times apart from the existence of a forum amongst many other typical of Roman cities. The tower of Church of Santa Maria do Olival itself, is hypothesized to be built on

the foundations of a pre-existing Roman mausoleum after an excavation (Santos, 2009). The construction of the structure was built with limestone slabs bound by mortar, aligned to Roman construction techniques and in sync with structures from Roman town of Sellium.

2.2 Visgothic period

The first migrant populations arrived in the form of Gothic contingents such as Suebi, Alans, Asding Vandala and Siling Vandala etc. to the Iberian Peninsula around 406 A.D. This migration generated instability and metamorphosis in the structure of local cities. This change was mainly invasion and mass destruction due to the disorganized martial populations causing deep damage in the societal structure mainly administrative, social and economic development. The local elite families faced the scenario where their political and socio-economic positions were threatened due to recurrent plundering and conquest of strategic cities. The urban center of Sellium was related to the Germanic tribes since it was located between borders of Suebi and Visigoth territories. The centralization of the Visigothic monarchy in the second half of the 6th century culminated in a civil war (Batata, 1997).

2.3 Paleochristianity

The Paleochristian mention of Sellium appears in the *Parochiale Suevicum* in the year 569 A.D. as a church in the diocese of Coimbra and subordinate to the episcopal seat of Braga (Ponte, 1997). In the early 6th century, structures related to paleochristianity have been discovered (Fabião, 2004).

Figure 2. The facade of Santa Maria do Olival, Tomar (DGMN).

The earliest structures are a set of buildings which served as the parish headquarters of Santa Maria do Selhos and other smaller buildings related to Santa Iria and São Pero de Fins. The location of Santa Maria do Selho is highly suspected to be in the same location of Santa Maria do Olival (Figure 2). The Church of Santa Iria still exists under the same name. The Church of São Pero de Fins seemed to exist between these two buildings, in the current area of Tomar cemetery (Ponte & Miranda, 1991).

2.4 Islamic Tomar

The conflict between the religious authorities and Visigothic monarchy lead to the benefit of the Islamic invader. This is explained by the monumental expansion of the Tariq Ibn Ziyad army in 711. Surprisingly there are no archaeological evidences apart from a single coin in the excavation (Ponte & Miranda, 1991). The Islamic population must have had little artistic and materialistic expressions and probable dispersion in the territory. During this period, the term Sellium was most likely replaced by Thomar, derived from the Islamic name of the Nabão River.

2.5 Reconquista and Order of the Christ

The Reconquista movement provoked by the Christian resistance moved the strategy to fortifications which has never been the specialty of Tomar. The left bank and a part of old Sellium were abandoned and on the opposite bank the Islamic rulers constructed a new fortified stronghold. In the bloody conflict of the Christian North and Muslim South, the borders were constantly redrawn based on the outcomes and flow of military campaigns. The 11th and 12th centuries were marked by a profound religious intolerance by both Christians and Muslims alike. The initiation of the Portuguese nationality is marked by the religious obligation of the war towards the South against the Muslims. In this scenarios, the religious orders began playing a larger role in military campaigns. The Templar Order of Portugal was given charge of the territories of Zêzere and Tejo.

In 1162, the first charter of Tomar was proclaimed by D.Gualdim Pais. On the legal basis of the charter, D.Gualdim Pais chose to undertake the task of building a fortified defensive structure of the Castle of Tomar starting from 1160. Two other structures were also being built along with the defensive constructions which were the Church of Santa Maria do Castelo and Charola. On the other bank of the river, the Church of Santa Maria do Olival was being constructed and developed as the core religious nucleus of religious activity. As the Reconquista progressed and the Islamic territory was pushed even south, urbanization of the settlement started with area around the castle

leading the metamorphosis. Commercial activities started gaining pace and attracted more immigrants from different regions to settle around the castle. The location of the church is in the same space as some Paleochristian structures of Sellium. This is supported by the fact that the monastery of Santa Maria do Selho was later designated as Santa Maria do Olival in medieval documentation. The church was most likely reformed under the orders of the Grand Master. From the previous structure only the Gothic façade was preserved with other elements altered to suit the era. The administration of the convent and pantheon passed from the hands of the Templar Order to the order of the Christ in 1307 after the dissolution of the former under the papal bull *Pastoralis praeeminentiae* issued by Pope Clement V. The Church of Santa Maria do Olival played an important role in the field of architecture as it served as a template for other churches built or renovated during the reign of D. Manuel I which concluded in the reign of D.João III (DGEMN, 1942:11).

The Church of Santa Maria do Olival was granted the rank of a Cathedral and Diocese by Pope Calisto III in 1455. In the reign of D. João III, a major reform of the religious order took place where the Order of Christ was subjected to the rigorous rules of cloister and the restrictions of the life in a convent were implemented strictly. The space surrounding the church was partitioned between different properties of the Order of Christ. Many other churches dedicated to St. Michael. St. Peter the Apostle, St. Mary Magdalena and Santo Ildefonso were demolished. An epigraph dating to 1175 reveals that the church was open to worship and burials were also permitted. The Directorate General of National Buildings and Monuments (DGEMN) in 1940s dismantled the ruins which were located around the church.

3. Archaeological Context

3.1 Necropolis of Santa Maria do Olival

Figure 3. An official document showing the area under the church of Santa Maria do Olival, DGMN Portaria publicada 259.

The focus here is the morphing of landscape in the context of the "old cemetery" due to the remodeling works of DGEMN and the construction of access roads to the Municipal Market and Marmelais Road. This funeral area surrounding the Church of Santa Maria do Olival has undergone several changes through the flow of time. The presumption that until the first half of the 19th century burials were made inside the church makes the origin of this funerary space difficult to explain. The burials during the Roman-Visgothic period were located in the immediate space to the structure of the church, more precisely in the churchyards (Santos, 2009). Archaeological interventions in the area began in 1977 after the discovery of tombstones and funerary stelae by Beleza Moreira (Batata, 1997). Major excavations made between 1989 and 1992 by Salete Ponte shed light on the spacio-temporal evolution of the necropolis (Ponte & Miranda, 1991). Ponte also states that the space surrounding the church was converted during the Gothic - Sellio period in to a scared area for praying and looking after the dead which is shown in Figure 3 (Santos, 2009). By the 12th century, the area has become a fixed space for religious activities. Archaeological evidence suggests that the space continues to be used for similar activities until the

end of 16th century. The stratigraphic units documented reveals the specific periods of history when the necropolis was used by the people in the Middle Ages. A part of the exhumed burials were assigned in the chronological period based on the burial type and stratigraphic units. Other major methodology was to identify the typology of burial goods associated with specific exhumations (Ponte, 1997:52). The lowest stratigraphic units which are also chronologically the oldest were dated to 5^{th}-12^{th} centuries which is between the Visgothic and Reconquista. These layers were followed by burials dating to post-Reconquista period. Mass burials were attributed to a period of 300 years where severe famines, bubonic plague and wars were common (Santos, 2009).

To this date the origins of this area are still shrouded in mystery. Under the Romans it was suburban space but later, it evolved to become an urban space of Tomar. The space which has remained constant is the necropolis and its constant role of being a space to honour the dead. Since the early 12^{th} century the space has stood isolated but over the time has started shrinking in size as the space began to be reused. The cemetery of Santa Maria do Olival continues to be sacred sanctum for people's belief in burying their dead.

The necropolis of the Church of Santa Maria do Olival was used by the population between the 11th and 18th centuries. The first excavation took place in 2007 and covered a part of the necropolis

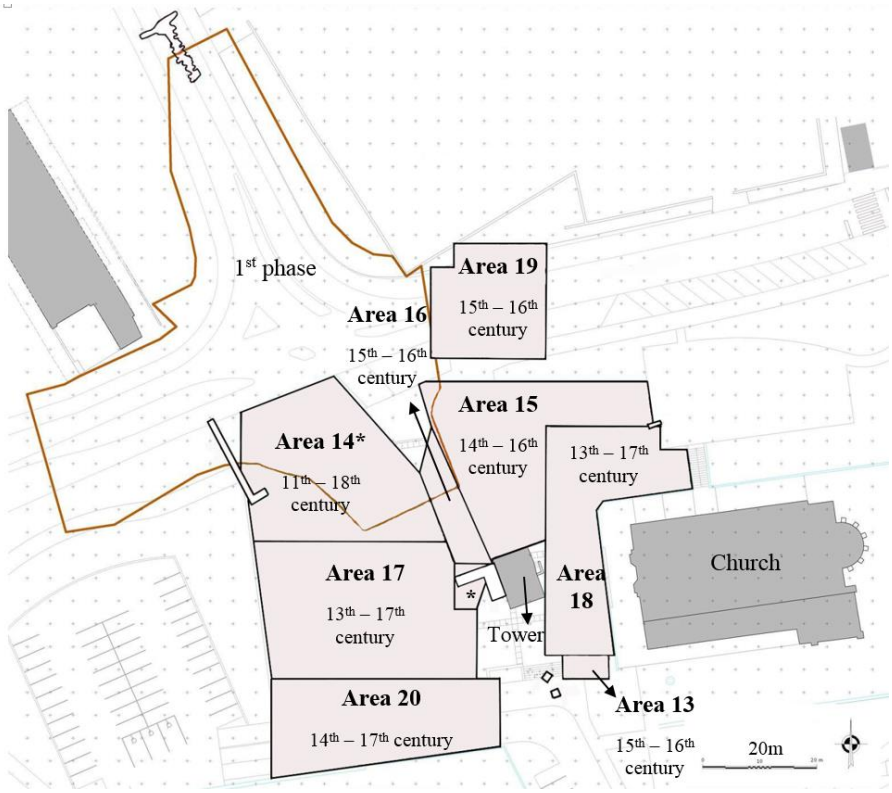

Figure 4: Excavation Map showing various areas of the necropolis.

which was divided into 11 areas whereas the second phase of the excavations took place in 2008 and covered 8 areas (13-20). Dental calculus is a part of the skeletal artefacts excavated in the Phase-II of archaeological interventions carried out in the area surrounding the church of Santa Maria dos Olivais in Tomar, district of Santarém, under the umbrella of urban requalification and environmental valuation of the Polis program. The interventions were mainly aimed at reducing the negative impact of the urban activities on the necropolis context. The unique characteristic of the site is the rich amount of archaeological remains found in all the numerous previous excavations. All these investigations have contributed to understanding the space of the dead i.e. the necropolis in this area of Tomar. This includes the death rituals starting from the Roman settlement of Sellium to the reconquered city of Tomar until the 18th century. The excavations lasted for 11 months beginning in April 2008 lasting until March 2009. The total excavation area is 4029.672 m^2 divided into 8 areas and 6 trenches as shown in Figure 4. The excavation was started in the Area 20 owing to emergency of building a platform access ramp.

3.2 Excavation Areas

Area 13 which was also excavated in an emergency is located to the south of the bell tower and Area 18. Sixty stratigraphic units, 15 burials, 6 ossuaries associated with burial and 1 isolated ossage were found. The burials were mostly pits excavated in the geological substrate. Many of the structures have been found violated leading to the belief that there has been reuse of the space for later inhumations. In regard of chronology of the area, it can be postulated that it approaches from late – Roman to upper medieval period. This is supported by the presence of structures oriented east to west, made of limestone and bound by clay which is characteristic of late – Roman period and for the upper medieval period, a single coin from the reign of Afonso V was found in a burial.

Area 14 is located to the north of Area 17 covering an area of 777.82 m^2. A sum total of 436 burials and 128 remains were recovered. The burials were found either in soil or in stone graves. Many of the recovered graves were Roman in context, oriented south to northeast (head to feet). Extensive overlapping has made determination of morphology of many pits very difficult. The chronology of the burials ranges from late Roman to Modern age through lower medieval age, which is indicated by burial goods such as coins, copper pins etc. typology.

Area 15 is located north of the Santa Maria do Olivais's bell tower, between Area 16 and Area 18 covering an area of 641.28 m^2. A large collection of remains numbering 235 burials, 145 partial remains associated with burials and 25 isolated bones were recovered. A vast majority of the burials were violated, as only 30 out of 235 skeletons were intact. The chronology of the burials date from the reign of King John I to the reign of Dom.Sebastião. However, the oldest archaeological material dates back to the late Roman period but are not associated with any burial.

Area 16 is located between Area 14 and Area 17 to the west and Area 15 to the east covering an area of 121.38 m^2. The area revealed an exceptional concentration of burials. A total number of 273 burials, 97 remains associated with burials and 12 isolated burials. The burials were in a position of "dorsal decubitus", with the head facing west or southwest grave. The chronology of the burials date from the reign of Sancho I to the reign of Dom.António.

Area 17 is located to the north of Area 20, in front of the Santa Maria do Olivais church covering an area of 850,986 m^2. A total of 220 burials were recovered from the area with the burials in

"dorsal decubitus" position, with the head towards the south. The chronology of burials range between 13th to 17th centuries.

Area 18 is located to the northwest of the Santa Maria do Olivais church covering an area of 570.33 m^2. A total of 342 burials, 188 burial related bones and 29 isolated bones were recovered. The burials were in a position of "dorsal decubitus", with the head towards the southwest or west and facing upwards. In this area there is a predominance of burials in relation to the other areas, with stones, mortars and masonry involved indicating work and monetary investment. This might have to do with the proximity of Santa Maria do Olivais church and the socioeconomic status of the deceased. The chronology of burials ranges from the reign of Dom.Sancho I until the reign of Dom.João IV.

Area 19 is located to the north of the church of Santa Maria dos Olivais and Area 15 with the current cemetery as the northern boundary. A total of 80 burials, 54 osteological remains associated with burials and 10 isolated bones were exhumed from this area. The chronology of the area seems to be between 15th to 16th centuries. However, further studies are required to precisely elucidate the limits of usage of the space.

Area 20 is located in the southern region to the side entrance of the Church of Santa Maria do Olivais with an area of 589.29 m^2. The burials are mostly oriented from south to north east direction. The chronology of the area ranges from the 14th to 17th centuries based on the burial goods recovered.

The samples were chosen from all the areas except Area 17 as equally as the sampling strategy allowed to have a representation of all the periods of the necropolis. Area 17 could not be represented as no individual had enough dental calculus to perform multiple analyses.

4. Diet in Medieval Portugal

It is essential to understand the variety of foods being consumed as diet is an aspect which abstrusely reflects the economic, political and social order of human society. To understand better the scientific data of the study, it is crucial to collect the contextual specificity and maintain the information about the dietary patterns practiced in Medieval Portugal. The synergy of food with spatiality and time are of the prime focus.

The Roman Empire is the predecessor of the Middle Age European kingdoms and one must trace the evolution of culinary practices from it if one wants to understand the medieval food preferences. The Roman Empire was very uniform with very slight variations in dietary practices. The standardized food customs and practices was based firmly on the classic trinity of wheat, wine and olive oil (Montanari and Bárbaros, 1998; R.Tannahill 1988). The Romans strongly believed that meat was the food of barbarians and practiced culinary customs based on cereals, vegetables, legumes and fruits. The sophisticated culinary techniques developed by the Romans were lost once its influence ended. Seasoning was limited to the essentials. With the flow of time, people developed dietary habits derived from integration of both cultures. The result was that people started consuming agricultural produce in conjugation with incessant intake of meat products such as cattle, game and fish (Montanari and Bárbaros, 1998; Montanari M. R., 1998; Tannahill.R, 1988). Medieval Portugal, like rest of Middle Age Europe made up the lack of quality of food with quantity and was usually a nutrient deficient and monotonous diet. Even though there were no major deficits in the supply of food even to the people in the lowest strata of the society. However, there were differences in the practices of food between social classes (Marques.A, 1987; Ferro.J.P., 1996).

The food in medieval Portugal was based on the new trinity of – cereals, wine and meat. The majority of time production of food was marred by climatic aberrations. This had direct impact on the interaction of people with food with respect to social and economic structures of the era. Peasants usually bore the brunt of the lower food production, as the consequences were increased food prices and lowering of purchase power. This lead to the formation of a restrictive barrier, denying the opportunity to consume a diverse range of food products (Ferro.J., 1996). This conformity lead to deficiencies of vitamin D, vitamin A and vitamin C. The consequence was weak resistance to pathogens leading to frequent epidemics (Marques.A.H.O, 1971). The other main

reason was that the cultivated land was not under the ownership of the peasantry but the aristocrats. The peasantry used the cultivated products to pay the rent and only keep a small part for self. The quantities of cereals and wine were just sufficient to fill their stomachs. The consumption of meat such as cattle, game and fish were governed by more sophisticated dynamics of abundance and religion. However, this pattern of absence and presence of foodstuffs along the flow of time shaped the culinary practices of the demography.

In Middle Ages Portugal, cereals occupied the largest share of cultivated area. Amongst the cereals cultivated, different kinds of wheat were the most produced and consumed. All other cereals such as corn, rye, and oats were less preferred (Marques.A.H.O, 1987). Rice was already known and being consumed in the 14th century though it was not widespread (Marques.A.H.O, 1968, 1987, 1987). Legumes were cultivated on a very small scale and amounted approximately 1% of the total cultivated land (Gonçalves. I, 1984; Marques.A.H.O, 1987). This indicates that meat was the primary source of proteins.

It is crucial however to understand the spatial variation in the cultivation patterns in Portugal. In Ribatejo region where Tomar is located, corn dominated wheat as the largest cultivated crop. However, this was after the discovery of the New World. In Trás-os-Montes region, rye was the most cultivated cereal and other cereals were hardly cultivated. In Beiras and Ribatejo, cereals were very widely cultivated, with an even distribution in the former region whereas in the later wheat dominated maize, barley and rye. In Extremadura and Alentejo, the situation was similar to Beiras as the soils had areas of high agricultural productivity. In a stark contrast, the Algarve region had to deal with inadequate levels of agricultural production (Marques.A.H.O, 1968, 1987).

Cereals were mostly consumed in the form of bread (.Marques.A.H.O, 1987; Ferro.J.P., 1996). An individual consumed about 1-2 kilograms of bread a day. The estimate could go up with socio-economic status. The majority of bread was made from wheat as it dominated the cultivation. Bread made from only wheat was white in colour and was consumed by the more well-off with the peasants consuming it on special occasions (Coelho.M.H.C, 1990; Marques.A.H.O, 1968). The lower classes consumed more of dark bread, manufactured from a mixture of flours. With crises in cereal production being frequent followed by soaring prices, people were forced to find replacements (Marques.A.H.O., 1987). In mountainous regions of the north where the climate is not suitable to cultivate cereals, chestnuts, acorn and legumes

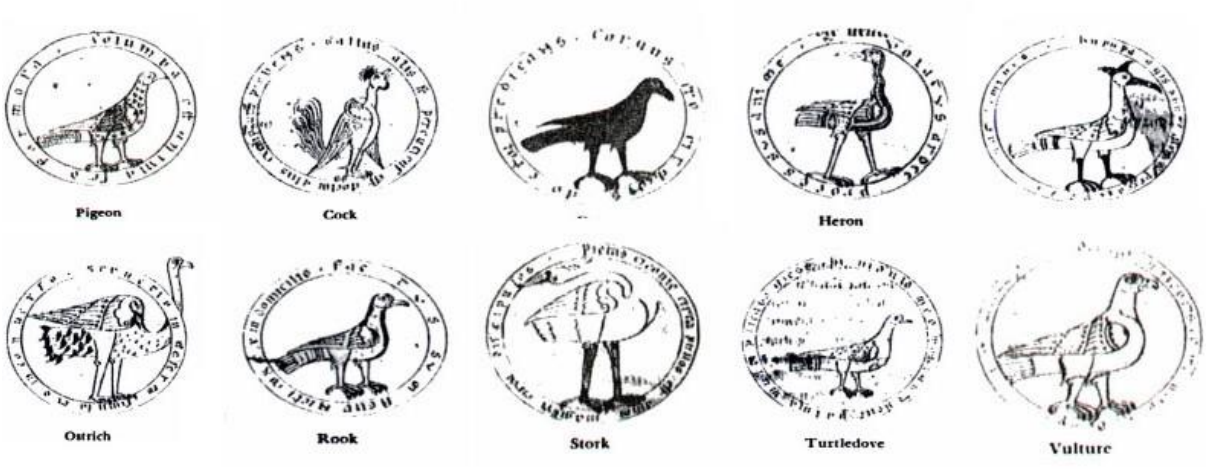

Figure 5. Birds which were cited in medieval Portuguese literature.

were being consumed. In highly populated regions, legumes such as fava beans, peas, lentils, chickpeas, peas, beans, and tremoço were imported from abroad to substitute cereals (Marques.A.H.O, 1987; Coelho.M.H.C, 1990; Gonçalves. I, 1988; Marques.A.H.O, 1987).

The staple diet of the people was predominantly meat and fish (Marques.A.H.O, 1971). Beef, pork, mutton and goat were the commercially available meats. Game and poultry were also consumed frequently. In the middle ages, Portugal was famous for gaming reserves and wilderness. Though hunting was a pastime for the aristocrats, it was an important source of subsistence for the peasantry. Fallow deer, deer, roebuck, hare and even bear were widely sold in the market along with a variety of fowl species such as crane, wild duck, teal, heron, redshank, bald coot, and partridge among many others out of which some are shown in Figure 5. Poultry was almost the same as today including chickens, ducks, geese, pigeons, pheasants and doves. Turkey was included in this list only after the discovery of the America. The peasants utilised the abundant

game and poultry accessible to them to cover a good part of the tribute they were obliged to pay such as rent and quitrents to the ruling class. Rabbits however were raised for food rather than being hunted to make various sort of cured meats (Marques.A.H.O, 1971).

Fish however seems to have been less consumed in comparison to the modern times not counting the economically well off class, who considered the partaking of these foods as important. This is shown in the famous cookbook by Domingos Rodrigues where 66% of the dishes were meat based and those based on fish were less than 10% (Rodrigues D., 1987). The content of the book is a reflection of the consumption patterns of the wealthy class. The consumption of the fish by the clergy was based on religion, as 68 days of abstinence from meat was obligatory for Catholics. Church recommended peas, fruit and small fish. In the deprived classes, fish played an important role (Marques.A.H.O, 1971). The peasantry consumed sardines and whiting (peixota). The economically well of preferred other marine and freshwater species such as snapper, tuna, trout, sea bream, shark, sardines, conger, eels, red

Figure 6. Geo-political situation during the Reconquista period. (Source: Pinterest)

snapper, sea bass, shad, surmullet were commonly consumed across all the socioeconomic classes. Crustaceans such as lobster, crab and molluscs such as clams, oysters along with whale and porpoise meat were also eaten (Marques.A.H.O, 1971). Tomar must have been influenced heavily by the presence of the various religious orders present throughout its history.

The dietary patterns also varied according to regional variation of religious practices. In the more Christian Coimbra in the twelfth century, pork and mutton were the most expensive whereas in the Muslim prominent Evora, price of beef was twice that of pork and more than twice that of mutton and goat. However, religion was not the only influencing factor at play in determining the price of the meat as pork is considered impure in Islam (Marques.A.H.O, 1987). Figure 6 shows the political situation of medieval Portugal during the Reconquista which influenced the local food prices.

The direct consumption of milk was not very widespread in Medieval Portugal. However, there were varied ranges of dairy products. They were specially used as side dishes or desserts and referred to as "Milk Victuals". Cheese, cream, butter and various pre-prepared dishes were very commonly consumed (Marques.A.H.O, 1987; Ferro.J.P, 1996). Due to abundance of poultry, eggs were used in large quantities as raw ingredients for more elegant dishes. Desserts were made with milk and sweets were improved upon biscuits and pastries. Honey was used as a sweetener as sugar was exorbitantly priced (Marques.A.H.O, 1987; Ferro.J.P, 1996).

Vegetables were not very preferred by the clergy in medieval Portugal. This is reflected in the cookbook of D. Rodrigues, less than 5% of the recipes are vegetarian (Rodrigues D., 1987). The poor class preferred fresh vegetables. Cabbage, cauliflower, spinach, cucumber, turnip, carrot, onion, broccoli, pumpkin, radish, and mushrooms were commonly consumed (Marques.A.H.O, 1987; Coelho.M.H.C, 1990; Gonçalves. I, 1988; Marques.A.H.O, 1987). Salads, predominantly lettuce based were commonly consumed on the side with meals. Vegetables served to vary the otherwise monotonous diet of the peasants, however they were reliant on the climate and market constraints.

Portugal was always abundant in the production of fruit. Various fruit bearing trees such as figs, pumice, apple, pear, peach, and cherry dotted the Portuguese landscape. Olives and grapes were also abundantly cultivated to produce olive oil and wine (Marques.A.H.O, 1987). Sweet orange became the most common tree after Vasco da Gama brought it back from the East. Fruits were also consumed with wine at night as a refreshment. Seasoning and condiments were really simple in Middle Ages. Usually it consisted of salts and fat - based products to food (Marques.A.H.O, 1987; Ferro.J.P, 1996). Olive oil played a central role as a condiment and base ingredient. Lard was also used as a seasoning by all social classes equally. Various herbs such as coriander, parsley,

and mint were used to refine the flavours by the wealthier classes. Spices such as clove, saffron, ginger, and mustard were very expensive and consumed only by the élite.

Medieval Portuguese population suffered periodic shortages of food which was mitigated by imports of non-indigenous agricultural products. The generally consumed food before the discovery of the American continent was the local produce and later started including the vegetables and fruits brought back by the explorers such as potatoes and corn. Investigating the composition of dental calculus may have seems to possess the potential to shed new light on the subsistence patterns of the inhabitants of Tomar.

5. Scientific Approach

5.1 Dental Calculus

5.1.1 Aetiology

The multi-dimensional nature of the aetiology of dental calculus was initially thought universally by anthropologists that an alkaline oral environment facilitates the increased precipitation of salts from the oral fluids (Hillson, 1979; Lieverse, 1999). Despite the multitude of studies to elucidate the process of calculus formation, comprehensive mechanism still evades discovery.

The process of formation of calculus begins with the evolvement of pellicle over the enamel surface due to adsorption of highly specific salivary glycoproteins as a preventive measure against the bacterial metabolic acids and the deposition of salivary minerals especially calcium phosphate (Samaranayake, 2006). This is followed by the formation of plaque which is composed by several species of bacteria, including but not limited to streptococci, staphylococci, lactobacilli and corynebacteria (Radini et al., 2017). The first colonisers of the pellicle are the facultative *Streptococcus sanguinis* and *Streptococcus mutans*, which replicate and form micro-colonies in a short time due to the oxygen rich environment. *Streptococcus mutans* is especially important as it produces enzymes glucosyltransferase and pyrophosphatase. The enzyme glucosyltransferase converts sucrose into exopolysaccharides (EPS). These EPSs act as adhesive agents for other bacterial species to adhere to the initial colonies, shielding them from acidic environment. The consequence of this phenomenon is that as the thickness of the plaque increases, the availability of oxygen is cut off to the initial colonies (T.M.Roberson, 2006). Starch granules have a higher probability than other substrate as the bacteria in the gingival crevice are principally proteolytic. The metabolism of the bacteria leads to production of compounds such as ammonia increasing the local oral pH (Marcotte & Lavoie, 1998). The process of plaque formation, if not dismissed, causes the surrounding pH to increase even further. This followed by mineralisation of the plaque leads to the formation of dental calculus. In case of the formed plaque not mineralising, which happens when the pH is lowered, caries is formed (Figure 7). The formation of calculus is usually prominent on the lingual surfaces of incisors and canines and the buccal surfaces of the maxillary molars owing to the proximity of the salivary duct openings (Hillson, 1979).

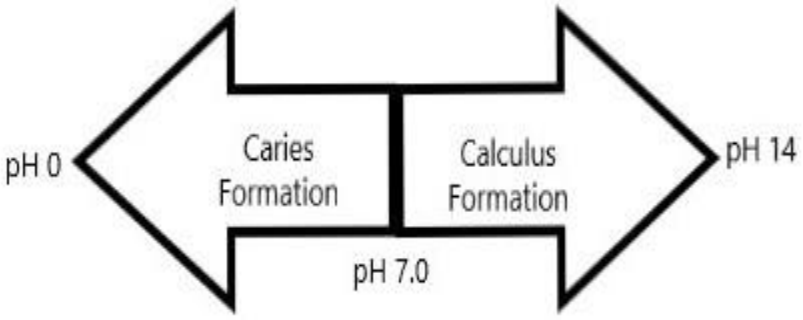

Figure 7. Oral pH and pathology associated with it.

A set of four mechanisms were termed to describe the formation of dental calculus out of which two describe the process of mineralization (Mandel, 1990). The first being termed the "Booster Mechanism" that propounds the formation of dental calculus as a crystal growth by spontaneous precipitation, relying on the supersaturation of calcium and phosphate ions in the oral fluids and a number of arbitrating factors such as local pH. This theory of simple precipitation is only feasible when calcium and phosphate ions are in ionised form (Schroeder & Shanley, 1969). The second theory, which is most widely supported, is termed as "Epitactic Concept". This takes into account that the calcium and phosphate ion concentrations are not high enough for spontaneous precipitation. However, the concentrations are sufficient to reinforce growth of calcium phosphate crystals once a "nucleus" or "seed" has formed. This is very similar to the formation of other ectopic calcifications such as urinary stones, and gall stones (Lieverse, 1999). This nucleation process requires an organic matrix which is available in the form of plaque, a biofilm and an occasional supersaturation of the calcium and phosphate ions to commence and persevere calculus growth (Mandel, 1990). The occurrence of dental calculus at certain sites and not everywhere is explained by the "Inhibition Theory". It has been established that oral bacteria play a key role in disrupting the inhibiting mechanisms of mineralisation (Scheie, 1989). When the inhibiting mechanism is obstructed, mineralisation occurs (Mandel, 1990). Pyrophosphatase is secreted by *Streptococcus mutans* hydrolyses pyrophosphate, a potent mineralisation inhibitor. Many proline rich proteins also bind with calcium and inhibit mineralisation. Proteolytic enzymes, produced by these bacteria, lyse them into peptides and amino acids (Scheie, 1989). The event of brushite and octocalcium phosphate precipitating first and acting as precursors hydroxyapatite and whitlockite is termed as "Transformation Theory" (Mandel, 1990). The theory is supported by the fact that in

immature deposits up to 3 months brushite crystals are the most abundant wherein mature calculus deposits of 6 months and above, hydroxyapatite crystals are the most abundant (Driessens & Verbeeck, 1989; Mandel, 1990).The four theories describe various aspects of the calculus formation process and it is prudent to say that they work in tandem with other factors, which are still unknown.

5.1.2 Archaeological Importance

The use of dental calculus as a proxy of the dietary reconstructions of living organisms from the past is relatively new (Hardy et al., 2015; Hardy, Radini, Buckley, Sarig, et al., 2016; Horrocks, Nieuwoudt, Kinaston, Buckley, & Bedford, 2014; Anita Radini et al., 2017; Tromp & Dudgeon, 2015). Biological matrices such as bones and teeth have been used for a relatively long time for the same purpose (Lee-Thorp et al., 1989; van der Merwe, 1991). This demands that the concernment as well as advantages of dental calculus as a valid proxy for the paleodietary reconstructions must be established.

The first most important facet which is exploited in archaeology is the entrapping of physical and biomolecular debris along with microbial flora in the dental calculus when the organism is alive (Buckley et al., 2014; Hardy et al., 2009; Radini et al., 2016; Wang et al., 2016; Warinner et al., 2014). The second facet is the lack of post-mortem alterations of micro-debris from the environment as the formation process of dental calculus ceases immediately after death (Middleton & Rovner, 1994). However, this does not rule out the alteration of the chemical signal due to diagenesis after death. Starch granule degradation has been reported due to complex diagenetic processes (Barton & Torrence, 2015; Collins & Copeland, 2011). Future crystallography studies can reveal the extent of alteration of the signal due to diagenesis. Finally, the last factor is the variability of the rate of formation of dental calculus from individual to individual which depends on a wide range of parameters, such as genetic factors, phosphate and calcium levels, mineral and silicon levels, salivary flow rate, oral microbiome, local pH, and oral hygiene (Lieverse et al., 2007; Marcotte & Lavoie, 1998). The fourth factor is the span of the lifetime, which the dental calculus represents. Chewing abrasive and fibrous material has the potentiality of mechanically dislodging the calculus deposits from the tooth surface (Gaar et al., 1989). The dental calculus, which is less than 3 months, is an immature deposit whereas a deposit older than

6 months is referred to as mature deposit. An immature deposit is not a reliable proxy for dietary reconstruction as it a too short period to represent an individual's life. One way to date the age of the deposit of calculus is to find the relative concentrations of hydroxyapatite, brushite, whitlockite and octocalcium phosphate as the concentration of brushite is the highest in immature deposits whereas hydroxyapatite is the most abundant in mature deposits. This might be reflected in the difference of carbon isotope ratios obtained from bones and dental calculus as only the former is an average representative of an individual's life (Salazar-García, Richards, Nehlich, & Henry, 2014). A recent study showed a correlation between the carbon isotope ratios of the inorganic fractions of bone and calculus of an individual (Price et al., 2018).

The advantage of dental calculus over other biological matrices is that it is not a part of the skeletal system. This makes it an ideal material to work with destructive techniques when the skeletal remains are parts of collections, and museum exhibits.

5.1.3 Debris

The first scientific evidences of dietary debris from dental calculus were phytoliths which formed the basis of the conclusions to understand the diet of the herbivore ungulates (Armitage, 1975). Along with phytoliths, other environmental indicative debris were also observed and reported. The first foreign bodies to be categorically identified were silicified oral bacteria (Gonzales & Sognnaes, 1960; Lustmann, Lewin-Epstein, & Shteyer, 1976). The recovery and identification of other debris from the calculus matrix such as charcoal, pollen, and plant fibers from wide periods of historical material by Dobney and Brothwell (1987, 1988) laid the final foundation for the usage of the dental calculus in archaeological dietary studies (Radini et al., 2017).

Any foreign material which enters the buccal cavity is primarily through three sources, with the primary being nutrition intake and the other two being environmental contaminants and debris due to behavioural tendencies. The debris due to nutrition intake usually consists of diatoms from drinking water (Dudgeon & Tromp, 2014), phytoliths from plant based raw material, starch granules from carbohydrate rich food and other trapped physical and biomolecular food components (Henry, Brooks, & Piperno, 2011; Henry & Piperno, 2008; King & Searcy, 2016; Li et al., 2010; Radini, Nikita, & Shillito, 2016; Warinner et al., 2014; Weber & Price, 2016). The environmental contaminants are usually encompassed into the dental calculus matrix by either

inhalation (both nasal and oral) or "secondary eating". Common particulate matter includes, charcoal particles, fibers (Hardy et al., 2015). The oral respiration is carried out while eating, interacting orally, panting and finally when respiratory passage is blocked by nasal mucus. This also includes micro-particles which have lodged or deposited on food or drinks, entering the oral cavity and get embedded in the dental calculus (Hardy et al., 2016; Radini et al., 2017). Sometimes this embedding of soil and grit particles can happen to the food during the initial stages of the raw material synthesis (Tromp & Dudgeon, 2015). A broad range of breathable inorganic and organic particulate material produced in sufficiently high concentrations due to different production activities such as stone tooling, agricultural processing, ceramics, cooking etc. which can cause various respiratory syndromes have been found in dental calculus. These particulate material include soot, micro-charcoal, spores etc. which are highly probable to be embedded into the calculus because of oral respiration (Hardy et al., 2015, 2016; Radini et al., 2017). Finally, the debris capsulated due to behavioural tendencies is usually because of the use of "mouth as third hand" behaviour or practices of introducing non-dietary material into the oral cavity such as the practices of chewing or smoking non-nutritional substances such as tobacco, coca (Yaprak et al., 2017; Klepinger, Kuhn, & Thomas, 1977; Blatt et al., 2011; Charlier et al., 2010; Radini et al., 2016). A more uncommon but interesting behavioural tendency, which has the potential to introduce micro-particles, is gastrophagy. Gastrophagy is the practice of eating the gut contents of hunted animals in some populations as a means of gaining nutrition without having much effort in digestion. The presence of yarrow and chamomile was suggested by Hardy et al., (2012) after finding molecular cursors indicative of them in the dental calculus of El Sidrón Neanderthals. However, Buck et al. (2015) propounded the possibility of gastrophagy as the mechanism of incorporation of these compounds into the dental calculus and that it should be considered as a potential factor in distorting the signal in dietary studies (Radini et al., 2017). Another widespread cause of non-dietary debris in dental calculus is the extramasticatory use of the teeth. The use of teeth as a force to apply on material which is too small in size to be worked by hands, often results in the material getting embedded in the dental calculus matrix (Blatt et al., 2011). As it has been proved beyond reasonable doubt that the mechanism of debris incorporation in dental calculus is multi-causal, conclusions should be drawn after careful considerations. The possibility of the scientific evidence being embedded by more than one process is highly probable. The attribution

of the chemical signal to the source is highly contested as of the current scenario (Radini et al., 2017).

5.1.4 Incorporation of Debris

Incorporation of debris in dental calculus is as multi-causal as it has multiple origins. The dietary debris is incorporated after the mastication process where as the non-dietary debris is incorporated when the mouth acts as a dust trap (Radini et al., 2017). The incisors cut the food into a chewable size and the canines, which tear harder food that cannot be cut by the incisors, carry out a parallel of this function. The food is then mixed with saliva by the tongue and then pushed to the premolars and the molars, which grind it, making it relatively smooth and easy to digest. Because of the positioning of the salivary glands, the formation of the dental calculus is more concentrated on the molars and the incisors (Watson, 2017). The food is then pushed down the throat by the peristaltic motion and it enters the oesophagus, this is called the bolus.

When the pH of the buccal cavity is alkaline and the concentrations of Ca^{2+} ions and PO_4^- ions are high enough for the ectopic formation of the dental calculus nucleus (Mandel, 1990), the food chewed in the mouth gets stuck on the various surfaces of the teeth including the dental calculus surface. The chance of food debris being stuck on the surface of the dental calculus surface is high due to the presence of the EPSs (exopolysaccharides). However, the stickiness of the food also plays a huge role in the amount of debris being incorporated. The subsequent rinsing of the mouth gets rid of the majority of the debris with the exception of very a small amount of debris remaining behind. The biomolecular debris is adsorbed by the calcium phosphate matrix whereas the physical debris is embedded by the next cycle of expansion of the nucleus of the ectopic calculus. This cycle keeps repeating until the dental calculus either dislodges from the surface of the tooth or the calculus formation stops due to the death of the individual. In case of the non-dietary debris, the cycle may or may not begin in the same way as the dietary debris depends on if it is a non-nutritional substance (e.g. tobacco, betel leaves, coca etc.) in which case it undergoes deposition as dietary debris. If it is an inedible substance, it begins with the deposition of the debris on the dental calculus surface. Then the subsequent cycle of the calculus expansion embeds the debris. The amount of debris should be relatively higher at the incisors and the molars than the remaining area of the mouth. The presence of the certain enzymes which hydrolyse inhibiting factors (e.g.

Pyrophosphatase) cause calcium phosphate to precipitate more than in other locations (Scheie, 1989).

The incorporation of debris into dental calculus is almost the same in all the scenarios. However due to various enzymes and other factors, the spatial incorporation of the debris is not homogenous. This is caused by the hydrolysis of the debris by suitable enzymes. A good example of this phenomenon is the higher incorporation of starch granules in sub-gingival crevice where the bacteria is proteolytic (Marcotte & Lavoie, 1998). In addition, the debris is relatively shielded by the salivary amylase (α-amylase). The mechanism and the factors controlling the spatial distribution of the debris plays a central role while sampling for scientific analysis.

5.2 Microremains

5.2.1 Phytoliths

The word "phytolith" is taken from two Greek words, "phytos" meaning plant and "lithos" for stone. In the past, this term has been used non-specifically for all forms of siliceous and calcareous mineralized secretions by plants. In current literature, when not mentioned otherwise, the term phytolith refers to siliceous depositions in an intracellular or extracellular locations in a plant.

Silica is an omnipresent component of plant and animal microorganisms. Silica is absorbed in to the cellular system in a soluble state from groundwater. Silica enters the plant body in the form of monosilicic acid, $Si(OH)_4$ when the soil pH ranges between 2 and 9 (Barber & Shone, 1966). Silica is present in underground water in soluble form mainly due to weathering of minerals such as quartz and feldspar (Dunne & Leopold, 1978). The growth of phytoliths in a plant is dependent on several factors such as climate, composition of soil, availability of water, age of plant and taxonomy of the plant. The process of phytolith development begins when the plants take in soluble silica present in groundwater via their roots. This silica is carried up to various organs in the transpiration process by the water conducting tissue, xylem. There are two pathways by which plants absorb water solubilized silica. The two proposed pathways are active transport of monosilicic acid and non-selective passive flow in the transpiration stream. In active transport mechanism, the plant has to expend energy to transport silica whereas it does not in the latter. There is sufficient evidence that passive uptake and active transport of silica occurs in plants based on their taxonomy (Raven, 1983). However, it has also been demonstrated that some species of

plants having low concentrations of phytoliths have some mechanism for rejecting silicic acid at the surface of the root.

When the monosilicic acid enters the plant it is polymerized and finally deposited in the form of silicon dioxide (SiO_2) in both intracellular and extracellular spaces. Though these deposits are referred to as opal silica, they behave more like silica gel (Lewin & Reimann, 1969). There are three loci in a plant where phytoliths occur: (1) cell wall deposits (2) infillings of the cell lumen and (3) in the intercellular spaces of the cortex. Patterns of local deposition are repeated in the same species and families of plants, independent of the environment of growth. This fact is exploited to identify families if not species of plants in archaeological context.

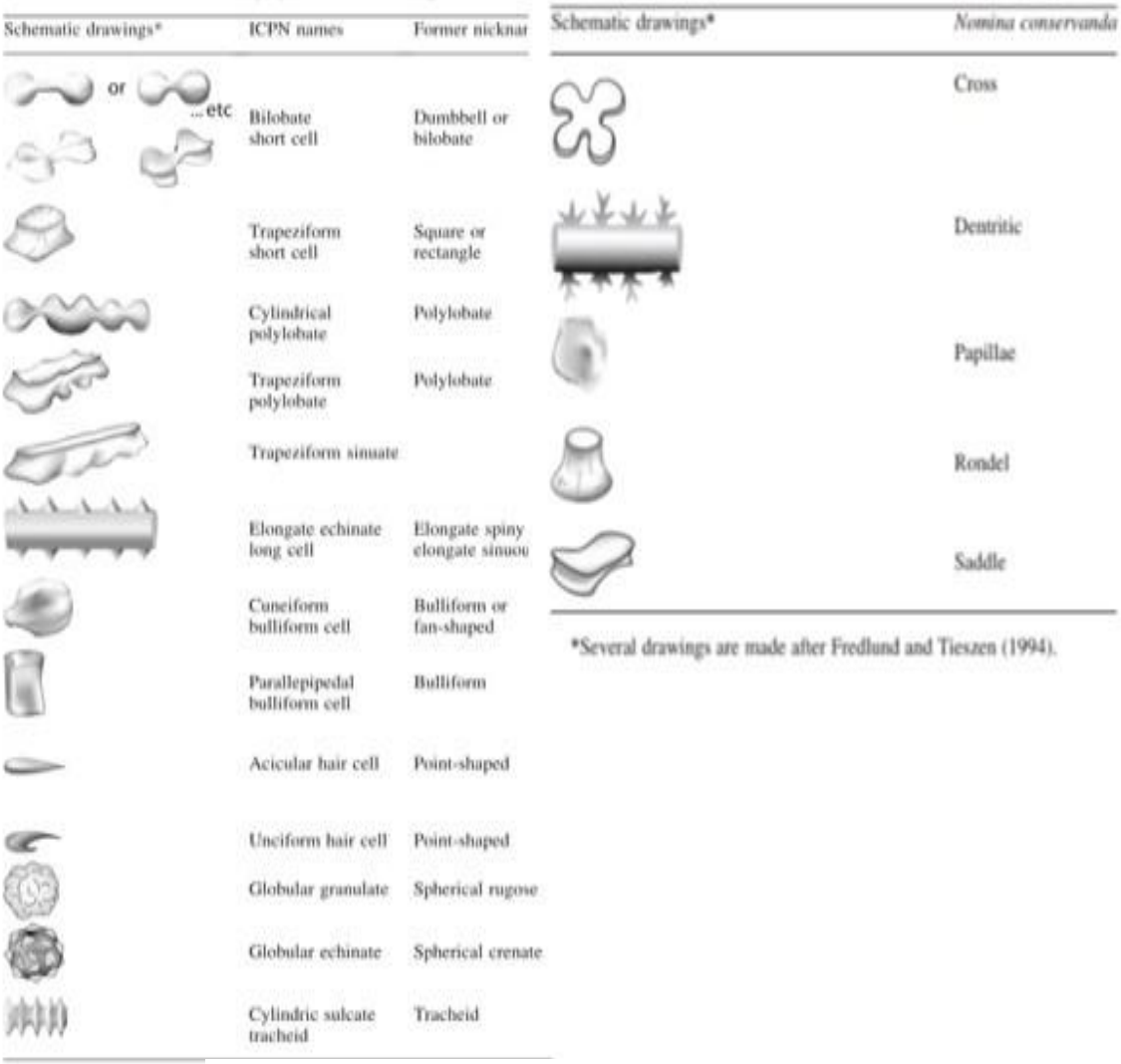

Figure 8. International Phytolith Nomenclature. Madella et al., 2005

The first report on phytoliths in archaeology was by Bryant who observed calcium oxalate crystals in coprolites (Bryant, 1974). Phytoliths being more or less ubiquitously present in archaeological

contexts when plant parts are involved. The presence of phytoliths are then subjected to further interpretation based on the surface they are observed. The application of phytoliths on archaeology ranges from economic importance of plant species, agricultural practices, domestication of plant species, dietary practices etc. The advantages of utilizing phytoliths are that they are resilient material, rarely transported by water or wind, extremely easy to evaluate the morphology and cheap analysed. However, phytoliths have their own pitfalls when acting as proxies for reconstruction of the past. Not every family of plant kingdom produce phytoliths. And phytoliths are erodible as well as dissolvable at extreme pH. Phytoliths are also subjected to mobility from surface to surface and also there is a huge dearth in the availability of reference material. Phytoliths are classified as shown in Figure 8 into various categories based on their morphology (Madella et al., 2005). The morphology of the phytoliths is based on the type of cell silicified. The morphometry of the phytolith can be utilized to identify the family of species of plant.

5.2.2 Starch Granules

Starch granules are the end products of plants after the completion of a cycle of photosynthesis. Starch is the stored form of food for plants in seeds, stems and underground organs such as roots, tubers and bulbs. Starch granules are highly utilized in archaeology as they are chemically inert and are morphologically specie specific. They are found preserved on surfaces of ancient artefacts and in paleorecords. Analysis of starch granules is usually used to reconstruct ancient subsistence patterns as well as plants which played a role in staple diet.

Starch granules have a point around which layers of protein are accumulated which is called as a hilum. Tubers and bulbs have an off-center hilum where the growth rings originate out from the hilum. The growth ring pattern is based on the formation geometry. As starch is the product of

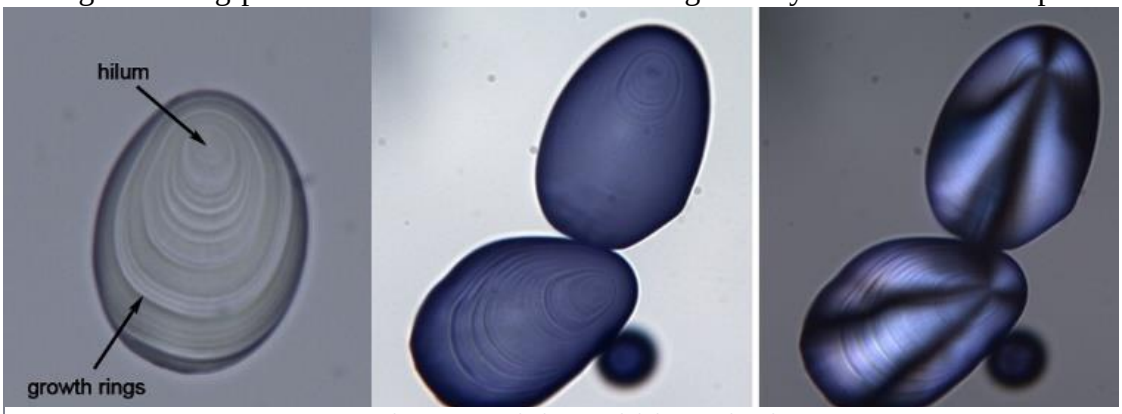

Figure 9. Starch grain morphology with hilum and maltese cross.
http://archaeobotany.dept.shef.ac.uk/wiki/index.php/Image:PotatoIKI.jpg

photosynthesis, its basic unit is glucose. Glucose can be linked into two types of starch chains namely amylose and amylopectin. The layers of amylose and amylopectin called lamellae are tightly packed into each of the rings. The dense packing along with the repeated pattern makes the starch grain partially crystalline. The second most identifying characteristic of a starch grain is its property of birefringence. Birefringence is a property of material where its refractive index is dependent on the direction. A starch grain under plain polarised light exhibits a cross shaped feature ending at its hilum. This is called an extinction cross or a Maltese cross (Figure 9). The third feature of starch granules is the presence of longitudinal fissure. The fissure is a sort of triangular trough originating from the hilum and extending outwards. This is a defining characteristic as some starch granules have it and some do not.

5.2.3 Phytoliths and Starches in Dental Calculus

The most widely used approach to extract the trapped microfossils consists in demineralization of the calcium phosphate matrix using HCl of varying concentrations. These extracted microfossils are then examined for morphology under a light microscope. A large amount of research has been conducted on both human and non – human dental calculus on the identification of phytoliths and starch granules. Usually the non – human samples are herbivores (ungulates) and extinct species such as *Gigantopithecus blacki*, mastodon etc. (Ciochon, Piperno, & Thompson, 1990; Gobetz & Bozarth, 2001; Middleton & Rovner, 1994). The majority of research has been focused on the extraction and identification of microfossils with specific emphasis on phytoliths and starch granules (Hardy et al., 2012; Henry, Brooks, & Piperno, 2011; Horrocks et al., 2014; Power, Salazar-García et al., 2014; Tromp, 2012; Tromp & Dudgeon, 2015). The other microscopy technique utilised for microfossil identification is the technique of scanning electron microscopy (SEM) coupled with energy dispersive X-Ray spectrometry. The technique has been exploited to study the micro - debris and its association with occupational and dietary habits (Charlier et al., 2010; Power et al., 2014). The technique has also demonstrated potential to identify possible drinking water sources by facilitating easy identification of diatoms (Dudgeon & Tromp, 2014). However, the main issue of the microfossil identification is that it involves the comparison of the extracted entities to be compared with reference collections (Pearsall, 2000). The usual method to explain the taphonomic processes affecting the survival of the microfossils is to compare them with residues extracted from other archaeological substrates (Barton & Torrence, 2015; Li et al., 2010). However, diagenetic alteration of starch granules has been reported and further research is

necessary to identify the integrity of dental calculus (Barton & Torrence, 2015; Horrocks et al., 2014).

5.3 Role of Stable Isotopes in Dietary Reconstruction

Isotopes are different atoms of the same element with same atomic number but different mass numbers (Schoeninger & Moore, 1992). In nature, isotopes exist in either radioactive or stable forms with the latter being more abundant. The stable isotopes of the same element possess the same chemical properties but slightly different physical properties. Due to the slight difference in the physical properties, one isotope (usually the lighter one) is favoured over the other isotope in a chemical process. The end product of this reaction is more enriched in the preferred isotope compared to the reactants, a process called isotopic fractionation (Malainey, 2011). The isotopic abundance of an element is measured with the aid of a mass spectrometer by combusting the sample in a controlled environment to liberate the element of interest in the form of a gas. In the case of dental calculus the gases liberated are CO_2 and N_2 as we are interested in carbon and nitrogen isotopes. Usually a magnetic sector is used to separate the molecules on the basis of their mass and a detector is used to measure the counts per second. A laboratory standard is also measured along with our samples as the former is calibrated to international standards.

Figure 10 shows the isotope fractionation application of stable isotopes which is quite varied in archaeology such as provenance studies, paleoclimatic reconstructions, diet and mobility of humans and fauna (Craig, Bondioli, Fattore, Higham, & Hedges, 2013; DeNiro & Weiner, 1988; Lee-Thorp et al., 1989; Sealy, Armstrong, & Schrire, 1995; van der Merwe, 1991). In the process of absorption and reuse of elements in the living tissue, the isotopic fractionation is dependent of the biochemical process the element goes through. In the case of dental calculus, the isotopic signal

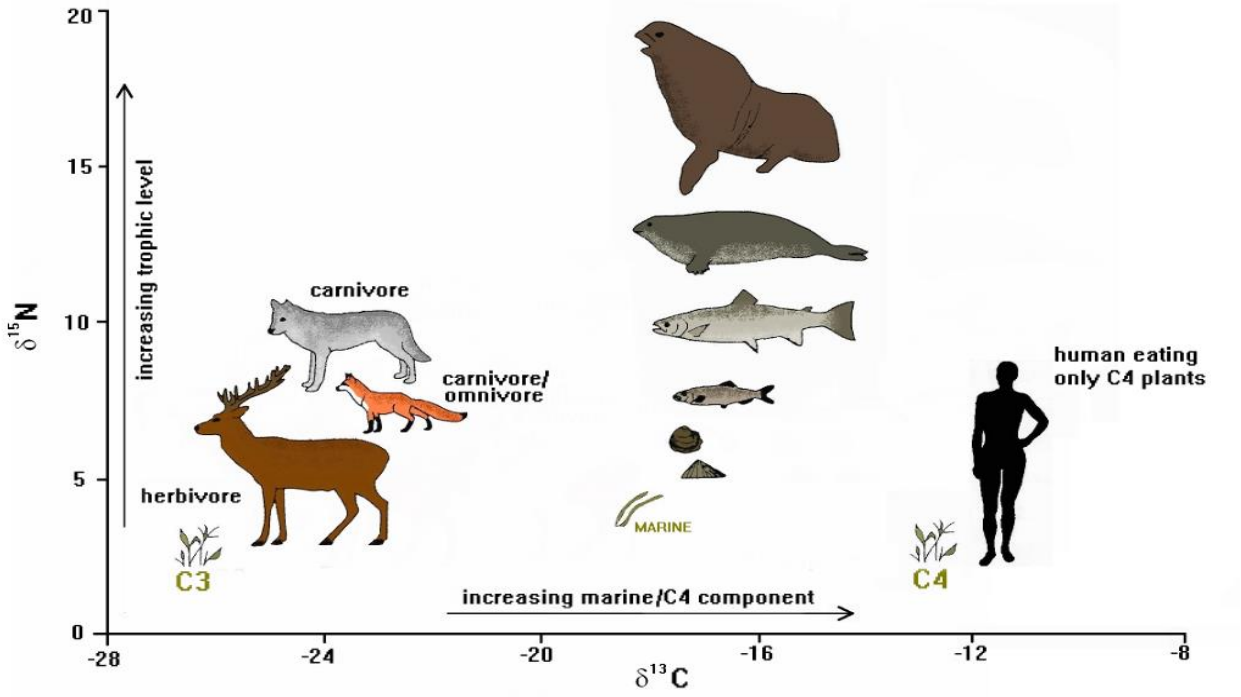

Figure 10. Carbon and nitrogen isotope fractionation. (Source: Schulting 1998)

is not subjected to any fractionation from the individual's metabolic process. Thus, the ratio of carbon and nitrogen isotopes in the dental calculus is the sum of the dietary debris trapped.

5.3.1 Stable Carbon Isotopes

^{12}C and ^{13}C are the stable isotopes of the element carbon where the abundance of the former is a 100 times greater than the latter (Malainey, 2011). In photosynthesis, the rate determining plant enzyme Rubisco (ribulose-1,5-biphosphate carboxylase/oxygenase) favours the lighter ^{12}C in comparison to the heavier ^{13}C (Caemmerer, Ghannoum, Pengelly, & Cousins, 2014; Leary, 2008). There are three different pathways of photosynthesis adapted by plants based on the climatic conditions they grown in. They are the C_3, C_4 and CAM (Crassulacean Acid Metabolism) respectively. Due to the difference in pathways, the end products have different $^{13}C/^{12}C$ ratios (DeNiro & Weiner, 1988; Lee-Thorp et al., 1989; van der Merwe, 1991). The majority of the vegetation of the world's terrestrial vegetation which includes rice, wheat, legumes and other tree species are C_3 in nature. Grasses which are from hot arid regions such as millet, sorghum, maize etc. are C_4 plants (Still et al., 2003). Usually in dietary analysis, osteological remains such as bones and teeth are measured which reflects the diet of the individual. The intake of C_3, C_4 and CAM plants in varying portions results in influencing the $^{13}C/^{12}C$ ratio reflected (DeNiro & Weiner, 1988; Sealy et al., 1995). The ratios are expressed as $\delta^{13}C$ values where the stable carbon isotope

ratio is expressed with respect to the value of Vienna Pee Dee Belemnite (VPDB). The deviation from the value of the VPDB if positive is referred to as enrichment and if negative as depleted. This is governed by the equation:

$$\delta^{13}C_{sample} = \frac{(^{13}C/^{12}C_{sample}) - (^{13}C/^{12}C_{reference})}{(^{13}C/^{12}C_{reference})} \times 1{,}000\% \quad (1)$$

From the equation one can observe that the more negative the $\delta^{13}C$ values, the lesser ^{13}C is present. A more positive $\delta^{13}C$ value indicates more ^{13}C in the sample. C_3 plants have $\delta^{13}C$ values ranging between ca. -22% to -30% with an average of -27% whereas C_4 plants have $\delta^{13}C$ values in between -9% to -19% with an average of -13% (Caemmerer et al., 2014; Leary, 2008; Roberts et al., 2017). Marine plants have a set of values in between the two and in cases may overlap. The $\delta^{13}C$ values from an herbivore are typically less negative than the plants it consumes and the $\delta^{13}C$ values from a carnivore will differ from those of the herbivore it feeds on. This further fractionation of isotopes when going up the trophic levels occurs because of all the extra metabolic activities involved. The extent of this difference depends also on the type of tissue as the process of imbibing the element varies from tissue to tissue intra-individual. For collagen from bones, a fractionation of 3-5% between plants and consumers with an additional fractionation of 1% in carnivores above primary feeders. However in case of dental calculus, the isotopic ratio should reflect the sum of the food consumed without any further fractionation.

5.3.2 Stable Nitrogen Isotopes

Amino acids are the building blocks of life with them acting as the fundamental units of proteins. Nitrogen is a necessary element for the synthesis of proteins which are made up of amines, amides and amino acids. The most abundantly found stable isotope is ^{14}N but it also occurs in the less abundant form of ^{15}N (Malainey, 2010). The $^{15}N/^{14}N$ ratio of the sample is measured against the $^{15}N/^{14}N$ ratio of an international standard which is atmospheric nitrogen (AIR – Ambient Inhalable Reservoir). This relation is governed by the equation:

$$\delta^{15}N_{sample} = \frac{(^{15}N/^{14}N_{sample}) - (^{15}N/^{14}N_{reference})}{(^{15}N/^{14}N_{reference})} \times 1{,}000\% \quad (2)$$

The nitrogen in atmosphere is depleted in ^{15}N, so the $\delta^{15}N$ will be close to 0% due to which most samples measured reflect a positive $\delta^{15}N$ value (Malainey, 2010). The $\delta^{15}N$ values of tissues from

an organism are more positive than that of the isotopic composition of their diet (Minagawa & Wada, 1984). Incorporation of ^{15}N is favoured by the metabolic reactions in comparison to ^{15}N, this makes the $^{15}N/^{14}N$ ratios useful in reconstruction of trophic levels and their related dietary sources (Minagawa & Wada, 1984; Schoeninger & Deniro, 1984). The comparison of the nitrogen isotopic ratios facilitates the possibility to reconstruct the subsistence pattern of an individual in terms of terrestrial versus aquatic food sources as well as legume versus non – legume plants. Nitrogen fixers, typically legumes have $^{15}N/^{14}N$ ratios which are quite lower than plants which accumulate all sorts of inorganic nitrogen. Consumption from these types of food sources can always affect the nitrogen isotopic ratios of the tissue samples (Minagawa & Wada, 1984; Schoeninger & Deniro, 1984). The other major influencing food are marine fauna such as fish, crabs etc. which have more positive $\delta^{15}N$ values when compared against terrestrial counterparts (Schoeninger & Deniro, 1984). The $^{15}N/^{14}N$ ratios of individuals are also affected by other factors such as weaning, stress periods etc. In case of weaning children, an enrichment of 2-4% is observed over non-weaning members.

Alone, the $^{13}C/^{12}C$ ratios and $^{15}N/^{14}N$ ratios are influenced by various factors such as precipitation, temperature, human activity, staple foods stuffs, geological factors making the comprehension quite difficult. But when the data is plotted together, they end up providing a picture on subsistence patterns. Populations consuming particular types of food have $\delta^{13}C$ and $\delta^{15}N$ values reflecting the diet after fractionation but when a combination of foods occur (which is the usual case), it results in intermediate values of both food types.

5.3.3 Stable Isotopes in Dental Calculus

Stable isotope analysis using elemental analyser – isotope ratio mass spectrometry (EA-IRMS) on dental calculus has furnished reasonably acceptable results, cementing the place of dental calculus as a proxy for ancient dietary studies (Price et al., 2018; Salazar-García, Richards, Nehlich, & Henry, 2014; Scott & Poulson, 2012). Some researchers have pointed out the fact that the signal from dental calculus is not the same as that from the bones (Salazar-García et al., 2014). This situation demands that the future research should be focused on developing standard ranges for isotopic ratios with varying trophic levels. Recent research has shown correlation between the starch granules and bone collagen isotope values as well as between the inorganic fraction of dental calculus and bone (Price et al., 2018; Wang et al., 2015).

5.4 Organic Residues

5.4.1 Organic Residues in Dental Calculus

Dental calculus is a reservoir of material entering the mouth which primarily includes food. The serial precipitation of calcium phosphate on to the biofilm secreted by facultative bacteria facilitate the storage of dietary record. The major nutritional molecules are carbohydrates, proteins, fats and vitamins. It is thus unsurprising to find sugars, amino acids, lipids, ribonucleic acids and other fundamental organic molecules which make up higher macromolecules. It was first reported that 17.1% of dental calculus is made up of organic material with proteins contributing 8.34%, fats a 2.71% and water along with unidentified organic fraction consists of 6.06% (Glock & Murray, 1938). Nothing was reported about the presence of cholesterol or related sterol compounds. Histochemical research revealed that the formation of salivary calculus is similar to other ectopic calcifications. Also it was reported that cholesterol, cholesterol esters, phosphor-lipids and fatty acids in the lipid fraction as well as reducing sugars in the carbohydrate fraction (Mandel, 1990). All amino acids except hydroxyproline and cysteine were found in dental calculus with aspartic acid and lysine being the most and least abundant respectively. The majorly occurring amino acids are glutamic acid, alanine, glycine, aspartic acid and lysine with rest of the amino acids being minor constituents (Stanford, 1957). Carbohydrates constitute around 16% of the total organic fraction of the dental calculus. The carbohydrates typically found were galactose, fucose, galactosamine, glucose, rhamnose, mannose, sialic acid, hexuronic acid and deoxyribose (Stanford, 1957). Further, a fraction of carbohydrate-protein complexes have been recovered which is attributed to be a mucoprotein (Stanford, 1957).

The organic fraction of the dental calculus also contains organic molecules which are associated with non-dietary ingestions. Not many cases have been reported about the recovery of these sort of biomarkers. Eerkens et al. reported the recovery of alkaloids from dental calculus, specifically nicotine confirming the use of tobacco in pre-contact California (Eerkens et al., 2018). Self-medication and cooking have been observed in Neanderthals from Atapuerca when non-nutritional bitumen, shale, and bitter tasting dihydroazulene and chamazulene which are bio-markers for plants such as chamomile and yarrow were recovered (Hardy et al., 2012). These cases though are very peculiar in their nature, theoretically it fits the facts that the compounds recovered are quite stable and dental calculus is quite inert as well as quite unaffected by diagenesis.

Fast and least preparative methods which have been employed are Thermal Desorption Gas Chromatography Mass Spectroscopy (TD-GCMS) and Pyrolysis Gas Chromatography Mass Spectroscopy (Py-GCMS). The two techniques can be carried out by the same instrumentation with different temperature programming. Thermal desorption involves slow heating of the sample at moderate temperatures to liberate relatively volatile organic molecules without breaking them down. However, in pyrolysis the sample is subjected to temperatures around 600 C^0 for a few seconds where the organic molecules are broken down in to smaller and stable compounds. The liberated compounds are then separated with gas chromatography and the molecules identified with mass spectrometry. TD-GCMS and Py-GCMS not only help in identifying the compounds in organic fraction of the dental calculus, they also help in checking for diagenetic alteration. The techniques can be exploited to identify bacterial compounds which can sometimes be diagnostic for a species.

The calcium phosphate matrix of dental calculus is an excellent environment to preserve a wide spectrum of organic molecules, which can be identified by gas chromatography techniques such as pyrolysis gas chromatography mass spectroscopy (Py-GCMS) etc. The biomarkers, which are trapped in the dental calculus matrix, are characteristic to the source of their origin. This can be exploited to identify diet, therapeutic compounds, addictive compounds and environmental pollutants such as carbohydrates, proteins, bitumen etc. (Buckley et al., 2014; Hardy et al., 2012, 2015). However, this framework of analysis has only been applied for paleolithic contexts and is yet to be tested for calculus from different periods. Py-GCMS in this study is being utilised in a medieval context and mainly to demonstrate the importance of spatiality in the sampling of dental calculus. Dental calculus is a very good reservoir of nucleic acids and other biomolecules of microorganisms (De la Fuente et al., 2013; Preus et al., 2011). The oral microbiome and its temporal evolution has been the core directive of the research in understanding past pathologies such as tuberculosis, domestication of plants etc. (Adler et al., 2013; Warinner et al., 2014; Christina Warinner et al., 2014 (1)). Biomolecules which are resilient such as globulin proteins have been utilised to study milk consumption (Warinner, et al., 2014). However, only some portions of the biomolecules act as signatures contextually as many of the molecules can be interpreted in multiple ways.

5.5 Trace Elements in Dietary Studies

Trace elements in terms of biological systems can be divided into two categories, namely essential elements or micro-nutrients which participate in biochemical reactions as co-factors or in form of metallo-enzymes and non-essential elements which are stored in passive state as a consequence of detoxification process. Due to similarity in size and charge with Ca^{2+}, many cations such as Zn^{2+} and Sr^{2+} are incorporated in to the hydroxyapatite structure of bone and teeth (Liu et al., 2013). This replacement also occurs with anions (PO_4^{3-} and OH^-), usually by CO_3^{2-} but by other anions as well (Cameron et al., 2012). This replacement leads to accumulation of elements such as Sr, Ba and Pb in case of calcium and OH^- is frequently replaced by F^- and Cl^-. Strontium and barium are the most focused elements in trace element studies for dietary reconstructions. Strontium is a non-essential element with no explained biochemical function but is treated by the body in a similar fashion as calcium (Ezzo, 1994). Strontium is concentrated in plants but is filtered out as it progresses up the trophic level (Claassen, 1998). Animals store less strontium in comparison to calcium and at each level in the food chain, the Sr/Ca decreases which is a process referred to as "biopurification" (Burton & Price, 2000). A similar biopurification trend is detected in the ratio between barium and calcium as the former is targeted for elimination along trophic levels, and is utilized to distinguish between marine and terrestrial diets (Bodoriková et al., 2013; Burton & Price, 2000; Claassen, 1998; Corti, Rampazzi, Ravedoni, & Giussani, 2013). Strontium is present in vegetables and cereals, acting as an indicator for carbohydrate consumption. The strontium values reported are in the range of 400-500 ppm for herbivores, 150-400 ppm for omnivores and 100-300 ppm for carnivores (Lazzati et al., 2016). Zinc is an element which is an essential element as it is a part of metallo-enzymes as well as a co-factor in metabolic processes in the body. Zinc is mainly present in animal based food products such as fish, eggs, dairy products, nuts, sea food and meat. Zinc has the reverse trend compared to strontium as it has a range of 90-150 ppm in herbivores, 120-220 ppm in omnivores and 175-250 ppm in carnivores (Buikstra, 1984). Copper, magnesium and vanadium are usually analysed along with other elements as they are probably indicative of specific foods. However, they are highly affected by diagenetic processes (Buikstra, 1984). Lead is usually analysed with the elements and it is used to evaluate postmortem integrity of the remains. It is used as a skeletal preservation marker as it usually leeches into the bone or teeth from the soil (Lazzati et al., 2016).

5.5.1 Trace Elements in Bones, Teeth and Dental Calculus

Teeth and bones undergo remodeling, while the dentine and bone are living tissues and the enamel is just a resistant matrix after its formation (Galiová et al., 2010; Webb et al., 2005). The hypothesis of this study is that dental calculus when not detached is in a dynamic of formation and remodeling in the form of precipitation and incorporation of elements. If the hypothesis is true then the concentrations of trace elements in dental calculus should be the same as that of teeth and bones. Thus, the analysis of dental calculus can reveal the nature of diet involved just as it is analysed by (Scott & Poulson, 2012).

The pitfall of the trace element approach is the interpretation of elements other than strontium and barium. Both strontium and barium belong to the same group as calcium which make them chemically similar to it. This leads to a simple model of biopurification where the elements are non-essential and are being incorporated into the bone. The initial controversy began with the interpretation of zinc in the list throws this disposition of being non-essential. Archaeologist's principle that "you are what you eat" is not as simple as stated. The review by Ezzo in 1994 on the role of zinc as paleodietary indicator listed the criteria for an element to qualify as an indicator paleodiet (Ezzo, 2010). The elements should be free of metabolic control and should be incorporated in the bone with concentrations due to incorporation being higher than that of post-depositional processes (Burton & Price, 2000). These criteria limit the elements to barium and strontium with lead qualifying in some cases. Dental calculus has so far has proven itself to be resilient to diagenetic processes due to its location as well as stratigraphic nature of its formation. The measurement of uranium and rare earth elements aid in understanding the extent of diagenesis as they are not present in living tissues (Burton & Price, 2000).

Trace element studies on dental calculus are very few in number but promising in nature. The potential has been demonstrated by synchrotron radiation multiprobe analysis, inductively coupled plasma mass spectrometry (ICP-MS) and neutron activation analysis (NAA). The earlier studies have not dealt with the association of trace element concentrations with their potential dietary source but recent studies have identified carbohydrates and marine diet from medieval Italy (Capasso et al., 1995; Lazzati et al., 2016; Molokhia & Nixon, 1984). Laser ablation inductively coupled plasma mass spectrometer (LA-ICPMS) seems to be suitable to conduct further studies as it is micro – destructive unlike the liquid mode of ICPMS, preserving it for further analysis and diagenesis can be evaluated by elemental imaging of rare earth elements.

6. Materials and Methods

6.1 Dental Calculus Sampling

From the Phase II of the Church of Santa Maria do Olival necropolis excavations, samples were chosen based on the degree of dental calculus deposited. The higher the degree, the more preference samples were given as it allowed the possibility of carrying out multiple techniques on the same samples. As the study is aimed at establishing standardized protocols for analyzing dental calculus, some techniques were carried out multiple times with varying parameters especially microscopy. A total of 12 human samples and 7 faunal samples were selected and analysed. The dental calculus is sampled from multiple teeth based on availability and if present on multiple teeth then the one with lowest sufficient dental calculus was chosen (Figure 11). Not all the techniques were performed on all calculus due to restrictions on sample availability.

Figure 11. Dental calculus before and after sampling.

Two approaches were taken to remove sediment from the surface of the dental calculus. The first one was to use a DREMEL® diamond coated drill to clean the surface whereas the second approach was to clean the surface with deionized water by utilizing a sterile toothbrush. After duly recording the degree of dental calculus deposition, the tooth (articulated or otherwise) is placed over a clean Whatmann® filter paper such that the calculus deposit to be sampled was facing upwards. The sediment adhering to the deposit is cleaned very carefully by one of the two methods mentioned above.

If it was observed that the sediment was adhering too strongly to clean with the toothbrush, the DREMEL® drill was utilised for cleaning. It was observed that drilling lead to adjacent calculus deposits to dislodge sometimes. In order to detach the dental calculus from the tooth surface, a sterile dental pick was used to gently pry the deposit. The detached fragment of dental calculus was collected on a clean Whatman® filter paper and then stored in a labelled Eppendorf® tube. The

microprobe was rinsed with ethanol and ultrasonicated after each individual was sampled while the Whatman® filter paper was replaced. In case of trace element analysis, a plastic pestle was utilised to dislodge the deposits to avoid contact with the metallic microprobe.

In the Tables 3 and 4, sample number is the archaeological sampling number which is substituted for a sample code representative of the site of origin for the sake of reducing sample naming complexity.

Table 1. List of samples with respective sampled teeth.

	Sample Numbe	Sample Cod	Tooth	Sample Typ	Site
Humans	Modern	E2	PM1 Mand Right	Human	Evora
	14.388	T1	I1 Mand Left	Human	Tomar
	14.420	T2	M3 Max Left	Human	Tomar
	14.72	T3	M1 Max Right	Human	Tomar
	14.271	T4	PM1 Mand Right	Human	Tomar
	16.113	T5	M1, I2 Mand Left	Human	Tomar
	16.255	T6	M3 Max Left	Human	Tomar
	18.100	T7	M3 Max Right	Human	Tomar
	18.212	T8	I1 Max Left	Human	Tomar
	18.3	T9	C Max Right	Human	Tomar
	19.19	T10	I2 Mand Left	Human	Tomar
	19.23	T11	M3 Max Left	Human	Tomar
	20.144	T12	M3 Mand Right	Human	Tomar
	ENT2	E1	I1 Max Right	Human	Evora
Fauna	14.1004F	A1	M1 Mand Right	Bos	Tomar
	14.1348F	A2	M3 Mand Left	Equus	Tomar
	14.1498F	A3	M3 Mand Right	Bos	Tomar
	14.252F	A4	M3 Mand Right	Bos	Tomar
	14.324F	A5	M2 Mand Left	Ovis/Capra	Tomar
	20.1194F	A6	M2 Mand Left	Bos	Tomar

Table 2. List of samples with the techniques applied on them.

	Sample Numbe	Sample Cod	Microscopy(OM+SEM	EA-IRMS	LA-ICPM	Py-GCM	FT-IF
Humans	Modern	E2	◊				◊
	14.388	T1	◊	◊	◊		
	14.420	T2	◊				
	14.72	T3		◊			
	14.271	T4			◊		
	16.113	T5				◊	
	16.255	T6	◊	◊			
	18.100	T7		◊	◊		
	18.212	T8	◊				
	18.3	T9	◊	◊		◊	
	19.19	T10	◊	◊	◊	◊	
	19.23	T11		◊	◊		
	20.144	T12	◊				
	ENT2	E1				◊	
Fauna	14.1004F	A1	◊	◊	◊		◊
	14.1348F	A2		◊	◊		
	14.1498F	A3		◊			
	14.252F	A4		◊			
	14.324F	A5		◊			
	20.1194F	A6		◊	◊		

6.2 Anthropological Information

The bioarchaeological collection of the necropolis of is very vast in terms of quantity. It consists of 1456 ossuaries and 3675 primary inhumations adding up to a total of 6792 minimum number of individuals. The burials were buried in conformation to the Christian funerary ritual, in dorsal decubitus and with orientation of west to east. The skeletons were often noted to be flexed at either at the lumbar or pelvic region and the lower limbs were mostly kept straight. Out of this vast number of recovered remains, fourteen individuals from different excavation areas were selected for this study on the basis of the availability of dental calculus. Five faunal samples were selected as well.

Table 3. List of selected calculus affected individuals.

Sample Number	Sample Code	Sex	Age
Modern	E2	Female	Old
14.388	T1	Male	Mature
14.420	T2	Unknown	Unknown
14.72	T3	Female	Old
14.271	T4	Unknown	Unknown
16.113	T5	Unknown	Unknown
16.255	T6	Male	Mature
18.100	T7	Male	Mature
18.212	T8	Unknown	Unknown
18.3	T9	Female	Unknown
19.19	T10	Male	Mature
19.23	T11	Male	Unknown
20.144	T12	Female	Young
ENT2	E1	Male	Young

Table 4. List of fauna chosen for the study.

Sample Number	Sample Code	Species
14.1004F	A1	Bos
14.1348F	A2	Equus
14.1498F	A3	Bos
14.252F	A4	Bos
14.324F	A5	Ovis/Capra
20.1194F	A6	Bos

6.3 Evaluation and Documentation of Dental Calculus

Documentation of dental calculus in a comprehensive approach is better than a simple "present or absent" approach. Having exclusively the frequency data indicates only the percentage of the population having tartar. The system of indices, proposed by Dobney and Brothwell, implemented in this study is aimed in assisting extraction of dietary information from archaeological calculus. Most of the techniques applied to the study of diet are destructive in nature. Thus it is mandatory to have the relative position of the deposits and also the accurate variation of the profile of dental calculus on the surface of the teeth (Dobney & Brothwell, 1987). The calculus index aids in the estimation of the rate of calculus accumulation, and the variation of the rate of accumulation within the dental arcade and within a sample. Further, it improves the knowledge with respect to the effect of calculus on dental pathologies (Greene, Kuba, & Irish, 2005).

The system consists of two components. The first one is simply a 5 grade scale namely: 0, normal; 1, slight; 2, mild; 3, severe; 4, gross. The method involves accurately gauging the thickness of the calculus deposit on the crown surface for both humans and fauna. The second is a scheme of initially dividing the tooth surface into three horizontal zones: A, B and C where A and B represent the upper and lower halves of the remaining area of the crown and C the region of the tooth below the cemento-enamel junction in case of humans.

	Sample No.																		
HUMAN	Tooth No.																		
	Bucc/Ling.	B	L	B	L	B	L	B	L	B	L	B	L	B	L	B	L	B	L
	Tooth Grade																		
	% Covered	A																	
		B																	
		C																	
		O																	
		M																	
		D																	
Zone Thickness Grades	Zone A																		
	Zone B																		
	Zone C																		

	Sample No.																		
HUMAN	Tooth No.																		
	Bucc/Ling.	B	L	B	L	B	L	B	L	B	L	B	L	B	L	B	L	B	L
	Tooth Grade																		
	% Covered	A																	
		B																	
		C																	
		O																	
		M																	
		D																	
Zone Thickness Grades	Zone A																		
	Zone B																		
	Zone C																		

Figure 12. Dobney-Brothwell Human Calculus Evaluation Proforma.

In case of fauna, the system was devised taking the series of distinctive cusps segregated by in folding and buttressing into consideration. Further, these zones are recorded separately for the occlusal, mesial and distal surfaces in both humans and fauna. The data is collected with the aid of a predesigned proforma which is different for humans and fauna with the human proforma shown in Figure 13. The system is practical and can be employed to quickly document the assessment accurately during the initial stages of research (Dobney & Brothwell, 1987). The system is accompanied by photographing samples recorded such that there is an image associated with each record.

6.4 Fourier Transform - Infrared Spectroscopy

An experimental approach was adapted in analyzing the crystalline structure of the dental calculus as literature cites that it mainly consists of calcium phosphate in various forms. A modern reference sample and a faunal sample (14.1004F) were subjected to ATR-FTIR analysis. Around 3 mg. of dental calculus was ground into fine powder with the aid of an agate mortar and pestle. A spectrometer from Bruker Alpha equipped with a single-reflection diamond ATR module (120 scans, spectral resolution of 4 cm^{-1}, between 4000 cm^{-1} to 375 cm^{-1}) was utilized to acquire infrared spectra. The ATR technique was used as it is convenient to prepare samples and its accuracy is not compromised in comparison to transmission FTIR. Opus/Mentor instrumental control software was used to record and correct the collected spectra for baseline as well as normalization. The infrared splitting factor (IRSF) and relative carbonate content (C/P) was calculated using the peak heights at 565 cm^{-1}, 590 cm^{-1} , 605 cm^{-1} 1415 cm^{-1} -1035 cm^{-1} (Weiner & Bar-Yosef, 1990).

$$\textbf{IRSF = (565ht+605ht)/590valley} \quad (3)$$

$$\textbf{C/P = 1415ht/1035ht} \quad (4)$$

$$\textbf{Mean Crystal Length (nm) = (IRSF-0.822)/0.048} \quad (5)$$

The equation given above allows the measurement of C/P ratio by dividing the carbonate peak at 1415 cm^{-1} by the phosphate peak at 1035 cm^{-1} which are independent of the peak splitting at 565 cm^{-1} and 605 cm^{-1} (Wright and Schwarz, 1996; Beasley et al., 2014).

The infrared splitting factor is mainly useful to calculate the mean crystal length to understand the crystallinity, which reflects the growth of crystals and the loss of smaller crystals (Weiner & Bar-

Yosef, 1990). This equation was developed for bones but has been used for dental calculus in this case.

6.5 Demineralisation and Extraction of Microparticles

Dental calculus being a mineralized deposition with a potential to act as a cornucopia of debris which enters the oral cavity. However, to extract the debris and characterize them, it is essential to separate the trapped material and the encasing mineral matrix. The procedure to separate the trapped debris and mineral matrix can be done either mechanically or by employing chemical agents. Dental calculus being a novel approach in studying the past populations, it has no standard protocol as of now. In this thesis one of the major goals is surveying various published methodologies and evaluating the efficiency of recovery along with ease of performing the extraction.

A majority of the protocols utilize chemical agents to decalcify the matrix to liberate the trapped microparticles. The most common agent is HCl which has been used in varying concentrations to decalcify. In some protocols, weak and cold HCl has also been proposed in order to prevent damage from the acid to the liberated microparticles (Buckley et al., 2014; Hardy et al., 2009, 2012; Tromp & Dudgeon, 2015; C. Warinner, Speller, et al., 2014). The most common methods use 5-10% but one instance of 20% has also been reported by Lazzati et al., 2016 (Blatt et al., 2011; Cummings, Yost, & So, 2016; Henry & Piperno, 2008; Horrocks et al., 2014; Leonard, Vashro, O'Connell, & Henry, 2015; Power, Salazar-García, Straus, González Morales, & Henry, 2015; Wesolowski, Ferraz Mendonça de Souza, Reinhard, & Ceccantini, 2010). The other popular reagent of decalcification is ethylene diamine tetra-acetic acid (EDTA) which has been used in ancient DNA (aDNA) studies as well as microparticle studies (Tromp et al., 2017; Warinner et al., 2014). Very few methods have not utilized any decalcification method but resorted to mechanical separation by grinding or crushing (Piperno & Dillehay, 2008; Power et al., 2014; Wang et al., 2016; Zhang et al., 2017). However, the results of decalcification have shown to be superior as there is not fragments from the calcium phosphate matrix obscuring the observation attempts to identify microparticles.

In the study, 5 methods have been chosen based on their representation of the wide variety of methods reported. They are presented in Table 5 below.

Table 5. Selected Protocols for Optical Microscopy Investigation.

Serial Number	Technique	Reagent	Concentration	Volume	Time	Washes	Additional
1	Hardy et al., 2016	HCl	2%	1.5 ml	15 mins	3, 13000 rpm for 15 mins	50% Glycerol Optical Microscopy (OM)
2	Lazzati et al., 2016	HCl	20%	1.5 ml	6-8 hours	3	Ultrasonification Dry at 70^0C SEM + OM
3	Dudgeon et al., 2012	HCl	21.9% (6N)	1 ml	48 hours	2	1.25 ml Calgon Vortex 24 hours 16000 rpm Rinse 3 times
4	Tromp et al., 2017	EDTA	17%	1 ml	30 mins – 1 week	3, 13000 rpm for 15 mins	----------
5	Power et al., 2015	Glycerin	25%	25 µL	1-3 hours	2000g for 10 mins	Positive pressure fume hood

1) **Hardy et al., 2016** – The dental calculus samples were placed in 2 ml. Eppendorf® tubes into which a volume of 1.5 ml. 2% HCl was added. The tubes were left undisturbed for 15 minutes. The tubes were then centrifuged at 13,000 rpm for 15 minutes and rinsed 3 times with deionized water. After the third rinse, 50% glycerol is added to the tubes before mounting it on a slide and observing it on the optical microscope.
2) **Lazzati et al., 2016 –** The dental calculus samples were placed in 2 ml. Eppendorf® tubes into which a volume of 1.25 ml. 20% HCl was added. The tubes were left undisturbed for 6 to 8 hours. The tubes were ultrasonicated for 20 minutes with no heating. The tubes were then rinsed 3 times with deionized water. The pellet was dried at 70 ^{0}C and then observed in both scanning electron microscope and optical microscopy.
3) **Dudgeon et al., 2016** – The dental calculus samples were placed in 1.5 ml. Eppendorf® tubes into which a volume of 1 ml. Calgon was added. The tubes were centrifuged and decanted after a brief period of rest and 1ml. of 21.9% HCl was added. The tubes were left

undisturbed for 48 hours. The tubes were then centrifuged at 16,000 rpm and rinsed 3 times with deionized water.

4) **Tromp et al., 2017 -** The dental calculus samples were placed in 1.5 ml. Eppendorf® tubes into which a volume of 1 ml. 17% EDTA was added. The tubes were left undisturbed for 30 minutes to 1 week depending on the complete demineralisation of the calcium phosphate matrix. The tubes were then centrifuged at 13,000 rpm for 15 minutes and rinsed 3 times with deionized water.
5) **Power et al., 2015 -** The dental calculus samples were crushed in sterile Eppendorf® tubes with a micropestle with 25 µl of glycerine to prevent loss of material and left for 1 to 3 hours. The samples were then centrifuged at 2000g for 10 minutes before mounting on to a slide. All the steps are carried out under a positive pressure hood.

Scanning electron microscopy was performed on four samples (T1, T2,T4 and T6) which have already been examined using optical microscopy. VP-SEM-EDS HITACHI 3700N SEM was used along with a detector for secondary electrons, an annular detector for backscattered electrons and an X-ray spectrometer BRUKER Xflash 5010SDD detector. Prior to the analysis, samples were sputter-coated with carbon.

6.6 Elemental Analysis – Isotopic Ratio Mass Spectrometry

The analysis of dental calculus to measure the isotopic ratios of carbon and nitrogen using the EA-IRMS involved two separate measurements, one for the organic fraction and the other for the bulk composition. In case of the bulk analysis, approximately 7 mg of dental calculus was weighed in combustible tin capsules. For the organic fraction, the protocol of Price et al., (2018) was used where approximately 7 mg was put in pre-weighed silver capsules (Price et al., 2018). With the aid of a micro-pipette, up to 60 µL 1M HCl was added slowly to liberate CO_2 from the carbonate of the apatite. The samples are left overnight to dry with an addition of another 60 µL of 1M HCl was added until no bubbling was observed under a stereo-microscope. These silver capsules were inserted in to tin capsules to increase burn intensity. These tin capsules of both bulk and organic fractions were folded and then loaded into the machine where they were combusted to form CO_2 and N_2 in an elemental analyser (EA Flash 2000 HT, Thermo Fisher Scientific®) in presence of oxygen, with pure helium acting as a carrier gas. The capsules were fed in a specific sequence in to the EA with blank capsules for monitoring the background and contamination checks. In the sequence were also international reference materials with standardized carbon and nitrogen

isotopic composition. These standards are mentioned below in Table 6. These standards are used for calibration of both carbon and nitrogen compositions as well as their isotopic ratios. However, the in-house nitrogen standards are in range for measuring the nitrogen composition accurately. The isotopic ratios were obtained on a Delta V Advantage Isotope Ratio Mass spectrometer (Thermo Fisher Scientific®).

Table 6. Standards utilised for measuring isotopic ratios of dental calculus.

Standard	Type	$\delta^{13}C$ (%)	$\delta^{18}O$ (%)	$\delta^{15}N$ (%)
CO8	International	-5.755	-22.685	----
L-SVEC	International	-46.499	-26.500	----
CICL (CO8)	Internal	-0.372	-9.334	----
CSPC (NBS19)	Internal	-28.690	-14.869	----
IAEA-N-1	International	----	----	+0.4
IAEA-N-2	International	----	----	+20.3

6.7 LA – ICP – MS Analysis

Trace element analysis was carried out using an Agilent 8800 ICP-MS Trip Quad instrument hyphenated to a Teledyne Systems CETAC® LSX – 213 G^{2+} laser ablation unit. The dental calculus samples were placed on double sided carbon tape with the aid of a pair of tweezers whose tips were Teflon® coated. The surface of the dental calculus adhering to the tooth was placed facing upwards to avoid any contamination from the soil. Using the real time video monitoring system, the stage was oriented to find the area of the dental calculus which was relatively flat. The instrument was calibrated using an NIST SRM 610 international glass standard reference prior to every analysis. Elemental fractionation was overseen using the $^{238}U/^{232}Th$ (≅ 102%) and the formation of oxides was gauged using the $^{248}ThO/^{232}Th$ (<0.15%) ratio. A different standard reference material, NIST SRM 612 was used in the analysis to correct for instrumental drift, to check for variations in certified values and to compare the ablation efficiency when the parameters are altered (Cameron et al., 2007; Dolphin et al., 2013; Galiová et al., 2010; Randall, 2016). The process is not completely foolproof as the 213 nm laser based ablation is matrix dependent and the ablation parameters are not perfectly matrix – matched. For each dental calculus sample, 4 spots were chosen to ablate on a relatively flat surface. In the beginning and the end of the analysis, 3

spots of NIST SRM 612 were ablated to monitor the ablation as well as quantify the target elements. The identification of flat area was rather difficult as dental calculus samples tend to be curved due to the conformation to the curvature of the tooth surface. Five human and three faunal samples were selected for shot analysis. One of the samples was used as a test sample to determine the optimal ablation conditions as the dental calculus is a novel material. ^{43}Ca was used as an internal standard with a stoichiometric value of 38% for hydroxyapatite to calculate the concentration of the analyte elements. The laser ablation parameters were (Table 7):

Table 7. Ablation parameters of dental calculus.

Spot Size	**100 µm**
Laser Energy	100%
Shot Frequency	20 Hz
Shutter Delay	10 secs
Burst Count	600

GLITTER® software was used to pre - process the data and reduce the data while correcting it for instrumental drifts. It was then used to calculate the concentrations of the analytes (in ppm) by using the NIST 612 as the certified reference material. Quantitative data was obtained based on the analysis of the following isotopes: Li^{7}, Na^{23}, Mg^{24}, Al^{27}, P^{31}, K^{39}, Ca^{43}, Ca^{44}, V^{51}, Cr^{52}, Mn^{55}, Fe^{57}, Co^{59}, Ni^{60}, Cu^{63}, Zn^{66}, As^{75}, Rb^{85}, Sr^{88}, Cd^{111}, Ba^{137}, Pb^{208}, Bi^{209}, U^{238}. The concentrations obtained for each sample were represented by 4 spots which were averaged to get a mean value representative of the sample.

6.8 Pyrolysis – Gas Chromatography – Mass Spectrometry

Organic residue was analysed by the technique of Py – GC – MS with a Frontier Lab PY-3030D double-shot pyrolyser coupled to a Shimadzu GC2010 gas chromatographer, also coupled to a Shimadzu GCMS-QP2010 Plus mass spectrometer. The interface between the furnace and the chromatograph was maintained at a temperature of 280 ºC. The separation was carried out using a capillary column Phenomenex Zebron-ZB-5HT (30 m length, 0.25 mm internal diameter, 0.50 µm film thickness) while helium was used as carrier gas with a flow rate of 1.5 mL min^{-1}.

The dental calculus samples chosen for Py-GC-MS analysis were placed in well labelled sterile glass tubes prior to analysis. A total of 4 individuals were chosen to be analysed for organic residue of dental calculus, out of which 3 individuals were from the necropolis of Santa Maria do Olival whereas 1 individual (E1) was from the Museum of Evora. Samples which were cleaned prior to analysis (T9) using a sterile Dremel® diamond coated drill to remove adhering sediment while the calculus deposit was still attached to the tooth.

After removing all the visible sediment, the samples were pried from the tooth using a microprobe and placed in a sterile glass tube. In case of unclean samples, the calculus deposit was pried with a microprobe and placed in a sterile glass tube. In addition to the dental calculus samples, an alkane mixture standard containing alkanes from C7 to C40 were pyrolysed in same instrumental conditions to have known retention times for n-alkanes and n-1 alkenes. The samples were then placed in a low mass 50 µL Ecocup® capsule and subsequently placed into the microfurnace using an Eco-stick®. The capsules were placed one at a time in the furnace – chromatograph interface, followed by a 2 minute helium purge. GC temperature programmed as follows: 40 ºC during 5 min, ramp until 300 ºC at 5 ºC min^{-1}, and then an isothermal period of 3 min. Source temperature was programmed to be at 240 ºC, and the interface temperature was regulated at 280 ºC. The mass spectrometer was set to acquire data between 40 and 850 m/z.

Table 8. Parameters of pyrolysis of dental human dental calculi.

Sample Code	Sample Weight	Clean/Unclean	Pyrolysis Method	Derivatisation
T9	2.080 mg	Clean	500 ^{0}C for 12 seconds	None
T9	2.080 mg	Clean	600 ^{0}C for 12 seconds	None
T9	3.191 mg	Unclean	600 ^{0}C for 12 seconds	None
T5.1b	Unclean	Unclean	600 ^{0}C for 12 seconds	None
T5.1l	3.443 mg	Unclean	600 ^{0}C for 12 seconds	None
T5.1m	1.204 mg	Unclean	600 ^{0}C for 12 seconds	None
T5.1d	3.737 mg	Unclean	600 ^{0}C for 12 seconds	None
T5.2	1.051 mg	Unclean	600 ^{0}C for 12 seconds	None
T5.TMAH	3.684 mg	Unclean	600 ^{0}C for 12 seconds	5 µL TMAH 2.5% in MeOH
T10	14.031 mg	Unclean	600 ^{0}C for 12 seconds	None
E1	2.274 mg	Unclean	600 ^{0}C for 12 seconds	None
Alkanes Standard	Alkane mixture	---------	No pyrolysis	---------

7. Results and Discussion

7.1 Structure of the calculus matrix

Fourier Transform – Infrared Spectroscopy was performed on E2, a modern dental calculus from Evora and A1 (see Appendix I) which is an archaeological faunal sample from Tomar. The primary aim of the study was to understand the chemical and crystal nature of the mineral matrix of the dental calculus. The spectra of both the samples are quite similar for the modern and the archaeological samples. Infrared splitting factor (IRSF), relative carbonate content (C/P), and mean crystal length (MCL), usually applied for bone mineral, were calculated and shown in Table 9 to estimate to the preservation state of the samples. Though the samples are not comparable to bones in terms of IRSF, C/P, and MCL due to the fundamental process of formation. Bone is formed through a systematic biomolecular process whereas dental calculus is formed as a precipitation of calcium phosphate. The crystal structure of dental calculus also seems to be mainly composed of hydroxyapatite but literature suggests the presence of whitlockite, octocalcium phosphate and brushite (Hayashizaki et al., 2008). The presence of ATR units at wavenumbers 600, 560 and 1021 cm^{-1} are confirmation for the presence of phosphate group. The carbonate group is confirmed by the presence of peaks at 1465, 1475, 861, and 869 cm^{-1} (Figure 13). The absorption bands of the carbonate ion in apatite matrix is different from those exhibited by the CO_3^{2-} of calcium carbonate (Le Geros, 2015).

Table 9. IRSF, C/P and MCL values of E2 and A1 samples.

Sample Code	Species	Context	IRSF	C/P	MCL (nm)
E2	Human	Modern	4.260	0.057	71.642
A1	Bos	Archaeological	4.034	0.124	66.925

The values of various calculated parameters are presented in Table 9. The IRSF values of the dental calculus are <5, indicating that the crystal are moderately sized with a regularly organized lattice structure of apatite (Beasley et al., 2014). The organic content of the bone is collagen with a smaller fraction of other proteins. In the case of dental calculus, the organic fraction is an assortment of biomolecules including lipids, proteins and sugars. Thus, the quantitative estimation of any one class of biomolecule is not easily achieved by non – destructive methods like FT-IR. The relative carbonate content is used to estimate the secondary calcite in the apatite matrix (Dal Sasso et al.,

2016) or the loss of carbonate during the burial, with modern reference bones having values between 0.23 and 0.34 (Beasley et al., 2014). Any values which are elevated or depleted are indicative of diagenetic alteration. But the presence of carbonate ions are integral components of the apatite structure (Le Geros, 2015). The mean crystal length is 71.642 nm and 66.925 nm for E2 and A1 respectively. The crystal length of calculus if compared with the values of bones, the

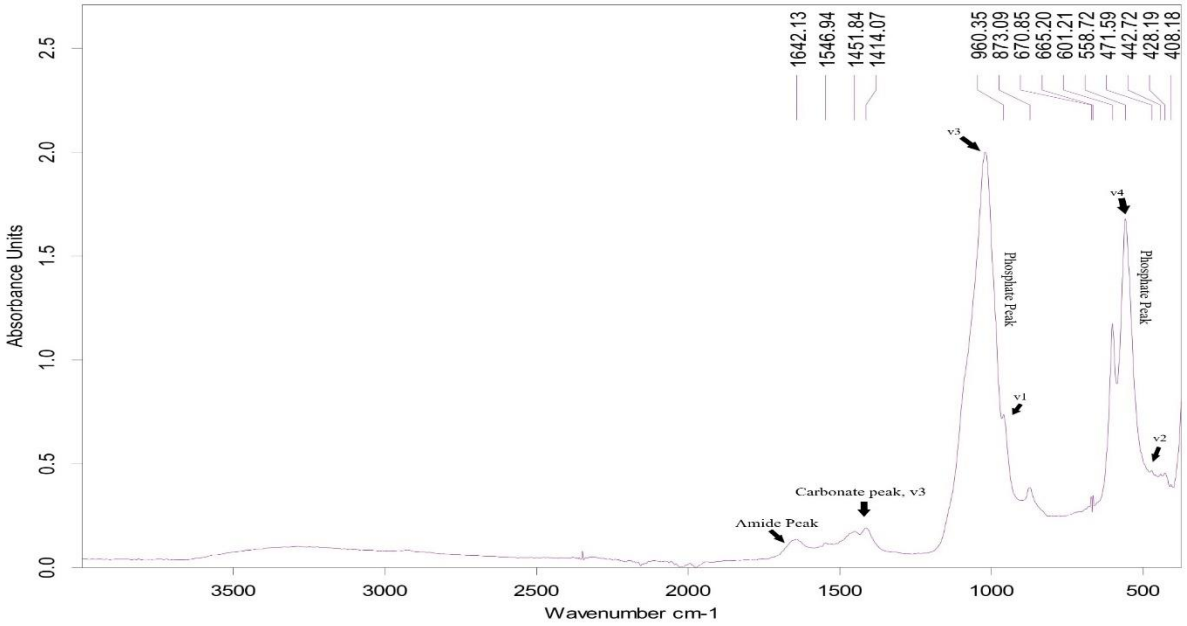

Figure 13. Infrared Spectra of dental calculus from individual E2.

former appears to be diagenetically altered. Trace element analysis for uranium and rare earth elements concentrations can further clarify the diagenetic alteration of the calculus samples. Also, the major hindrance in dental calculus studies is the lack of values for diagenetically unaffected calculus samples.

7.2 Micro-Debris

A modified Hardy et al., 2016 protocol was utilised which showed the best results where the small quantity of recovered biogenic silica was not obscured by any geological sediment. A 0.1% HCl solution was used to remove the sediment adhered to the sample by letting the samples rest for half an hour in Eppendorf® tubes. The tubes were then vortexed and rinsed quickly with deionized water. The sediment free dental calculus samples were then suspended in 2% HCl for 15 minutes. The samples were then rinsed three times at 13,000 rpm for 15 minutes and glycerol was added before observing under a microscope.

Micro-debris were primarily investigated through the use of optical microscopy and scanning electron microscopy. Since archaeological dental calculus are present in little amounts, series of tests were made on E2 which is an early 19th century sample from Evora. The collected calculus from E2 was divided into 2 samples of 0.055 grams each to suffice carrying out all the protocols which were chosen for the study as mentioned in the methods section.

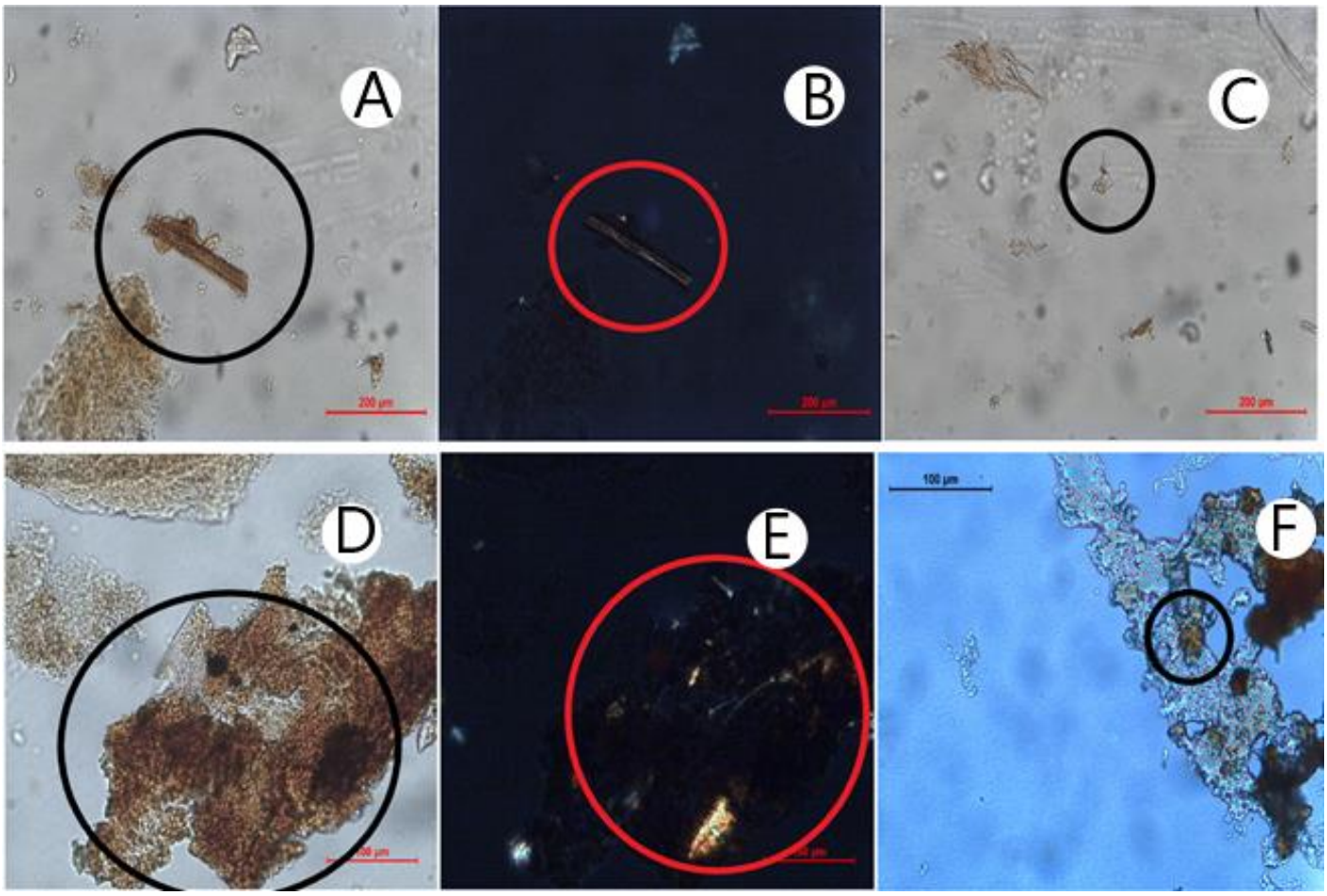

Figure 14. Micro-debris from modern sample E2 where biogenic silica (A), biogenic silica in cross polar (B), Rondel shaped phytolith (C), Brown coloured substance and the same in cross polar field (D & E) and a starch grain (F) using Hardy et al. (2016).

The samples were mostly analysed using optical microscope equipped with cross – polarising filter. The cross – polarising filter was used to confirm the identity of suspected starch grains on the slide (Hardy et al., 2016). The protocol of Hardy et al., (2016) was processed first and some of the results are shown in figure 14. The modern sample is filled with a brown coloured substance which is suspected to be organic matter. This brown coloured substance is a hindrance to the process of recording biogenic silica and starch grains. This can be observed in the Figure 14 in section A partially and completely in D. In section F of figure 14 it can be observed that a starch

grain is obstructed from clear viewing by the brown organic substance. But the maltese cross of the grain can be clearly viewed in panel F of Figure 14. Some biogenic silica are observed in Panel A, B, C, D and E of Figure 14 but they are too obscured to be attributed to any plant family or species. The one shown in section C of Figure 14 is suspected to be a rondel form phytolith belonging to the Poaceae family.

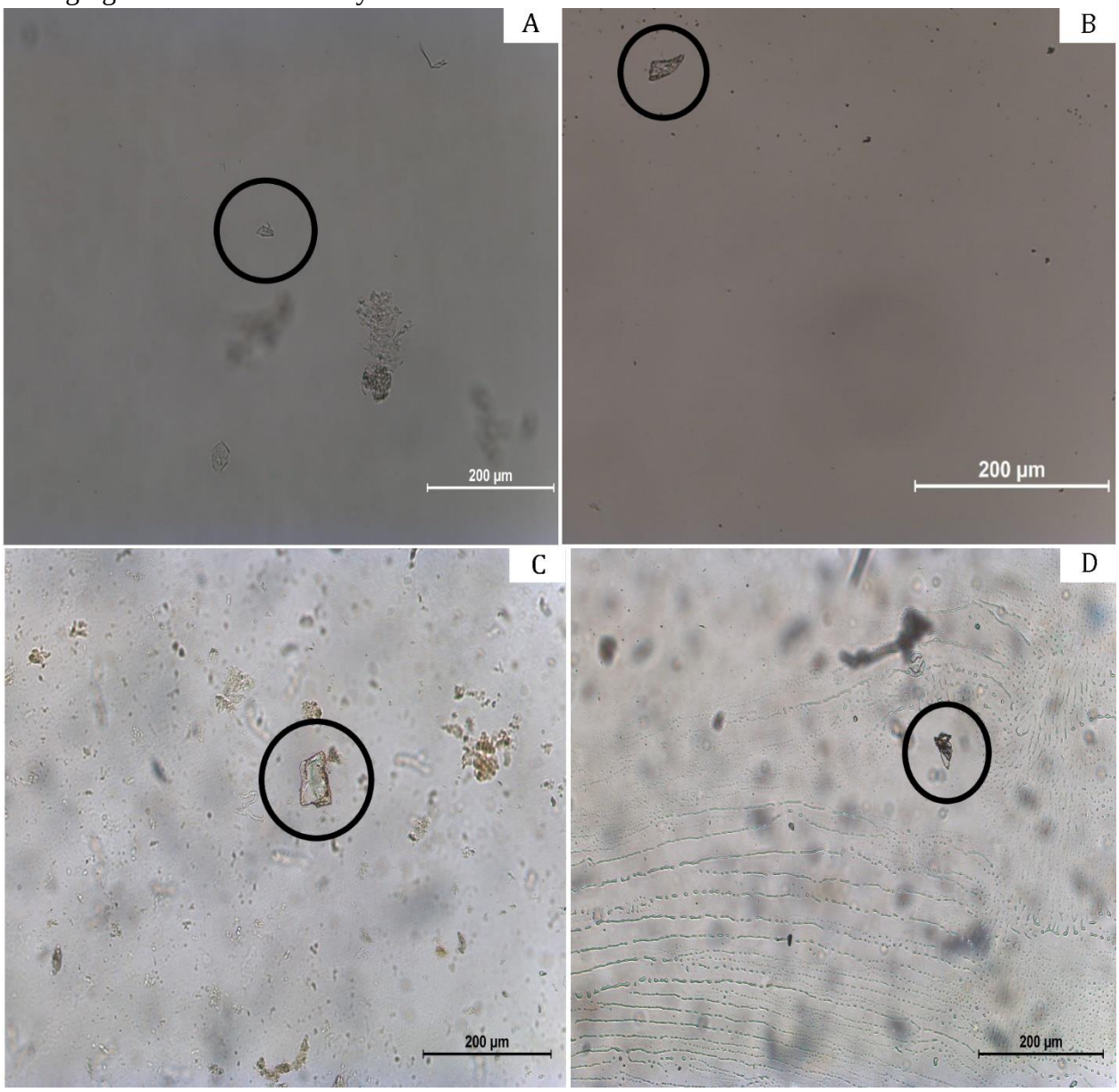

Figure 15. Modern human sample E2 analysed using protocols of Dudgeon et al., (2012) (A), Lazzati et al., (2016) (B), Tromp et al., (2017) (C) and Power et al., (2015) (D).

The next protocol to be tested was based on Dudgeon et al., (2012) (see section A – Figure 15). Section A contains a rondel shaped phytolith. Section B of Figure 15 represents results obtained from Lazzati et al., (2016) and shows a corroded morphotype. Tromp et al., (2017) who used

EDTA for demineralisation is shown in section C. The biogenic silica in section C of the same figure is block morphotype. Finally, Power et al., (2015) protocol is represented by section D. The biogenic silica in section D is cuneiform bulliform.

Of all the techniques chosen for this study, Hardy et al., (2016) was decided to be the most suitable. This is because it utilises the least concentrated HCl (2%) allowing the recovery of starch grains easily as well as for the fact that it takes the least amount of time for preparation (15 minutes). One of the major issues, encountered in the lab is the aerial particulate material which settles on the slides while examining. Aerial particulate material in general contains fibers, diatomaceous matter and other miscellaneous particulates (Tromp & Dudgeon, 2015). One of the most common particulates in the lab includes banded and blue coloured fibers as shown in Figure 16.

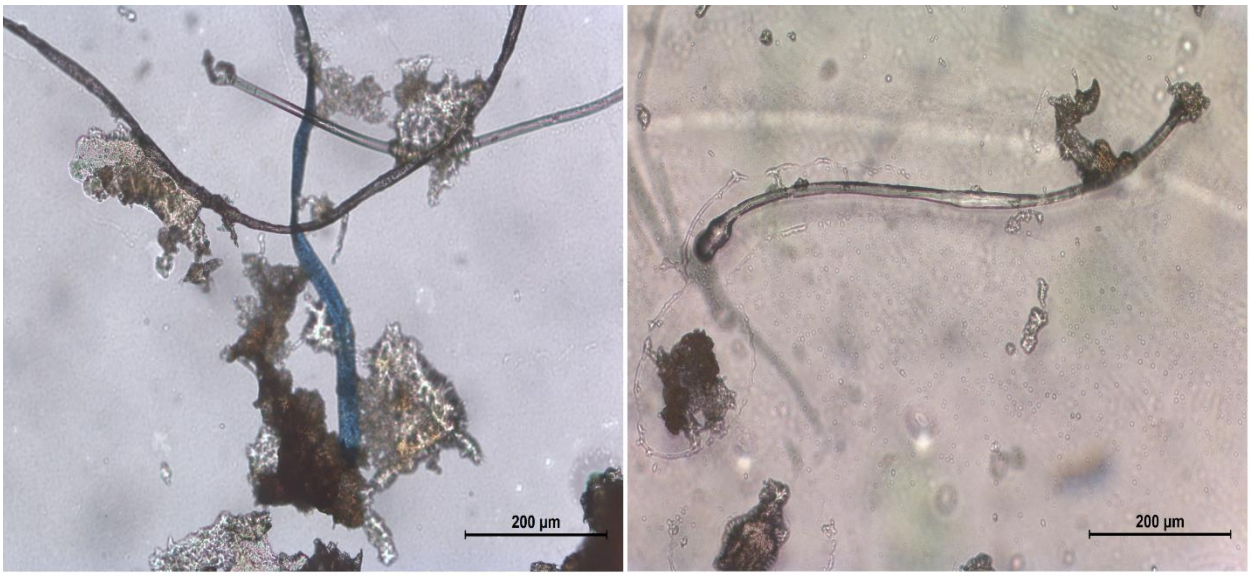

Figure 16. Aerial particulate material in the laboratory.

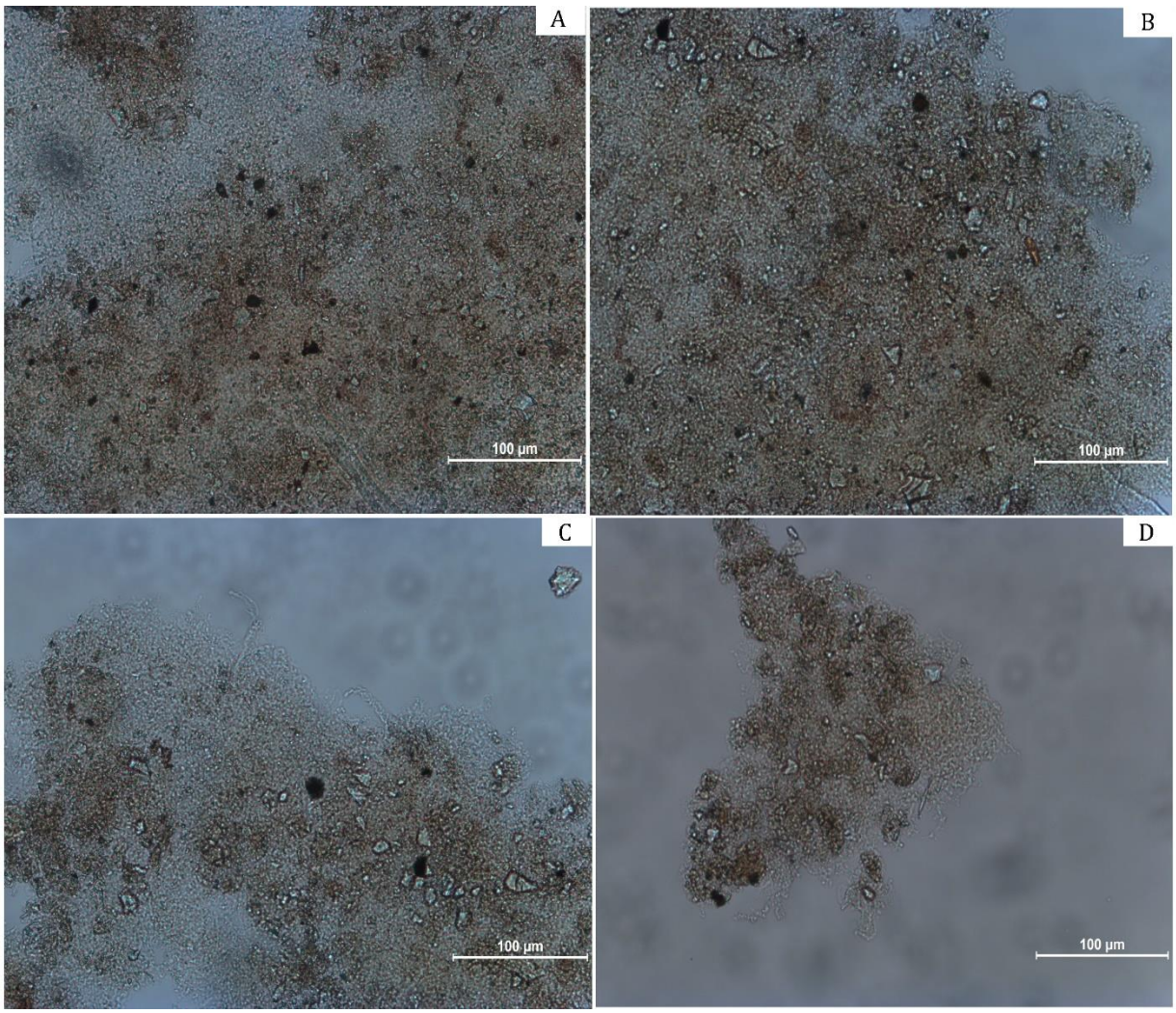

Figure 17. Faunal sample investigated using Hardy et al., (2016) protocol.

The second phase of studies involved the faunal calculus from sample A1 to test the protocol of Hardy et al., (2016) to check its efficiency of microparticle extraction on archaeological material. Sample A1 was chosen for this as it has acute dental calculus deposits of grade 4 (see Appendix I). Figure 17 shows that it calculus extracted from sample A1 yields different kinds of phytoliths from Poaceae family such as cuneiform bulliform, rondel, trapeziform polylobate, corroded morphotype, and paralelepipedal sinuate bulliform cells. However, no intact silica skeletons or starches were recovered which denies the possibility of elucidating the identity of the plants involved in diet of this cow.

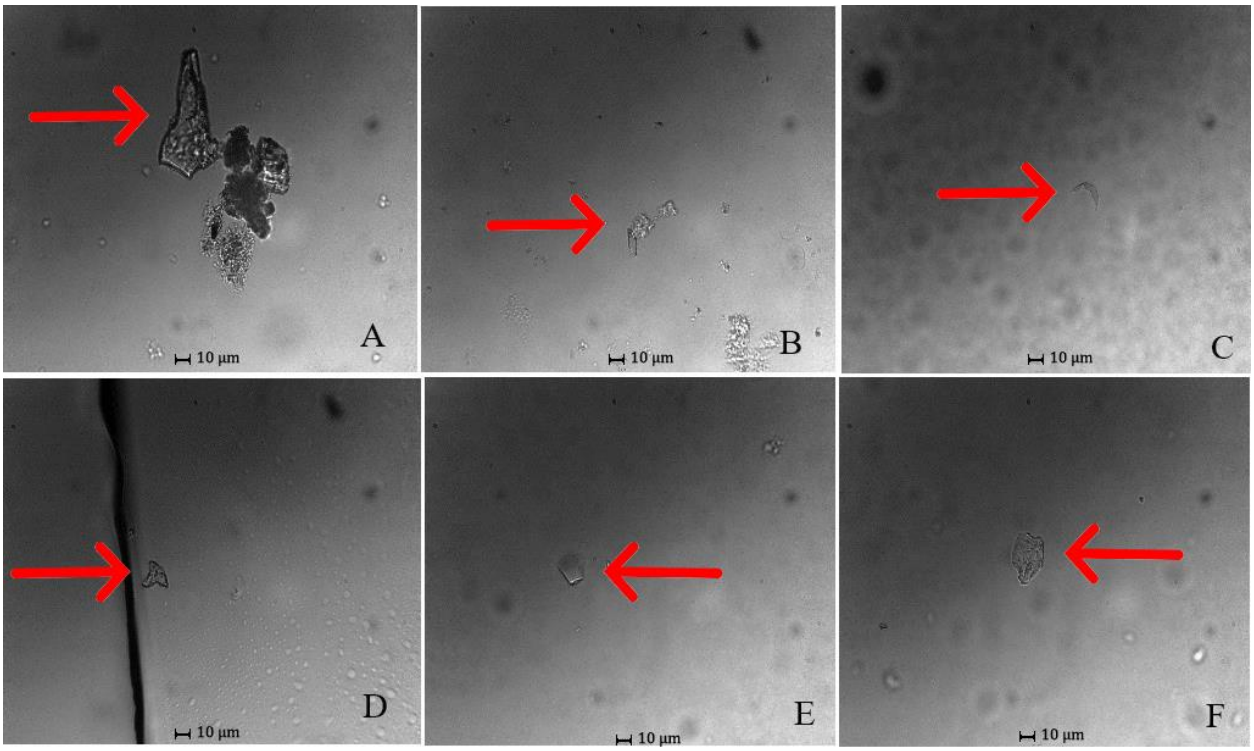

Figure 18. Phytoliths from human archaeological dental calculus sample T2 from medieval Tomar.

The microscopic analysis of dental calculus from human samples from medieval Tomar also had similar results to that of the faunal sample A1. The Figure 18 shows the recovered biogenic silica from the individual T2.

The phytoliths recovered are mainly cuneiform, acicular hair cells, phytoliths from wood, rondel, saddle type, and scutiform – bulliform. These phytoliths are characteristic of Poaceae family and

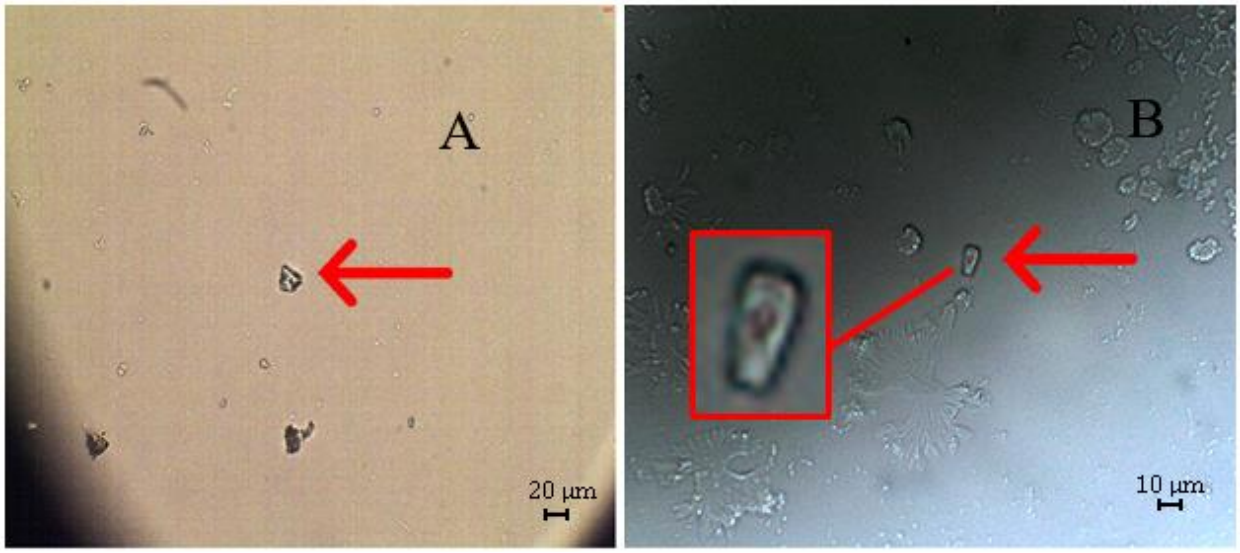

Figure 19. Phytoliths from individual T6.

might be originating from a wide variety of dietary plants mainly from cereal family such as barley, millet, and rice.

In Figure 19, section A is from individual T6, showing a trapeziform phytolith and section B is showing a saddle type phytolith. Another 3 individuals were analysed and they did not yield any results. One of the main issues of identifying the phytoliths and attributing them to a specific plant is the lack of phytolith reference database in the laboratory. The types of phytoliths are rather limited and occur in most genuses. What makes them unique is the combination of occurrence which is family specific. Also the non-availability of heavy liquids for separating sediment from the biogenic silica made the analysis rather cumbersome (Madella et al., 1998).

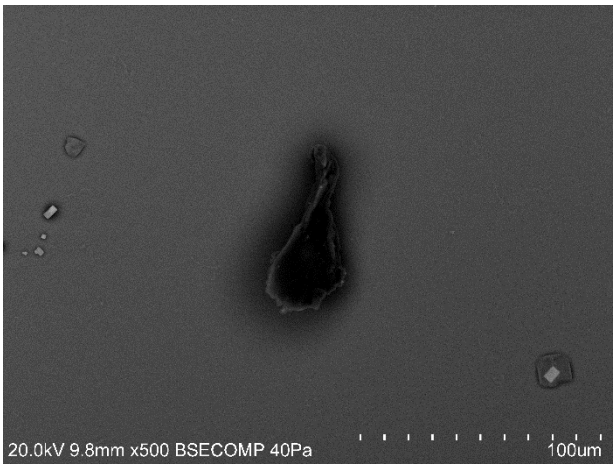

Figure 20. A cuneiform bulliform phytolith observed under SEM from individual T2.

Scanning electron analysis was carried out on four samples but only one sample (T2) is presented. This was done to test the potential of the technique and one of the few observed biogenic silica is presented in figure 20 which is a cuneiform type characteristic of Poaceae family. It was rather difficult to carry out as microscopy slides are made from silica, the same material as phytoliths. From published literature it was discovered that borosilicate slides are effective in this aspect (Dudgeon & Tromp, 2014; Tromp, 2012). Also the sample needs to devoid of any coverslip which makes it suffer aerial particulate contamination. These factors limited the possibility of carrying out more examination of more samples using SEM but other researchers seem to have some amount of success (Dudgeon & Tromp, 2014; Lazzati et al., 2016; Power et al., 2014). The phytoliths observed under the SEM are characteristic of Poaceae family as is in the case of optical microscopy.

7.3 Carbon and Nitrogen Stable Isotopes in Calculus and Collagen

The study's primary focus is to identify the potential of dental calculus as a replacement and/or complement for bones and teeth as paleodietary proxies. It has already been established that stable isotope ratios of dental calculus are not the same as those obtained from both bones and teeth (Salazar-garcía et al., 2014; Scott & Poulson, 2012). However, Scott & Poulson, in 2012 demonstrated for the first time that isotope ratios from dental calculus could be interpreted in a similar pattern to isotope ratio from bones. Their conclusions while comparing data from dental calculus with published isotope values of medieval European bones were that even if the absolute values of calculus and bones differ, the trend remains the same (Scott & Poulson, 2012). The initial sample size in this study consists of 3 humans and 2 faunal samples. This is a pilot examination to verify if we can get reliable results, where the organic fraction of the dental calculus was examined in order to compare it to data obtained from collagen.

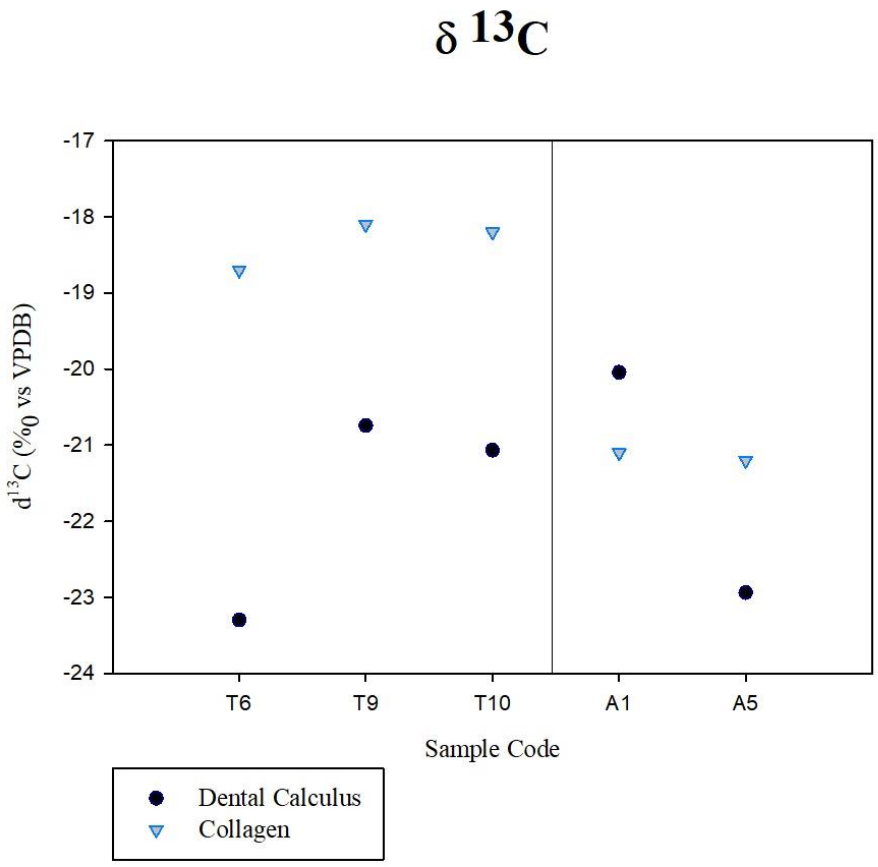

Figure 21. $\delta^{13}C$ values of dental calculus and bone collagen comparison. Faunal bone collagen values are represented by the mean values (Curto et al., 2018) of their respective species.

The $\delta^{13}C$ values of the organic fraction of the dental calculus in comparison to those from collagen are illustrated in Figure 21. The values of human calculi range between -20.7% and -23.3% while the fauna had values of -20‰ (A1) and -22.9‰ (A5) for their respective species of Bos and Ovis/Capra. These values are generally more negative than the values from bone collagen. In the case of faunal samples, isotopic values from collagen is higher in the case of A5 whereas A1 exhibits the same trend as humans. Curto et al., (2018) reported $\delta^{13}C$ values of bone collagen for humans as -19.4‰ and -17.3‰ whereas fauna had between -21.3‰ and -20.1‰. This was interpreted that the diet was primarily C_3 plant consumption for both herbivores and humans. Human collagen showed slight enrichment due to aquatic protein intake rather than consumption of C_4 plants (Chisholm et al., 1982; Curto et al., 2018). This was based on the findings of oyster and cockles shells at the excavation areas. The $\delta^{13}C$ values from dental calculus appear to be from individuals consuming C_3 plants but slight enrichment cannot be really commented upon due to limited sample size and lack of standard value ranges for dental calculus. And the results are in

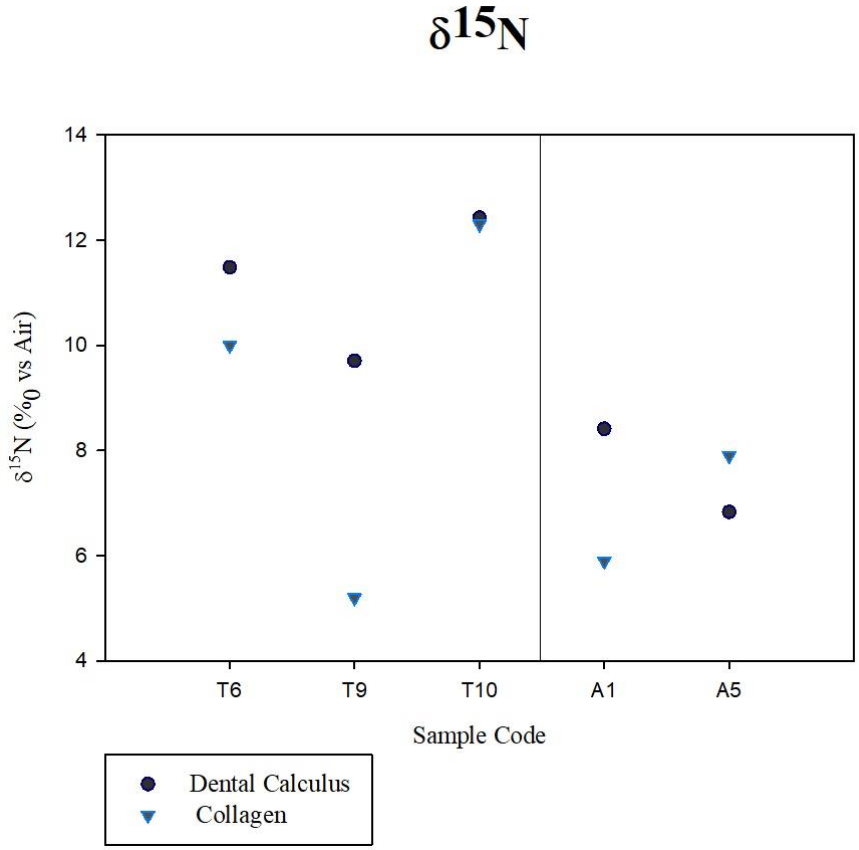

Figure 22. $\delta^{15}N$ values of dental calculus and bone collagen. Faunal bone collagen values are represented by the mean values of their respective species of Bos and Ovis/Capra.

agreement with conclusions from published literature that the carbon isotope ratio values of dental calculus are different from the values obtained from bones.

The $\delta^{15}N$ values of the calculus organic fraction in comparison with those obtained from bone collagen are shown in Figure 22. The values of human calculi range between 9.7‰ and 12.4‰ with fauna having values of 6.8‰ (A1) and 8.4‰ (A5). The $\delta^{15}N$ values from organic fraction of dental calculus are higher than those from bone collagen except in one case. The reported $\delta^{15}N$ value range from bone collagen for humans is 9.0‰ to 12.5‰ and for fauna is 4.8‰ to 7.8‰ (Curto et al., 2018). One of the samples (T10) has almost the same values with a variation of just 0.1‰. The elevation of the values between organic fraction of calculus and bone collagen can be explained by the presence of bacterial compounds and other dietary components which have not undergone metabolic fractionation processes. The difference in the human $\delta^{15}N$ values can be explained by trophic increment.

The main issue with the reliable interpretation of isotopic values from dental calculus is due to the non-availability of the specific range of values for C_3 consumers and C_4 consumers. The problem with comparing the isotopic values of dental calculus with those from bone collagen is that the values obtained from the latter are post metabolic fractionation processes. The organic content of dental calculus is not subjected to these processes but result from a summation of the dietary entrapped components. Carbon and nitrogen analysis on bone and dentine collagen exhibit no correlation with that of bulk dental calculus (Salazar-garcía et al., 2014) but it has been shown recently that the inorganic fraction of the dental calculus shows strong correlation with the inorganic fraction of the bone (Price et al., 2018).

7.4 Trace Element Analysis using LA – ICP – MS

Dental calculus is made of calcium phosphate matrix. The ratio between the concentrations of calcium and phosphorus (Ca/P) can be utilised to check the preservation condition of the crystal structure of the bone mineral. The range of Ca/P values for dentine is between 2.1 and 2.2 whereas for enamel, values range between 1.91 and 2.17 (Hillson, 1979). As shown in Figure 23, the Ca/P ratios of the study are between 1.80 and 2.94 which are slightly outside the accepted range for both dentine and enamel, attributing this to the difference in formation process. Though dental calculus is shielded better than bones from diagenesis due to its location in the human body, they can still be affected by burial conditions (Radini et al., 2017). Sample T10 has very low Ca/P value compared to other samples which indicates phosphorus enrichment and is attributed to diagenetic alteration.

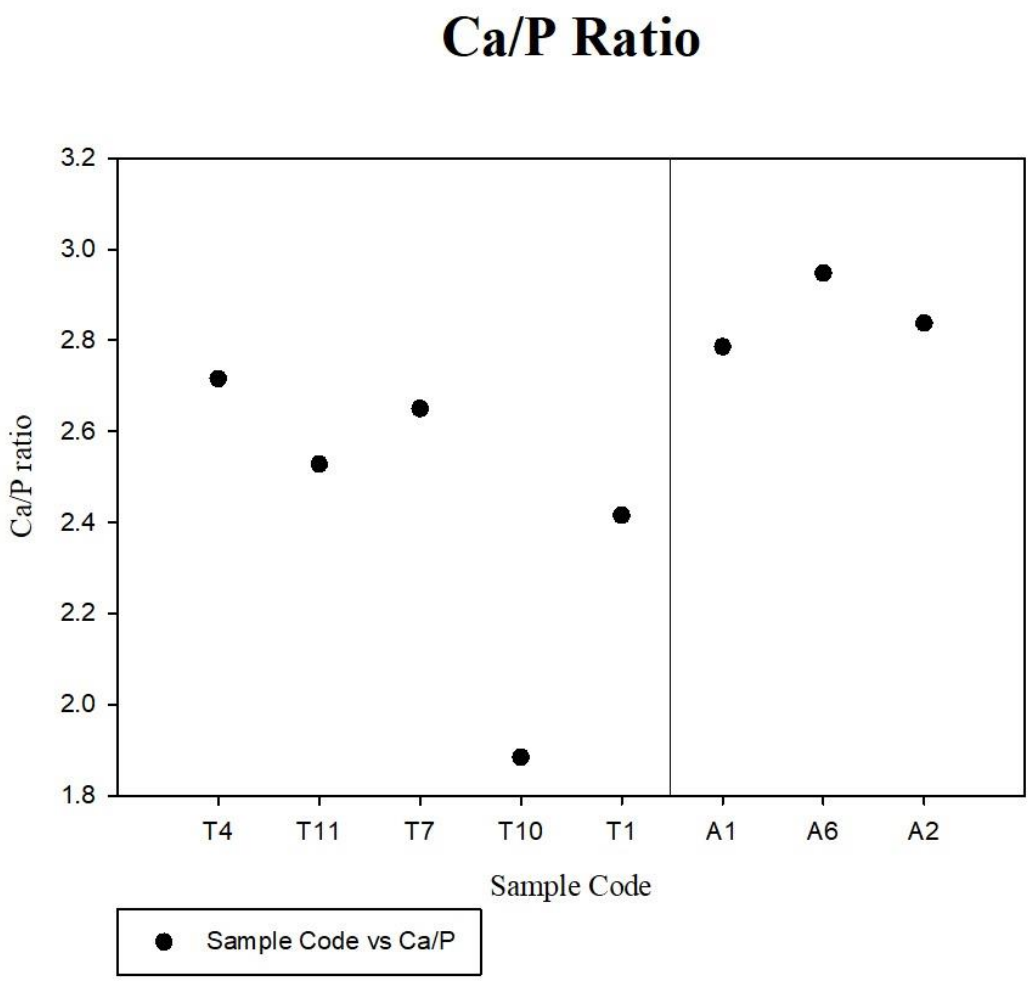

Figure 23. Ca/P ratios of dental calculus.

Rare earth elements (REE) and uranium are used as indicators for post-burial alterations (Lazzati et al., 2016). The concentrations of uranium and REE in modern teeth are noted to be less than 1 ppm as these elements are not naturally retained in the human tissue. Concentrations higher than 1 ppm are treated as diagenetic products and used to support evidences of possible alteration of other elements such as strontium and barium which can give information about diet. In case of dental calculus, uranium and REE should be present in higher amounts than skeletal tissue as the process of incorporation in the former does not involve any metal transporting enzymes. This is illustrated in Figure 24. For our study, vanadium (V) and uranium (U) were chosen to explain diagenesis. Vanadium and uranium show similar behaviour across all samples indicating that there is a consistent effect of burial environment on samples. Samples having uranium concentration greater than 10 ppm are considered to be diagenetically altered. Sample A6 exhibits uranium

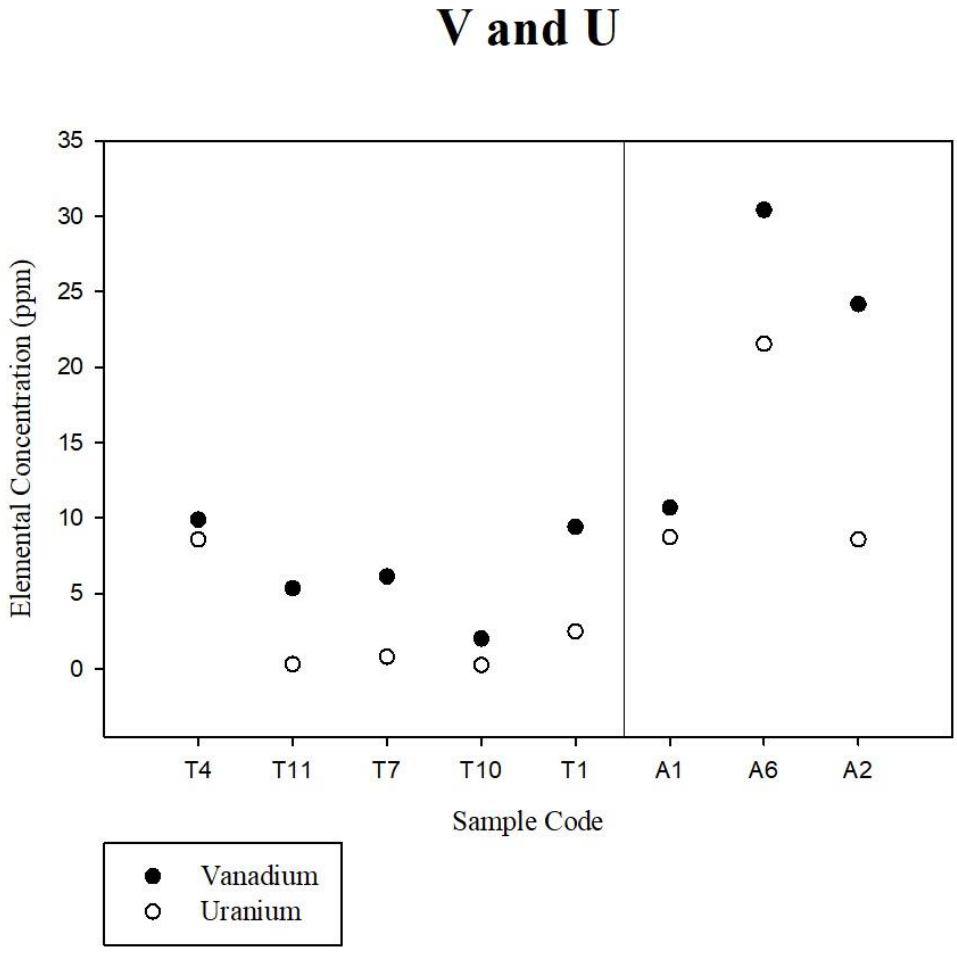

Figure 24. Vanadium and Uranium concentrations in dental calculus samples.

concentration greater than 10 ppm, leading to the conclusion that it is diagenetically altered. In case of vanadium, the reported value ranges are 0.0–0.6 ppm for both human and non-human teeth, < 1.5 ppm for dentine and < 0.08 ppm in case of bones (Grimstead et al., 2017). Based on these values, the dental calculi of both humans and fauna seem to be altered during burial.

Strontium and barium have no known physiological functions but due to their chemical similarity to calcium, they are treated by the body just as the latter as explained in Chapter 5. Both Sr and Ba are removed preferentially from the body with respect to calcium at each trophic level (Arnay-de-la-Rosa et al., 2009). In the biopurification process, the Sr/Ca and Ba/Ca ratios decrease through accumulated preference for calcium over strontium and barium when moving up the trophic levels. Thus, the ratios in the body tissues will always be lower than the ratios in the consumed food. In Figure 25, the Sr/Ca and Ba/Ca ratios of humans and fauna dental calculi are shown.

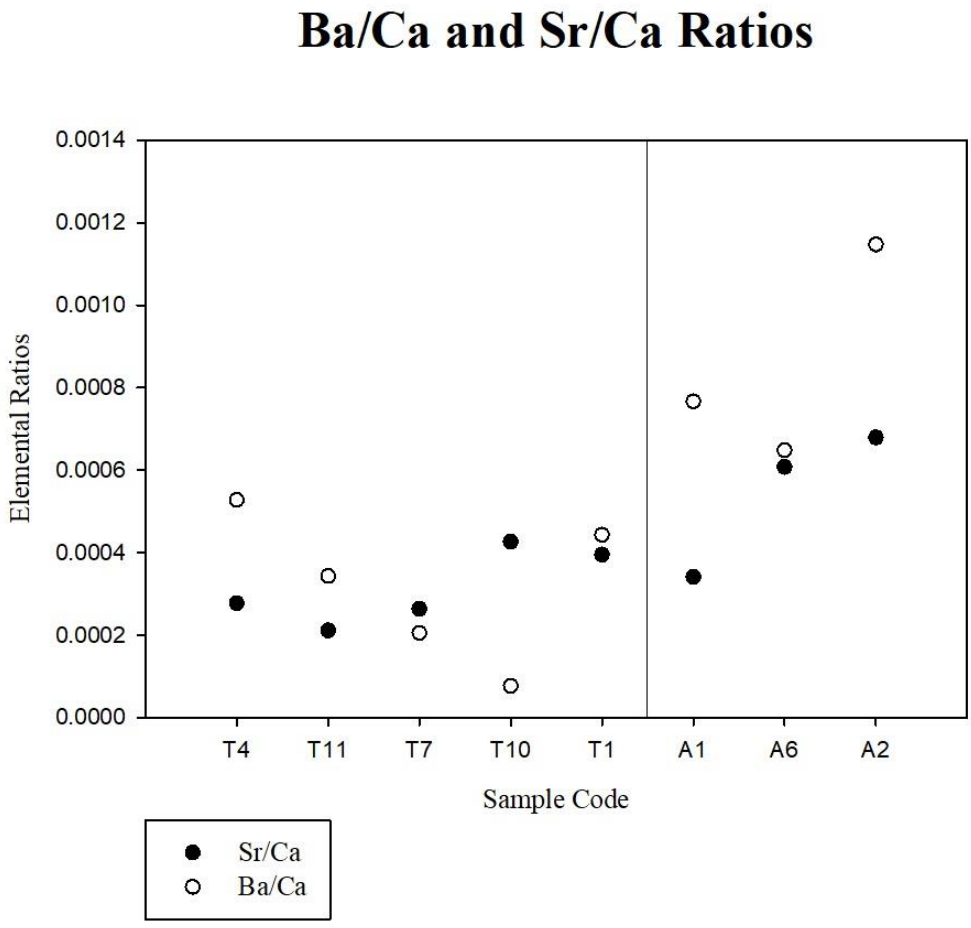

Figure 25. Sr/Ca and Ba/Ca ratios of dental calculus.

In Figure 25, it can also be observed that the faunal samples which are herbivores hailing from *Bos* family (A1 and A6) and *Equus* family (A2) have higher barium values than the humans. This is very similar to the trends expected from bones and teeth as herbivores being at a lower trophic level have higher barium values. In the case of strontium, the same trend as for barium is observed with the exception of one faunal sample A1. It is possible that A1 is subjected to diagenesis. Though the trends are similar to that observed in bones and teeth, the absolute values of dental calculus are not the same as the ones from bones (Lazzati et al., 2016). Barium shows more variability than strontium which might be due to diagenetic alteration.

Ba/Sr has been demonstrated to distinguish marine food resources from terrestrial ones in skeletal tissue (Burton & Price, 2000; Claassen, 1998). The values of Ba/Sr ratio of humans and faunal dental calculi are represented graphically in Figure 26.

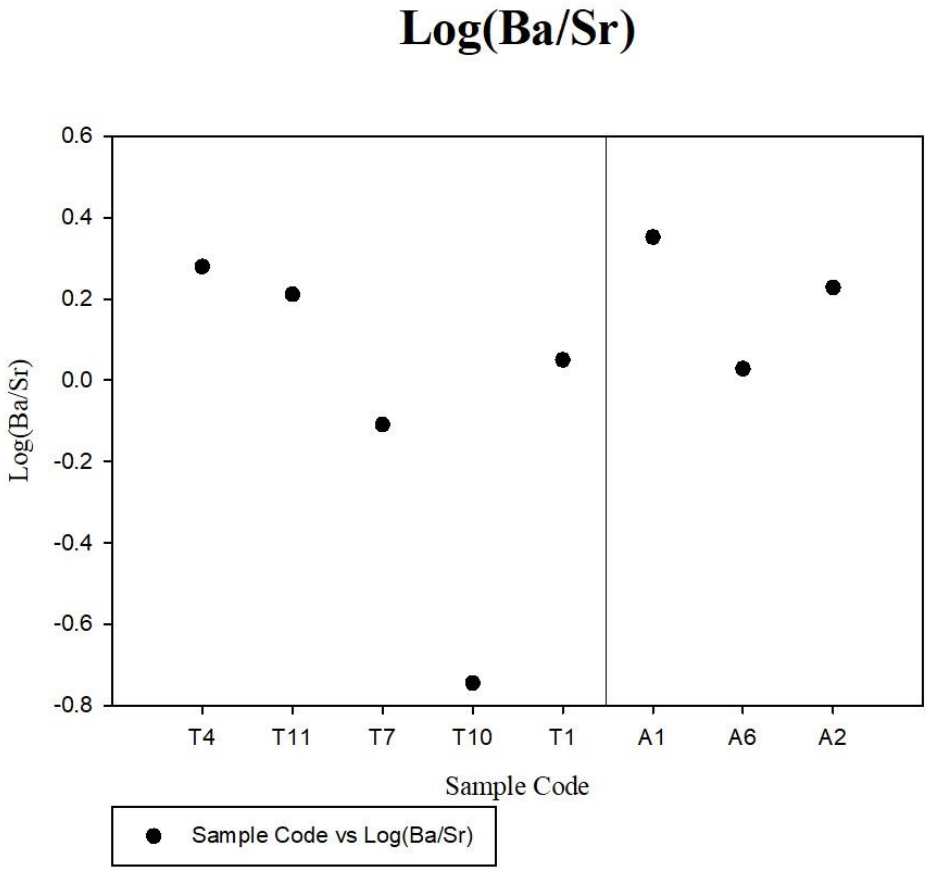

Figure 26. log (Ba/Sr) ratios of dental calculus.

The log (Ba/Sr) values range between -0.7 to 0.39 which appear to be in a certain range with the exception of T10 which also exhibited low Ca/P values Barium and strontium are found in an almost equal abundance in terrestrial environments (Ba/Sr =1) (Arnay-de-la-Rosa et al., 2009;

Lambert et al., 1985). In marine environments, this ratio lowers by a few orders of magnitude due to high sulphate content of seawater which removes available barium in form of insoluble barium sulphate (barite). This leads to enrichment of strontium (± 8.1 ppm) relative to barium (± 0.03 ppm) (Ba/Sr <0.001) (Arnay-de-la-Rosa et al., 2009; Burton & Price, 2000).

Trace elemental analysis on dental calculus shows potential for reliable information provided that the burial conditions are good. The analysis of non-metabolic elements has demonstrated interpretable results but the lack of standard range of values for the elemental concentrations and their ranges has cast a bit of trouble in attributing the levels to specific phenomenon.

7.5 Biomolecular Analysis using Py – GC – MS

The various elucidated pyrolysis products were classified into different categories based on the nature of the molecule of origin. The major classes of the compounds are proteins, fatty acids, carbohydrates, char and unknown. The application of Py – GC – MS technique to material of dental calculus is relatively new and the dynamics of the compounds being pyrolysed are entirely not understood to reconstruct the macromolecular composition (Hardy et al., 2012, 2015; Mickleburgh & Pagán-Jiménez, 2012). A series of tests were made using a very limited number of samples to understand the behavior of the compounds in pyrolysis and also to see if varying parameters of pyrolysis would to what extent alter the pyrograms. This study is only preliminary as no replicate analysis were run for each test and sampling was not done in a manner which guarantees the homogeneity of the samples studied.

Pyrograms of all the samples exhibited a lot of benzene, toluene and xylene biomarkers which can indicate proteins but because of being widespread in nature with many synthetic origins. Pyridines, pyrroles and indenes are attributed to the presence of proteins. n-1-Alkenes and n-alkanes are indicative of C_4 to C_{30} unsaturated and saturated fatty acids which are derived acyl lipids and plant waxes. Phenols, naphthalenes, fluorine, pyrene and anthracenes are attributed to combustion markers formed by incomplete combustion possibly from wood fires. The first major compound eluted in the pyrolysate is carbon dioxide which results from the breakdown of carbonates in the hydroxyapatite structure as well as decarboxylation of carboxylic acids of the calculus deposits (Hardy et al., 2015). In the case of protein class compounds, between 400 – 600 ^{0}C the proteins breakdown into amino acids which undergo further reactions with other breakdown compounds. Pyridinic-N and pyrrolic-N are mainly synthesized due to cyclisation reactions of the amino acids

especially leucine, lysine, proline, and arginine, whose polar side-chains are long enough to form 5- or 6- membered N-heterocyclic rings by dehydration, deamination, or dehydrogenation reactions (see Figure 27). Other amino acids such as valine, aspartic acid and glutamic acid can undergo dimerization reactions leading the formation of pyridinic-N and pyrrolic-N as demonstrated by equations 1 – 3 in Figure 27 (Wei et al., 2017). A lot of indoles and its derivatives were observed which can be easily explanied by the loss of their side functional groups of phenylalanine, tyrosine and tryptophan (Figure 28). However, at higher temperatures pyridines and pyrroles are known to undergo cracking reaction to form pyridinic-N, pyrrolic-N, and quarternary-N (indoles) from equation 10 (Figure 29) (Wei et al., 2017).

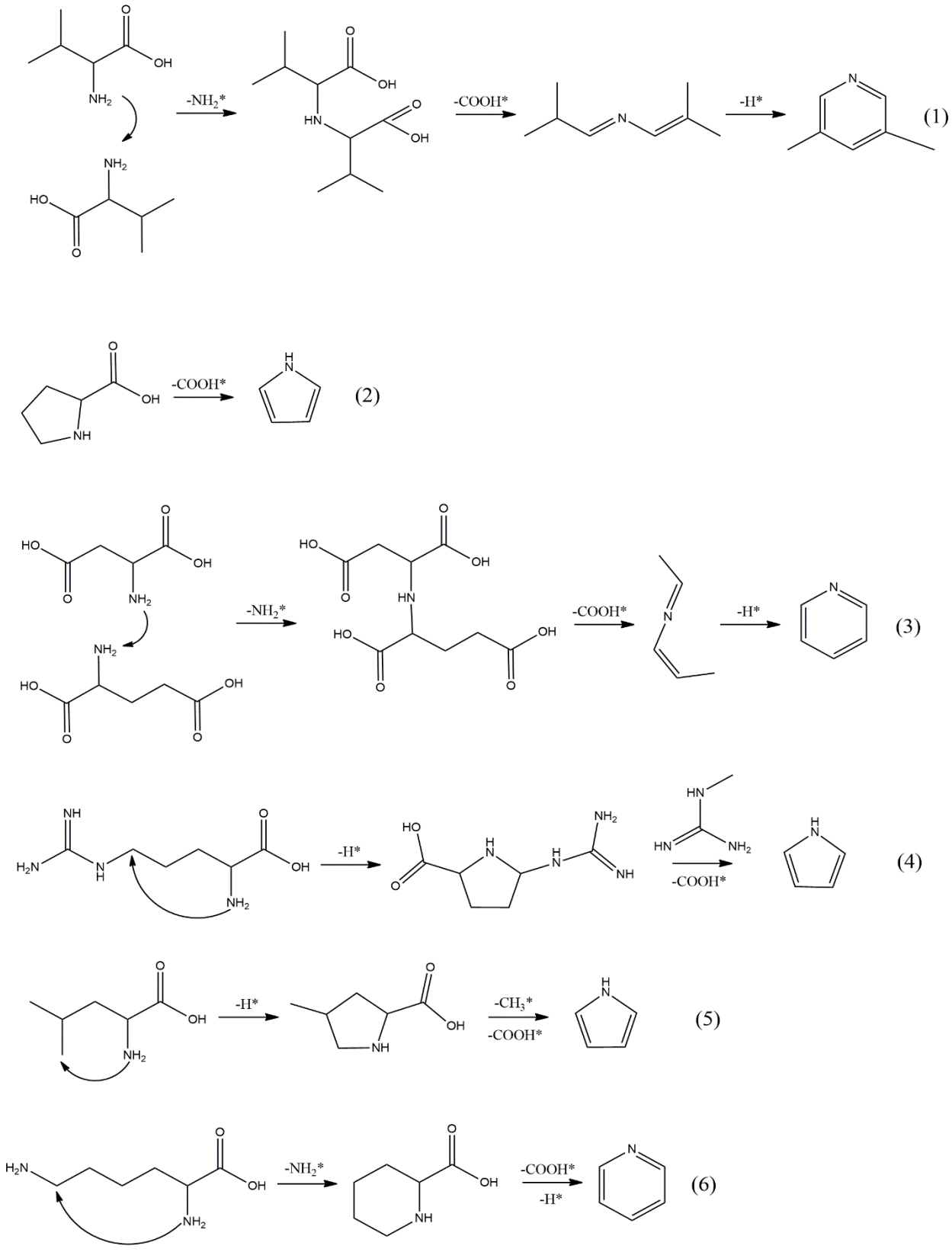

Figure 27. Cyclisation reaction of amino acids (Wei et al., 2017).

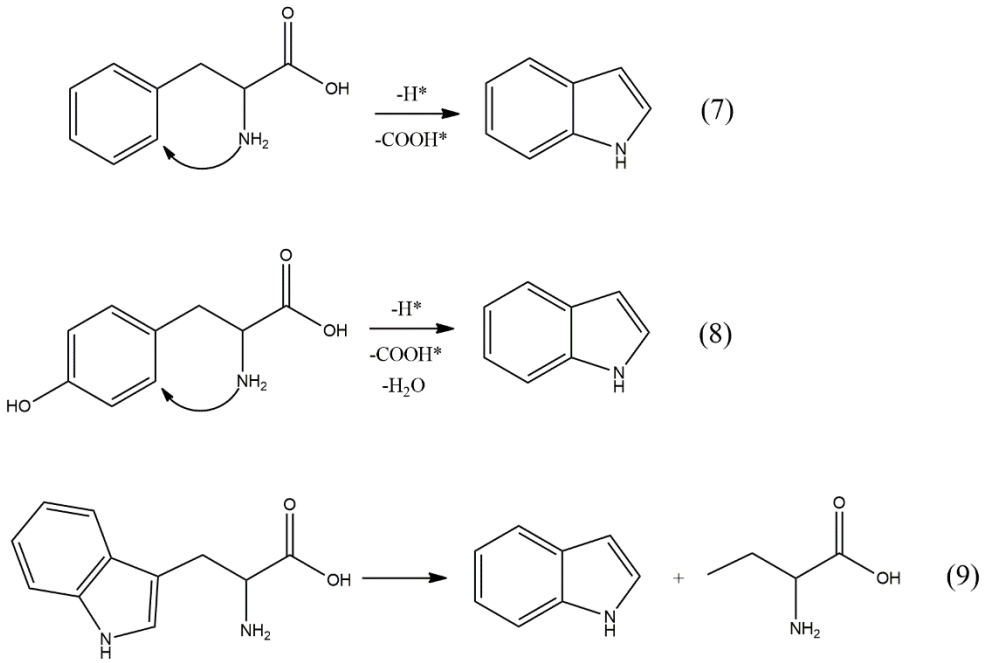

Figure 28. Side functional group loss of phenylalanine, tyrosine and tryptophan (Wei et al., 2017).

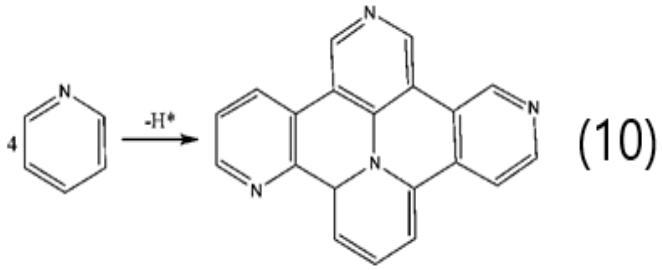

Figure 29. Ring condensation reaction of pyridinic – N (Wei et al., 2017).

Quarternary-N compounds are formed due to ring condensation of the pyridinic-N formed through earlier reactions. Additionally, NH_2^* groups relaeased as part of these reactions usually react with other intermediates to form ammonia as in equations 11 – 12 (Figure 30) (Wei et al., 2017).

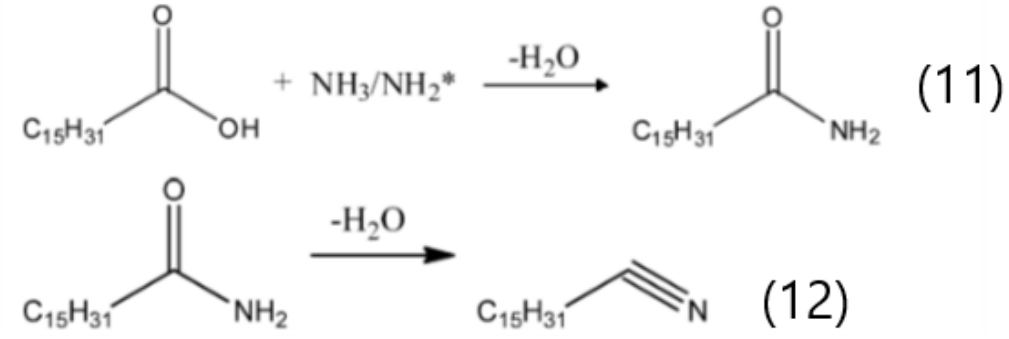

Figure 30. NH_2^* free radical group release and formation of other intermediates (Wei et al., 2017).

Fatty acids under decarboxylation, reduction and release carbon dioxide and form a variety of compounds such as alkanes, alkenes, aldehydes, alcohols etc. (Hardy et al., 2015). Nitriles are generated due to cracking of amino acids and dehydration of amides as shown in Figure 30. Amines and amides are formed primarily from long chained fatty acids which react with either ammonia or NH_2^* free radicals formed in the pyrolitic reaction to form long chained amides and amines if decarboxylated (Figure 31). Ion extraction for m/z (55 and 57) was performed for all the spectra and a series of n-1 alkenes with n- alkanes were observed. Apart from the dental calculus samples, two standard alkane mixtures ranging from C7 – C40 were pyrolysed to investigate fatty acid composition. This pattern of n-1-alkenes and n-alkanes is charactersitic of polymerised fatty acids (Hardy et al., 2015).

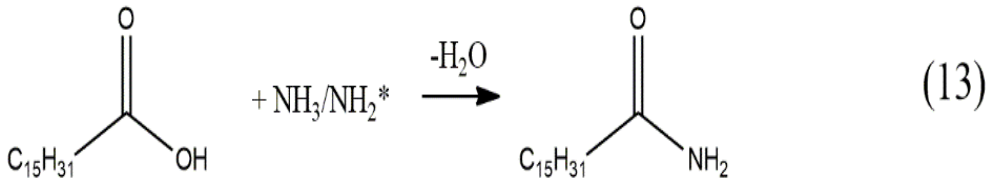

Figure 31. Amide formation due to fatty acid reaction with amine free radicals or ammonia (Wei et al., 2017).

The pyrolysis products of carbohydrates are dependent on the number of carbon atoms initially present before the pyrolysis. The pyrolysis of trioses and tetroses generates similar pyrolysis compounds to higher sugars under initial heating and condensation. They usually generate carboxylic acids, hydroxycarboxylic acids, and various lactones (Moldoveanu, 2010). Pentoses typically generate H_2O, carbon dioxide, aldehydes, ketones, furan and pyran derivatives which is usually furfural compounds as well as various deoxy sugars. Hexose pyrolysis elucidates small molecules such as formaldehyde, hydroxyacetaldehyde, furan derivatives, pyran derivatives, dioxane derivatives, and organic compounds with C_1 to C_4 atoms due to a variety of reactions including but not limited to eliminations, fragmentations, and rearrangements (Moldoveanu, 2010). Pyrolysis of disaccharides is very similar to those of monosaccharides with only the proportion of pyrolysate compounds varying.

A considerable number of compounds identified in the pyrolysate are classified as char compounds. This class represents compounds which are generated due to incomplete combustion of biomass. Wood smokes, wood smoked foods, coal or oil usually generate various compounds of di- and tri- methyl phenol family. Combustion markers for wood fires, formation of gas or coal or oil are usually naphthalenes, fluorenes, anthracenes, and pyrenes (Hardy, Radini, Buckley,

Sarig, et al., 2016). Apart from these classes, a large number of compounds are widely present in nature and cannot be attributed to any one particular source. These compounds are classified as unknown. In the pyrograms, relative abundance is presented to facilitate comparisons between different samples in a quantitative sense.

The sample T9 was pyrolysed at 500 ^{0}C for 12 seconds and the eluted pyrolysate was subjected to gas chromatography mass spectrometry (Figure 32). Subsequently the same sample was pyrolysed at 600 ^{0}C for 12 seconds (Figure 33) and the eluted pyrolysate was subjected to gas chromatography mass spectrometry to see the effect the of pyrolysing temperature on detected compounds. The classes on compounds, namely proteins, carbohydrates, fatty acids, char and finally unknown compounds. From the pyrograms, it can be observed that there is still a fraction of molecules which had not been pyrolysed at the lower temperature.

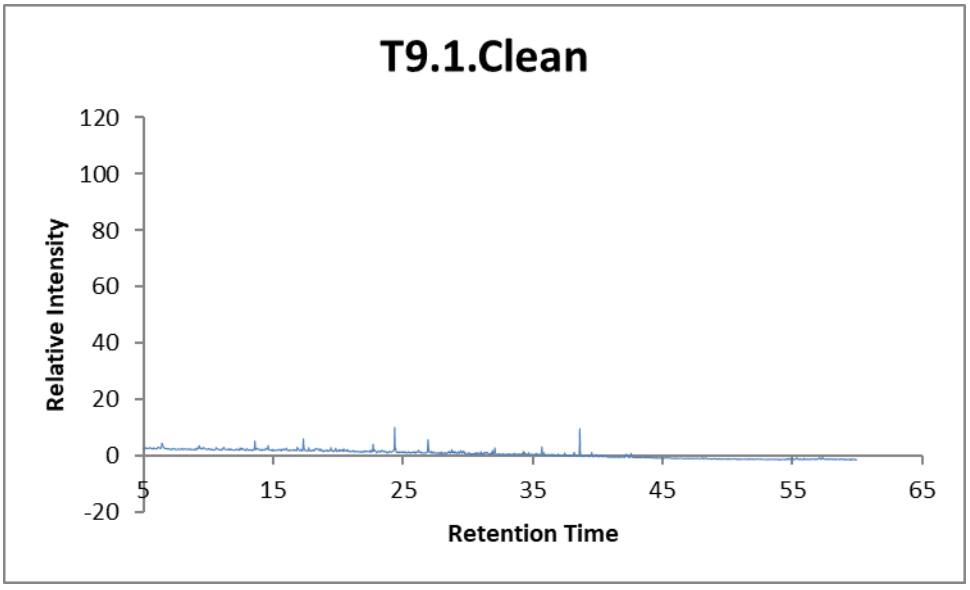

Figure 32. Pyrogram of cleaned sample T9.1.

At 600 ^{0}C, some pyrolysed compounds are identified from protein, fatty acid, carbohydrate, char and unknown class. As it can be seen in the pyrograms (Figure 32, Figure 33) that the relative intensity of eluted compounds is reduced. It was concluded in this case that pyrolysing at 600 0C was better in order to extract the greater majority of the compounds and to have a better representation of the sample in the pyrogram. The compounds observed are presented in Appendix II.

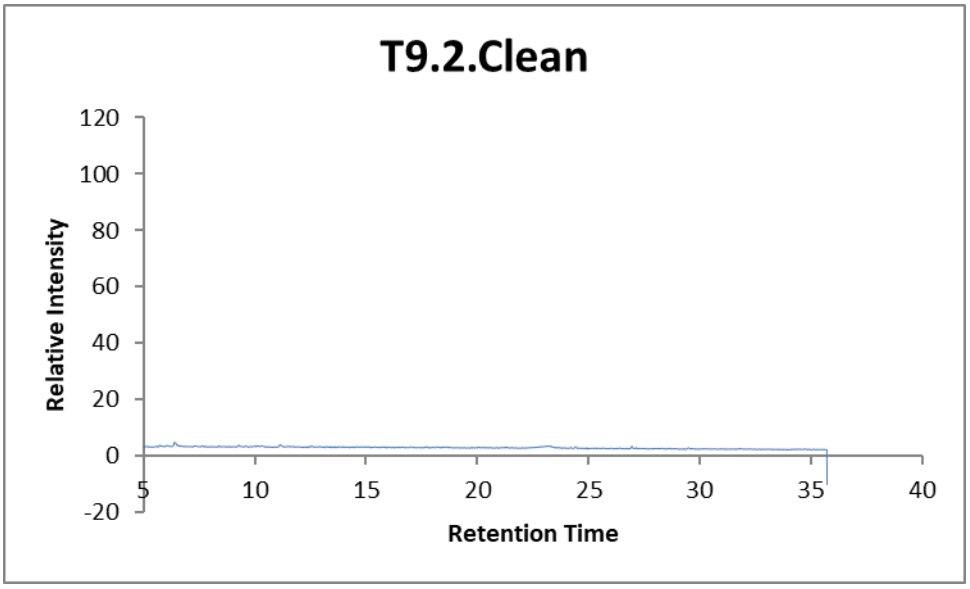

Figure 33. Pyrogram of cleaned sample T9.2.

The second condition which was altered, was the presence or absence of adhering sediment to see the extent of contamination. A part of the same sample (T9) was not cleaned of the adhering visible sediment and labelled T9_UNCLEAN whereas the previous sample T9_CLEAN was cleaned with a DREMEL® diamond coated drill. The uncleaned sample was pyrolysed at 600 ^{0}C for 12 seconds. The pyrogram (Figure 34) shows greater relative intensity of elucidated compounds and the observed compounds (Appendix II) are very similar to the ones identified in the cleaned sample (T9.1.Clean). No compounds indicative of bacterial contamination have been identified (Radini et al., 2017). Thus, it was decided to directly pyrolyse the samples without cleaning the sediment unless the adhered sediment was too large in quantity. This also indicates that in this specific case the dental calculus samples were not contaminated from the soil.

Py – GC – MS was then used to investigate the spatial variability of dental calculus along the different faces of the same tooth. These intra – tooth signal was then compared to dental calculus from another tooth of the same individual to see inter – tooth signal variability. The individual T5 (see Figure 34 and Figure 35) was chosen with one calculus deposit from left mandibular M1 and other from left maxillary I1 for intra – tooth and inter – teeth analysis respectively. The buccal,

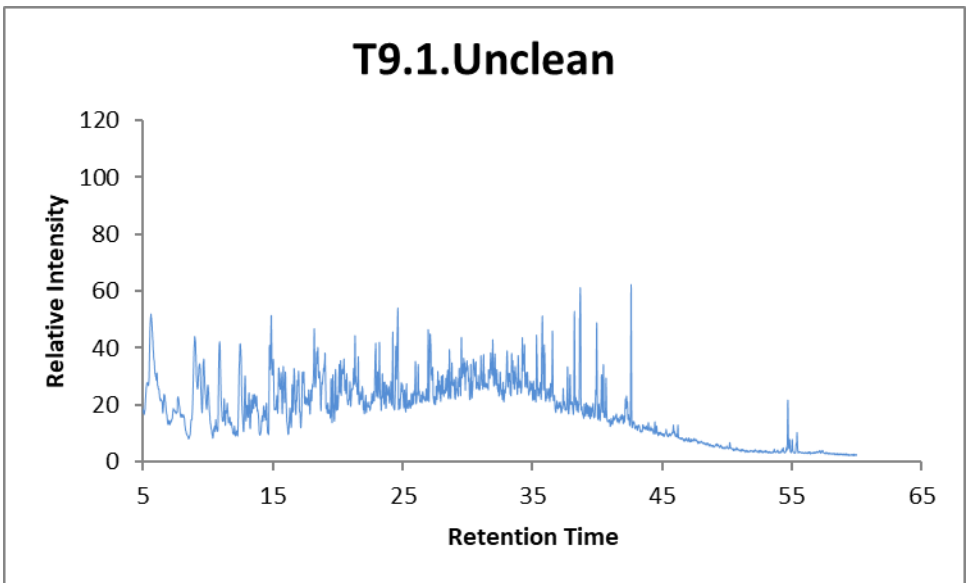

Figure 34. Pyrogram of uncleaned sample T9.1.

lingual, mesial and distal surfaces of M1 were labelled T5.1b, T5.1l, T5.1m, T5.1d whereas the calculus deposit from I1 was labelled T5.2.

The pyrograms of T5.1b, T5.1l, T5.1m, and T5.1d are presented in the Appendix II, it was observed that changing the face of the tooth has not brought about much variation in the composition of the compounds in the pyrograms. The samples from mesial and distal faces, T5.1m and T5.1d show larger number of compounds indicative of carbohydrates where as T5.1b and T5.1l from buccal and lingual faces show one or two compounds. The results can be explained by the preservation of starch and other sugars in the sub-gingival region due to absence of saccharolytic bacteria and the low concentrations of salivary amylase (Radini et al., 2017). Though it appears that the spatial variability of the signal from the different surfaces of the tooth are not very different, this methodology needs to be extended to a large number of samples from different contexts before generalized conclusions could be drawn.

When the sample T5.1 was compared to T5.2 to see inter – tooth deposit, the results were similar to the intra – tooth variability. No major variation of compound distribution was observed between the samples in this case as well (Figure 35). This is an important observation as usually calculus deposits are very scarce on archaeological teeth. In most of the cases, it is present on a few teeth and if the variability of the compound distribution is different based on its location in the buccal cavity then the interpretation of the results must be based on that fact as well.

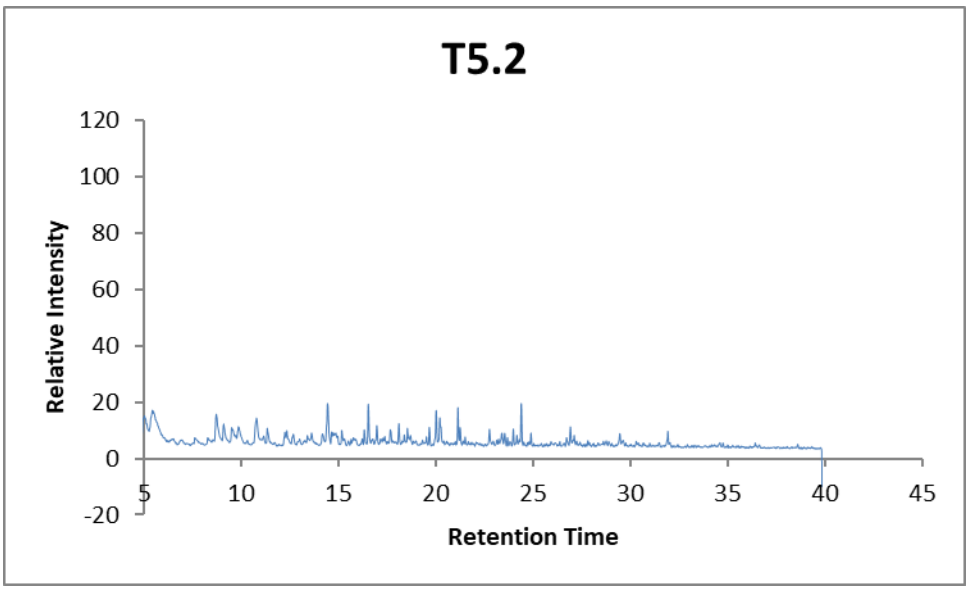

Figure 35. Pyrogram of uncleaned sample T5.2..

Another investigation was performed by derivatising sample T5 (Figure 36) the sample with 5 µL of TMAH in 2.5% methanol. It was observed that the relative intensity of the elucidated compounds improved but no new compounds were detected. In case of low amounts of organic traces in the sample, derivatising the sample seems to give improved sensitivity.

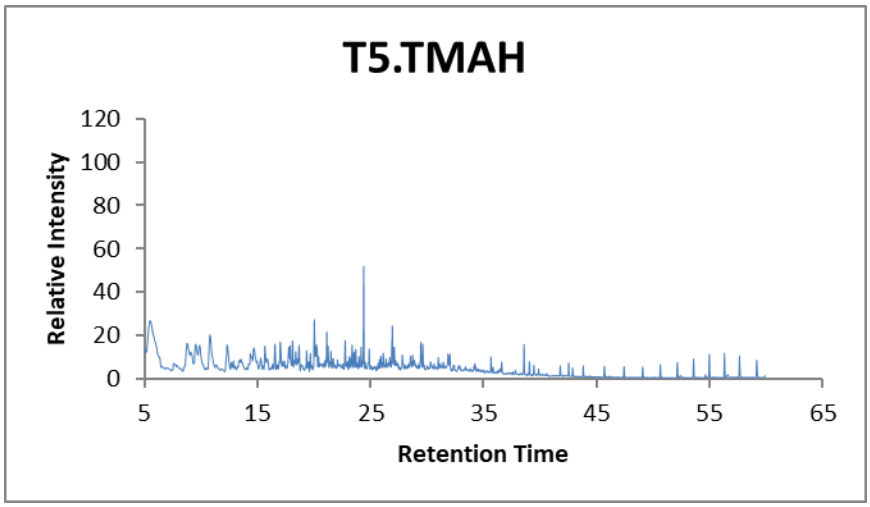

Figure 36. Pyrogram of sample T5 derivatised using TMAH.

In order to compare the samples of the necropolis of Santa Maria do Olival, one sample (E1) from the human remains retrieved from the Museum of Evora was analysed. The pyrogram (Figure 37) shows similar compounds to that of the samples from Tomar indicating a diet high in proteins and an environment of char compounds. An ion extract (m/z = 55, 57) was applied to see n-1-alkenes

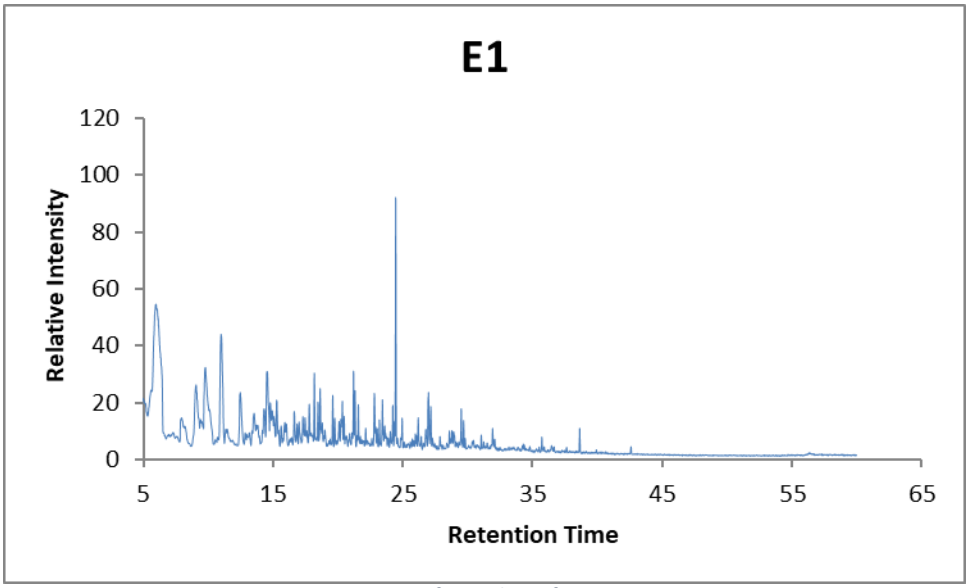

Figure 37. Pyrogram of sample E1 from Evora Museum.

and n-alkanes. The presence of these compounds indicates polymerised fatty acids. These compounds were present in all the samples (Appendix II).

In general, all the samples exhibit a number of carbohydrate markers, indicative of a range of carbohydrates. 2-methyl-2-cyclopenten-1-one; 2,3-dimethyl-2-cyclopenten-1one; ,4-dimethyl-2-cyclopenten-1one; 3,4,5-trimethyl-2-cyclopenten-1-one, furan and its derivatives, and pyran and its derivatives are present in almost all the samples indicating high carbohydrate consumption. Toluene, xylene and o, m and p-xylene are found in high abundances along with high abundances of pyridine, 2-methyl pyridine, 3-methyl pyridine, 4-methyl pyridine, pyrrole and pyrrole derivatives suggesting the presence of protein component. Aliphatic nitriles and amides presence indicate protein lipid condensation products and also the presence of fats or oils. Phenols 2,4-dimethylphenol, 2,3,5-trimethylphenol and 2,3,6-trimethylphenol, along with other combustion markers fluorene, 1-methyl-9H-fluorene, 2-methyl-9H-fluorene, 1-methylanthracene, 2-methylanthracene, 3,6-dimethylphenathrene, 1-methylfluoranthene, pyrene, 1-methyl pyrene, 7H-benzo[c]fluorene, and a number of indene and naphthalene and its derivatives were present in high quantities in all samples indicating exposure to partial wood combustion or partial biomass combustion or consumption of smoked meats.

7.6 Implications in Diet

The various microdebris observed are all originating from the Poaceae family which consists of all grasses. These is not really a diagnostic feature for identifying various plant sources at species level. No starch granules are observed which can be interpreted in two ways. One is that the burial conditions were not favourable for preservation of the entrapped material of dental calculus. The second reason could be that people were consuming low starch based diet and in taking other food. If this is the case then, it also explains the absence of silica skeletons in the recovered debris. This indicates that the people were consuming more animal based food. The $\delta^{13}C$ isotopic ratios indicate a diet based primarily on C_3 plants in both humans and fauna. In case of $\delta^{15}N$ values, the reflected values from calculus are higher from those of bone collagen. The higher values though can be explained as increase in trophic levels, it is not prudent to conclude so. The initial conclusions from stable isotope ratios is substantiated by trace element ratios. The faunal samples which are herbivores exhibit higher barium to calcium ratios indicating lower trophic level when compared to humans. In case of strontium to calcium ratios, except for the faunal sample A1 all others exhibit similar trend. It is difficult to conclude due to non-availability of concentration ranges for trace element concentrations of dental calculus. Finally, Ba/Sr ratios have been calculated but could not be interpreted to understand the consumption of marine food due to the issue of non-availability of ranges for terrestrial and marine sources. However, it can be established by analysing $\delta^{34}S$ values which makes it easy to establish the standard values for different sources. The organic residue analysis reveals a high amount of partially combusted biomass. This is suspected to originate from bad air quality as well as from the consumption from grilled and charred meat which was consumed a lot in medieval Portugal. Indoles were found in high concentrations throughout the samples which is a pyrolysis product of the amino acid tryptophan. Tryptophan is present in abundant quantities in red meat, eggs, chestnuts, acorns, oats, milk, fish and lentils. According to historical data, all of these foods formed a staple diet in medieval Tomar. Even fish which was expensive, it was consumed due to compulsion of religious fasts. Alternating n-1-alkenes and n-alkanes indicates polymerised fatty acids which is something other than olive acid which the population was consuming. Future analysis is needed to identify this specific polymerised fatty acid.

8. Conclusions

Dental calculus has shown potential to act as a complementary source of paleodiet proxy to bones and teeth. The study has taken a multi-analytical approach to investigate the reliability of dental calculus on 14 humans and 6 faunal samples from Tomar. An archaeological sample and a modern sample were added to the study to have comparative information from the same period. The analyses showed that the preservation conditions seem to affect the retrieval of dietary signal and the notion of dental calculus being impervious to diagenesis needs to be revisited. Micro-debris, isotopic and organic residue analysis have revealed to be promising directions of analysis. Nevertheless, a limitation of the approach concerns the recovery of micro-debris, which has not been as successful as anticipated with respect to published literature. This drawback has been attributed to poor preservation conditions as well as dietary practices. $\delta^{13}C$ and $\delta^{15}N$ isotopic ratios have proven to be interpretable as well as the respective values from bone collagen though the absolute values are not the same. This needs to be substantiated by analysing a larger number of analyses to establish a relation between the isotopic values of bone collagen and dental calculus. Study of non-dietary elements such as barium and strontium have shown promising results as they have shown expected trends where their ratio with calcium decreased with increase in trophic level. Also, Ba/Sr ratio from dental calculus has shown to have potential to be utilised to differentiate between marine and terrestrial diets but the lack of sulphur isotope ratio values and specific standard values of the ratios for dental calculus made the interpretation difficult. Organic residues suggested a high protein based diet with some polymerised fatty acids. Also compounds which are typical indicators of partial combustion of biomass suggestive of exposure to smoky environment. Based on the results obtained, it can be concluded that human diet at Medieval Tomar most probably included terrestrial protein, marine protein and C_3 food sources. The general diet was rich in proteins and carbohydrates. Another interesting aspect concerns the quality of the air quality. According to high amount of biomarkers for charred biomass, in fact, in Medieval Portugal the quality of the air must have been of very low quality much like anywhere else in the world due to the wood burning for heat energy requirements.

9. Bibliography

A.H.O, M. (1987). *A Sociedade Medieval Portuguesa Aspectos da Vida Quotidiana*. Lisbon: Sá da Costa.

Adler, C. J., Dobney, K., Weyrich, L. S., Kaidonis, J., Walker, A. W., Haak, W., … Cooper, A. (2013). Sequencing ancient calcified dental plaque shows changes in oral microbiota with dietary shifts of the Neolithic and Industrial revolutions. *Nature Genetics*, *45*(4), 450–455. https://doi.org/10.1038/ng.2536

Armitage, P. L. (1975). The extraction and identification of opal phytoliths from the teeth of ungulates. *Journal of Archaeological Science*, *2*(3), 187–197. https://doi.org/10.1016/0305-4403(75)90056-4

Arnay-de-la-Rosa, M., González-Reimers, E., Gámez-Mendoza, A., & Galindo-Martín, L. (2009). The Ba/Sr ratio, carious lesions, and dental calculus among the population buried in the church La Concepción (Tenerife, Canary Islands). *Journal of Archaeological Science*, *36*(2), 351–358. https://doi.org/10.1016/j.jas.2008.09.019

Ase, F., & Rqueológicos, D. E. T. R. A. (2009). GeoArquE Relatório Antropológico Final de Escavação.

Barber, D. A., & Shone, M. G. T. (1966). The absorption of silica from aqueous solutions by plants. *Journal of Experimental Botany*, *17*(3), 569–578.

Barton, H., & Torrence, R. (2015). Cooking up recipes for ancient starch: Assessing current methodologies and looking to the future. *Journal of Archaeological Science*, *56*, 194–201. https://doi.org/10.1016/j.jas.2015.02.031

Batata, C. (1997). *As Origens de Tomar*. Tomar: City Council of Tomar.

Beasley, M. M., Bartelink, E. J., Taylor, L., & Miller, R. M. (2014). Comparison of transmission FTIR, ATR, and DRIFT spectra: implications for assessment of bone bioapatite diagenesis. *Journal of Archaeological Science*, *46*, 16–22.

Blatt, S. H., Redmond, B. G., Cassman, V., & Sciulli, P. W. (2011). Dirty teeth and ancient trade: Evidence of cotton fibres in human dental calculus from Late Woodland, Ohio. *International Journal of Osteoarchaeology*, *21*(6), 669–678. https://doi.org/10.1002/oa.1173

Bodoriková, S., Tibenská, K. D., Katina, S., Uhrová, P., Dörnhöferová, M., Takács, M., & Urminský, J. (2013). Dietary reconstruction from trace element analysis and dental microwear in an Early Medieval population from Gáň (Galanta district, Slovakia). *Anthropologischer Anzeiger*, *70*(2), 229–248. https://doi.org/10.1127/0003-5548/2013/0256

Bryant, V. M. (1974). Prehistoric diet in southwest Texas: the coprolite evidence. *American Antiquity*, *39*(3), 407–420.

Buckley, S., Usai, D., Jakob, T., Radini, A., & Hardy, K. (2014). Dental calculus reveals unique insights into food items, cooking and plant processing in prehistoric central Sudan. *PLoS ONE*, *9*(7), 1–10. https://doi.org/10.1371/journal.pone.0100808

Buikstra, E. (1984). Ancient Human Diet from Inorganic Analysis of Bone. *Acc. Chem. Res.*, *85*(6), 298–305. https://doi.org/10.1021/ar00105a001

Burton, J. H., & Price, T. D. (2000). The use and abuse of trace elements for paleodietary research. *Biogeochemical Approaches to Paleodietary Analysis Kluwer Academic/Plenum: New York*, 159–171. https://doi.org/10.2993/0278-0771-35.1.60

Caemmerer, S. von, Ghannoum, O., Pengelly, J. J. L., & Cousins, A. B. (2014). Carbon isotope discrimination as a tool to explore C4 photosynthesis. *Journal of Experimental Botany*, *65*(13), 3459–3470. https://doi.org/10.1093/jxb/eru127

Cameron, N. E., Balks, M., Littler, R., Manley-harris, M., & Awekotuku, N. Te. (2007). An Investigation by LA-ICP-MS of Possum Tooth Enamel as a Model for Identifying Childhood Geographical Locations of Historical and Archaeological Human Remains from New Zealand, *3*(1).

Capasso, L., di Tota, G., Jones, K. W., & Tuniz, C. (1995). Synchrotron radiation microprobe analysis of human dental calculi from an archaeological site: A new possible perspective in palaeonutrition studies. *International Journal of Osteoarchaeology*, *5*(3), 282–288. https://doi.org/10.1002/oa.1390050307

Charlier, P., Huynh-Charlier, I., Munoz, O., Billard, M., Brun, L., & Grandmaison, G. L. de la. (2010). The microscopic (optical and SEM) examination of dental calculus deposits (DCD). Potential interest in forensic anthropology of a bio-archaeological method. *Legal Medicine*, *12*(4), 163–171. https://doi.org/10.1016/j.legalmed.2010.03.003

Chisholm, B., Nelson, D. E., & Schwarcz, H. P. (1982). Stable-carbon isotope ratios as a measure of marine versus terestrial protein in anciet diets. *Science*, *216*(216), 11131–11132.

Ciochon, R. L., Piperno, D. R., & Thompson, R. G. (1990). Opal phytoliths found on the teeth of the extinct ape Gigantopithecus blacki: implications for paleodietary studies. *Proceedings of the National Academy of Sciences*, *87*(20), 8120–8124.

Claassen, C. (1998). *Shells*. Cambridge University Press. Retrieved from https://books.google.de/books?id=s4gLYlBjOl8C

Coelho.M.H.C. (1990). Apontamentos sobre a comida e a bebida do campesinato coimbrão em tempos medievos. In *Homens, Espaços e Poderes. Séculos XI-XVI. Vol. I «Notas do Viver Social»* (pp. 9–22). Lisbon.

Collins, M. J., & Copeland, L. (2011). Ancient starch: Cooked or just old? *Proceedings of the National Academy of Sciences*, *108*(22), E145–E145. https://doi.org/10.1073/pnas.1103241108

Corti, C., Rampazzi, L., Ravedoni, C., & Giussani, B. (2013). On the use of trace elements in ancient necropolis studies: Overview and ICP-MS application to the case study of Valdaro site, Italy. *Microchemical Journal*, *110*, 614–623. https://doi.org/10.1016/j.microc.2013.07.001

Craig, O. E., Bondioli, L., Fattore, L., Higham, T., & Hedges, R. (2013). Evaluating marine diets through radiocarbon dating and stable isotope analysis of victims of the AD79 eruption of vesuvius. *American Journal of Physical Anthropology*, *152*(3), 345–352. https://doi.org/10.1002/ajpa.22352

Cummings, L. S., Yost, C., & So, A. (2016). Plant microfossils in human dental calculus from Nemrik 9 , a Pre-Pottery Neolithic site in Northern Iraq. https://doi.org/10.1007/s12520-016-0411-3

Curto, A., Maurer, A., Barrocas-dias, C., Mahoney, P., Fernandes, T., & Fahy, G. E. (2018). Did military orders influence the general population diet ? Stable isotope analysis from Medieval Tomar , Portugal.

D., R. (1987). *Arte de Cozinha*. Lisbon: Imprensa Nacional Casa da Moeda.

Dal, G., Lebon, M., Angelini, I., Maritan, L., Usai, D., & Artioli, G. (2016). Bone diagenesis variability among multiple burial phases at Al Khiday (Sudan) investigated by ATR-FTIR spectroscopy. *Palaeogeography, Palaeoclimatology, Palaeoecology*, *463*, 168–179. https://doi.org/10.1016/j.palaeo.2016.10.005

DE LA FUENTE, C., FLORES, S., & MORAGA, M. (2013). DNA FROM HUMAN ANCIENT BACTERIA: A NOVEL SOURCE OF GENETIC EVIDENCE FROM ARCHAEOLOGICAL DENTAL CALCULUS. *Archaeometry*, *55*(4), 767–778. https://doi.org/10.1111/j.1475-4754.2012.00707.x

DeNiro, M. J., & Weiner, S. (1988). Chemical, enzymatic and spectroscopic characterization of "collagen" and other fractions from prehistric bones. *Geochimica et Cosmochimica Acta*, *52*, 2197–2206.

Dobney, K., & Brothwell, D. (1987). A method for evaluating the amount of dental calculus on teeth from archaeological sites. *Journal of Archaeological Science*, *14*(4), 343–351. https://doi.org/10.1016/0305-4403(87)90024-0

Dolphin, A. E., Naftel, S. J., Nelson, A. J., Martin, R. R., & White, C. D. (2013). Bromine in teeth and bone as an indicator of marine diet. *Journal of Archaeological Science*, *40*(4), 1778–1786. https://doi.org/10.1016/j.jas.2012.11.020

Driessens, F. C. M., & Verbeeck, R. M. H. (1989). Possible pathways of mineralization of dental plaque. *Recent Advances in the Study of Dental Calculus*, 7–17.

Dudgeon, J. V., & Tromp, M. (2014). Diet, Geography and Drinking Water in Polynesia: Microfossil Research from Archaeological Human Dental Calculus, Rapa Nui (Easter Island). *International Journal of Osteoarchaeology*, *24*(5), 634–648. https://doi.org/10.1002/oa.2249

Dunne, T., & Leopold, L. B. (1978). *Water in environmental planning*. Macmillan.

Eerkens, J. W., Tushingham, S., Brownstein, K. J., Garibay, R., Perez, K., Murga, E., … Gang, D. R. (2018). Journal of Archaeological Science : Reports Dental calculus as a source of ancient alkaloids : Detection of nicotine by LC- MS in calculus samples from the Americas, *18*(November 2017), 509–515. https://doi.org/10.1016/j.jasrep.2018.02.004

Ezzo, J. A. (2010). Society for American Archaeology Zinc as a Paleodietary Indicator : An Issue of Theoretical Validity in Bone-Chemistry Analysis Published by : Society for American Archaeology Stable URL : http://www.jstor.org/stable/282336 ZINC AS A PALEODIETARY INDICATO, *59*(4), 606–621.

Fabião, C. (2004). *A Antiguidade Tardia e a desagregação do Império*.

Gaar, D. (1989). Comparison of the rate of formation of supragingival calculus in an Asian and a European population. *In Recent Advances in the Study of Dental Calculus*.

Galiová, M., Kaiser, J., Fortes, F. J., Novotný, K., Malina, R., Prokeš, L., … Laserna, J. J. (2010). Multielemental analysis of prehistoric animal teeth by laser-induced breakdown spectroscopy and laser ablation inductively coupled plasma mass spectrometry. *Applied Optics*, *49*(13), C191. https://doi.org/10.1364/AO.49.00C191

Glock, G. E., & Murray, M. M. (1938). Chemical Investigation of Salivary Calculus. *Journal of Dental*, 257–264.

Gobetz, K. E., & Bozarth, S. R. (2001). Implications for late Pleistocene mastodon diet from opal phytoliths in tooth calculus. *Quaternary Research*, *55*(2), 115–122.

Gonçalves. I. (1984). *O Temporal do Mosteiro de Alcobaça nos Séculos XIV e XV*. Lisbon: Faculdade de Ciências Sociais e Humanas.

Gonçalves. I. (1988). Acerca da Alimentação Medieval. In *Imagens do Mundo Medieval* (pp. 201–217).

Gonzales, F., & Sognnaes, R. F. (1960). Electronmicroscopy of Dental Calculus. *Science*, *131*(3394), 156–158. https://doi.org/10.1126/science.131.3394.156

Greene, T. R., Kuba, C. L., & Irish, J. D. (2005). Quantifying calculus: A suggested new approach for recording an important indicator of diet and dental health. *HOMO- Journal of Comparative Human Biology*, *56*(2), 119–132. https://doi.org/10.1016/j.jchb.2005.02.002

Grimstead, D., Clark, A., & Rezac, A. (2017). Uranium and Vanadium Concentrations as a Trace Element Method for Identifying Diagenetically Altered Bone in the Inorganic Phase. *Journal of Archaeological Method and Theory*.

Hardy, K., Blakeney, T., Copeland, L., Kirkham, J., Wrangham, R., & Collins, M. (2009). Starch granules, dental calculus and new perspectives on ancient diet. *Journal of Archaeological Science*, *36*(2), 248–255. https://doi.org/10.1016/j.jas.2008.09.015

Hardy, K., Buckley, S., Collins, M. J., Estalrrich, A., Brothwell, D., Copeland, L., … Rosas, A. (2012). Neanderthal medics? Evidence for food, cooking, and medicinal plants entrapped in dental calculus. *Naturwissenschaften*, *99*(8), 617–626. https://doi.org/10.1007/s00114-012-0942-0

Hardy, K., Radini, A., Buckley, S., Blasco, R., Copeland, L., & Hardy, K. (2016). Diet and environment 1 . 2 million years ago revealed through analysis of dental calculus from Europe ' s oldest hominin at Sima del Elefante , Spain, *2*, 7–11. https://doi.org/10.1007/s00114-016-1420-x

Hardy, K., Radini, A., Buckley, S., Sarig, R., Copeland, L., Gopher, A., & Barkai, R. (2015). Dental calculus reveals potential respiratory irritants and ingestion of essential plant-based nutrients at Lower Palaeolithic Qesem Cave Israel. *Quaternary International*, *398*, 129–135. https://doi.org/10.1016/j.quaint.2015.04.033

Hayashizaki, J., Ban, S., Nakagaki, H., Okumura, A., Yoshii, S., & Robinson, C. (2008). Site specific mineral composition and microstructure of human supra-gingival dental calculus. *Archives of Oral Biology*, *53*(2), 168–174. https://doi.org/10.1016/j.archoralbio.2007.09.003

Henry, A. G., Brooks, A. S., & Piperno, D. R. (2011). Microfossils in calculus demonstrate consumption of plants and cooked foods in Neanderthal diets (Shanidar III, Iraq; Spy I and II, Belgium). *Proceedings of the National Academy of Sciences of the United States of America*, *108*(2), 486–491. https://doi.org/10.1073/pnas.1016868108

Henry, A. G., & Piperno, D. R. (2008). Using plant microfossils from dental calculus to recover human diet: a case study from Tell al-Raqā'i, Syria. *Journal of Archaeological Science*, *35*(7), 1943–1950. https://doi.org/10.1016/j.jas.2007.12.005

Hillson, S. W. (1979). Diet and dental disease. *World Archaeology*, *11*(2), 147–162. https://doi.org/10.1080/00438243.1979.9979758

Horrocks, M., Nieuwoudt, M. K., Kinaston, R., Buckley, H., & Bedford, S. (2014). Microfossil and Fourier Transform InfraRed analyses of Lapita and post-Lapita human dental calculus from Vanuatu, Southwest Pacific. *Journal of the Royal Society of New Zealand*, *44*(1), 17–33. https://doi.org/10.1080/03036758.2013.842177

J.P, F. (1996). *Arqueologia dos hábitos alimentares*. Lisbon: Dom Quixote.

King, D., & Searcy, M. T. (2016). Plant Microfossils Recovered from Dental Calculus at Casas Grandes , Mexico, 1–3.

Klepinger, L. L., Kuhn, J. K., & Thomas, J. (1977). Prehistoric dental calculus gives evidence for coca in early coastal Ecuador. *Nature*, *269*(5628), 506–507. https://doi.org/10.1038/269506a0

Lambert, J. B., Vlasak, S., Simpson, Szpunar, C. B., & Buikstra, J. E. (1985). Bone diagenesis and dietary analysis. *Journal of Human Evolution*, *14*(5), 477–482. https://doi.org/10.1016/S0047-2484(85)80026-9

Lazzati, A. M. B., Levrini, L., Rampazzi, L., Dossi, C., Castelletti, L., Licata, M., & Corti, C. (2016). The Diet of Three Medieval Individuals from Caravate (Varese, Italy). Combined Results of ICP-MS Analysis of Trace Elements and Phytolith Analysis Conducted on Their Dental Calculus. *International Journal of Osteoarchaeology*, *26*(4), 670–681. https://doi.org/10.1002/oa.2458

Le Geros, R. Z. (2015). Variations in the Crystalline Components of Human Dental Calculus : I . Crystallographic and Spectroscopic Methods of Analysis, (Fig 1), 45–50.

Leary, M. H. O. (2008). Carbon Dynamics in Plants. *Carbon*, *38*(5), 328–336.

Lee-Thorp, J., Sealy, J., & van der Merwe, N. (1989). Stable carbon isotope ratio differences between bone collagen and bone apatite, and their relationship to diet. *Journal of Archaeological Science*, *32*, 1459–1470.

Leonard, C., Vashro, L., O'Connell, J. F., & Henry, A. G. (2015). Plant microremains in dental calculus as a record of plant consumption: A test with Twe forager-horticulturalists. *Journal of Archaeological Science: Reports*, *2*, 449–457. https://doi.org/10.1016/j.jasrep.2015.03.009

Lewin, J., & Reimann, B. E. F. (1969). Silicon and plant growth. *Annual Review of Plant Physiology*, *20*(1), 289–304.

Li, M. Q., Yang, X. Y., Wang, H., Wang, Q., Jia, X., & Ge, Q. S. (2010). Starch grains from dental calculus reveal ancient plant foodstuffs at Chenqimogou site, Gansu Province. *Science China Earth Sciences*, *53*(5), 694–699. https://doi.org/10.1007/s11430-010-0052-9

Lieverse, A. R. (1999). Diet and the Aetiology of Dental Calculus. *International Journal of Osteoarchaeology*, *9*(4), 219–232. https://doi.org/10.1002/(SICI)1099-1212(199907/08)9:4<219::AID-OA475>3.0.CO;2-V

Lieverse, A. R., Link, D. W., Bazaliiskiy, V. I., Goriunova, O. I., & Weber, A. W. (2007). Dental health indicators of hunter–gatherer adaptation and cultural change in Siberia's Cis-Baikal. *American Journal of Physical Anthropology*, *134*(3), 323–339. https://doi.org/10.1002/ajpa.20672

Lustmann, J., Lewin-Epstein, J., & Shteyer, A. (1976). Scanning electron microscopy of dental calculus. *Calcified Tissue Research*, *21*(12), 47–55. https://doi.org/10.1007/BF02547382

Madella, M., Alexandre, A., & Ball, T. (2005). International code for phytolith nomenclature 1.0. *Annals of Botany*, *96*(2), 253–260. https://doi.org/10.1093/aob/mci172

Madella, M., Powers-Jones, A. H., & Jones, M. K. (1998). A Simple Method of Extraction of Opal Phytoliths from Sediments Using a Non-Toxic Heavy Liquid. *Journal of Archaeological Science*, *25*(8), 801–803. https://doi.org/https://doi.org/10.1006/jasc.1997.0226

Malainey, M. E. (2011). Elemental Analysis. In *A Consumer's Guide to Archaeological Science: Analytical Techniques* (pp. 493–495). New York, NY: Springer New York. https://doi.org/10.1007/978-1-4419-5704-7_38

Mandel, I. D. (1990). Calculus formation and prevention: an overview. *Compendium (Newtown, Pa.). Supplement*, (8), S235-41. Retrieved from http://europepmc.org/abstract/MED/3474065

Marcotte, H., & Lavoie, M. C. (1998). Oral microbial ecology and the role of salivary immunoglobulin A. *Microbiology and Molecular Biology Reviews : MMBR*, *62*(1), 71–109. https://doi.org/1092-2172/98/$04.0010

Marques.A.H.O. (1968). *Introdução à História da Agricultura em Portugal*. Lisbon.

Marques.A.H.O. (1971). *Daily Life in Portugal in the Late Middle Ages*. Wisconsin: University of Wisconsin.

Marques.A.H.O. (1987). Portugal na Crise dos Séculos XIV e XV. In *Nova História de Portugal*. Lisbon.

Mickleburgh, H. L., & Pagán-Jiménez, J. R. (2012). New insights into the consumption of maize and other food plants in the pre-Columbian Caribbean from starch grains trapped in human dental calculus. *Journal of Archaeological Science*, *39*(7), 2468–2478. https://doi.org/10.1016/j.jas.2012.02.020

Middleton, W. D., & Rovner, I. (1994). Extraction of opal phytoliths from herbivore dental calculus. *Journal of Archaeological Science*. https://doi.org/10.1006/jasc.1994.1046

Minagawa, M., & Wada, E. (1984). Stepwise enrichment of " N along food chains : Further evidence and the relation between 615N and animal age.

Moldoveanu, S. C. (2010). Chapter 16 Pyrolysis of Carbohydrates. In S. C. Moldoveanu (Ed.), *Pyrolysis of Organic Molecules with Applications to Health and Environmental Issues* (Vol. 28, pp. 419–470). Elsevier. https://doi.org/https://doi.org/10.1016/S0167-9244(09)02816-9

Molokhia, A., & Nixon, G. S. (1984). Studies on the composition of human dental calculus. *Journal of Radioanalytical and Nuclear Chemistry Articles*, *83*(2), 273–281. https://doi.org/10.1007/BF02037141

Montanari M. Romanos, Bárbaros, C. (1998). Na Alvorada da Cultura Alimentar Europeia. In *História da Alimentação* (pp. 247–250).

Montanari M. Romanos. (1998). Estruturas de Produção e Sistemas Alimentares. In *História da Alimentação* (pp. 251–259). Lisbon.

Pearsall, D. M. (2000). *Paleoethobotany: A handbook of procedures*. https://doi.org/10.1093/oxfordjournals.jhered.a102689

Piperno, D. R., & Dillehay, T. D. (2008). Starch grains on human teeth reveal early broad crop diet in northern Peru. *Proceedings of the National Academy of Sciences*, *105*(50), 19622–19627. https://doi.org/10.1073/pnas.0808752105

Ponte, S. da;, & Miranda, J. (1991). *"Relatório de escavações – 1990". Boletim Cultural da Câmara Municipal de Tomar*. Tomar.

Power, R. C., Salazar-García, D. C., Straus, L. G., González Morales, M. R., & Henry, A. G. (2015). Microremains from El Mirón Cave human dental calculus suggest a mixed plant-animal subsistence economy during the Magdalenian in Northern Iberia. *Journal of Archaeological Science*, *60*, 39–46. https://doi.org/10.1016/j.jas.2015.04.003

Power, R. C., Salazar-García, D. C., Wittig, R. M., & Henry, A. G. (2014). Assessing use and suitability of scanning electron microscopy in the analysis of micro remains in dental calculus. *Journal of Archaeological Science*, *49*(1), 160–169. https://doi.org/10.1016/j.jas.2014.04.016

Preus, H. R., Marvik, O. J., Selvig, K. A., & Bennike, P. (2011). Ancient bacterial DNA (aDNA) in dental calculus from archaeological human remains. *Journal of Archaeological Science*, *38*(8), 1827–1831. https://doi.org/10.1016/j.jas.2011.03.020

Price, S. D. R., Keenleyside, A., & Schwarcz, H. P. (2018). Testing the validity of stable isotope analyses of dental calculus as a proxy in paleodietary studies. *Journal of Archaeological Science*, *91*, 92–103. https://doi.org/10.1016/j.jas.2018.01.008

Radini, A., Buckley, S., Rosas, A., Estalrrich, A., de la Rasilla, M., & Hardy, K. (2016). Neanderthals, trees and dental calculus: new evidence from El Sidrón. *Antiquity*, *90*(350), 290–301. https://doi.org/10.15184/aqy.2016.21

Radini, A., Nikita, E., Buckley, S., Copeland, L., & Hardy, K. (2017). Beyond food: The multiple pathways for

inclusion of materials into ancient dental calculus. *American Journal of Physical Anthropology*, *162*(June 2016), 71–83. https://doi.org/10.1002/ajpa.23147

Radini, A., Nikita, E., & Shillito, L. M. (2016). Human dental calculus and a medieval urban environment. *Everyday Life in Medieval Europe: Environmental and Artefactual Approaches to Dwelling in Town and Country. Belgium: Brepols. Http://Dx. Doi. Org/10.1073/Pnas*, *1018116108*. https://doi.org/https://doi.org/10.1484/M.HDL-EB.5.109548

Randall, J. L. (2016). *Recent Advances in Laser Ablation ICP-MS for Archaeology*. https://doi.org/10.1007/978-3-662-49894-1

RAVEN, J. A. (1983). The transport and function of silicon in plants. *Biological Reviews*, *58*(2), 179–207.

Roberts, P., Fernandes, R., Craig, O. E., Larsen, T., Lucquin, A., Swift, J., & Zech, J. (2017). Calling all archaeologists: guidelines for terminology, methodology, data handling, and reporting when undertaking and reviewing stable isotope applications in archaeology. *Rapid Communications in Mass Spectrometry*, (August 2017), 361–372. https://doi.org/10.1002/rcm.8044

Salazar-garcía, D. C., Richards, M. P., Nehlich, O., & Henry, A. G. (2014). Dental calculus is not equivalent to bone collagen for isotope analysis : a comparison between carbon and nitrogen stable isotope analysis of bulk dental calculus , bone and dentine collagen from same individuals from the Medieval site of El Raval (Alica. *Journal of Archaeological Science*, *47*, 70–77. https://doi.org/10.1016/j.jas.2014.03.026

Samaranayake, L. (2006). *Essential Microbiology for Dentistry*. Churchill Livingstone.

Santos, H. (2009). PONTE ENTRE O FLECHEIRO E O MERCADO , E REMODELAÇÃO DO AÇUDE DO MERCADO – TOMAR OBRA 1.

Scheie, A. A. (1989). The role of plaque in dental calculus formation: a review. *Recent Advances in the Study of Dental Calculus*, 47–55.

Schoeninger, M. J., & Deniro, M. J. (1984). Nitrogen and carbon isotopic composition of bone collagen from marine and terrestrial animals, *48*.

Schoeninger, M. J., & Moore, K. (1992). Bone stable isotope studies in archaeology. *Journal of World Prehistory*, *6*(2), 247–296. https://doi.org/10.1007/BF00975551

Schroeder, H. E., & Shanley, D. (1969). Formation and Inhibition of Dental Calculus. *Journal of*

Periodontology, *40*(11), 643–646. https://doi.org/10.1902/jop.1969.40.11.643

Scott, G. R., & Poulson, S. R. (2012). Stable carbon and nitrogen isotopes of human dental calculus: A potentially new non-destructive proxy for paleodietary analysis. *Journal of Archaeological Science*, *39*(5), 1388–1393. https://doi.org/10.1016/j.jas.2011.09.029

Sealy, J., Armstrong, R., & Schrire, C. (1995). Beyond lifetime averages: Tracing life histories through isotopic analysis of different calcified tissues from archaeological human skeletons. *Antiquity*, *69*(263), 290–300. https://doi.org/10.1017/S0003598X00064693

Stanford, J. W. (1957). Analysis of the Organic Portion of Dental Calculus, 128–135.

Still, C. J., Berry, J. A., Collatz, G. J., & DeFries, R. S. (2003). Global distribution of C_3 and C_4 vegetation: Carbon cycle implications. *Global Biogeochemical Cycles*, *17*(1), 6-1-6–14. https://doi.org/10.1029/2001GB001807

T.M.Roberson. (2006). *Sturdevant'S Art & Science Of Operative Dentistry* (6th ed.). Elsevier (A Divisionof Reed Elsevier India Pvt. Limited).

Tannahill.R. (1988). The Silent Centuries. In *Food in History* (pp. 92–102). New York: Three River Press.

Tromp, M. (2012). Large-Scale Analysis of Microfossils Extracted From Human Rapanui Dental Calculus: a Dual-Method Approach Using Semeds and Light Microscopy To Address Ancient Dietary Hypotheses. *Department of Anthropology Idaho State University*, 121.

Tromp, M., Buckley, H., Geber, J., & Matisoo-Smith, E. (2017). EDTA decalcification of dental calculus as an alternate means of microparticle extraction from archaeological samples. *Journal of Archaeological Science: Reports*, *14*(June), 461–466. https://doi.org/10.1016/j.jasrep.2017.06.035

Tromp, M., & Dudgeon, J. V. (2015). Differentiating dietary and non-dietary microfossils extracted from human dental calculus: The importance of sweet potato to ancient diet on Rapa Nui. *Journal of Archaeological Science*, *54*, 54–63. https://doi.org/10.1016/j.jas.2014.11.024

van der Merwe, N. J. (1991). Light Stable Isotopes and the Reconstruction of Prehistoric Diets. *Proceedings of the British Academy*, *77*(February 1991), 247–264. Retrieved from http://cat.inist.fr/?aModele=afficheN&cpsidt=6120282

Wang, T. T., Fuller, B. T., Wei, D., Chang, X. E., & Hu, Y. W. (2015). Investigating Dietary Patterns with Stable Isotope Ratios of Collagen and Starch Grain Analysis of Dental Calculus at the Iron Age Cemetery Site

of Heigouliang, Xinjiang, China. *International Journal of Osteoarchaeology*, *26*(4), 693–704. https://doi.org/10.1002/oa.2467

Warinner, C., Hendy, J., Speller, C., Cappellini, E., Fischer, R., Trachsel, C., … Collins, M. J. (2014). Direct evidence of milk consumption from ancient human dental calculus. *Scientific Reports*, *4*, 1–6. https://doi.org/10.1038/srep07104

Warinner, C., Rodrigues, J. F. M., Vyas, R., Trachsel, C., Shved, N., Grossmann, J., … Cappellini, E. (2014). Pathogens and host immunity in the ancient human oral cavity. *Nature Genetics*, *46*(4), 336–344. https://doi.org/10.1038/ng.2906

Warinner, C., Speller, C., & Collins, M. J. (2014). A new era in palaeomicrobiology: prospects for ancient dental calculus as a long-term record of the human oral microbiome. *Philosophical Transactions of the Royal Society B: Biological Sciences*, *370*(1660), 20130376–20130376. https://doi.org/10.1098/rstb.2013.0376

Watson, R. R. (2017). *Nutrition and funtional foods for healthy aging*.

Webb, E., Amarasiriwardena, D., Tauch, S., Green, E. F., Jones, J., & Goodman, A. H. (2005). Inductively coupled plasma-mass (ICP-MS) and atomic emission spectrometry (ICP-AES): Versatile analytical techniques to identify the archived elemental information in human teeth. *Microchemical Journal*, *81*(2), 201–208. https://doi.org/10.1016/j.microc.2005.04.002

Weber, S., & Price, M. D. (2016). What the pig ate: A microbotanical study of pig dental calculus from 10th-3rd millennium BC northern Mesopotamia. *Journal of Archaeological Science: Reports*, *6*, 819–827. https://doi.org/10.1016/j.jasrep.2015.11.016

Wei, C., Haiping, Y., Yingquan, C., & Chen, X. (2017). Transformation of Nitrogen and Evolution of N-Containing Species during Algae Pyrolysis. *American Chemical Society*, *51*(December), 6570–6579. https://doi.org/10.1021/acs.est.7b00434

Weiner, S., & Bar-Yosef, O. (1990). States of preservation of bones from prehistoric sites in the Near East: a survey. *Journal of Archaeological Science*, *17*(2), 187–196.

Wesolowski, V., Ferraz Mendonça de Souza, S. M., Reinhard, K. J., & Ceccantini, G. (2010). Evaluating microfossil content of dental calculus from Brazilian sambaquis. *Journal of Archaeological Science*, *37*(6), 1326–1338. https://doi.org/10.1016/j.jas.2009.12.037

Yaprak, E., Yolcubal, Sinanoğlu, A., Doğrul-Demiray, A., Guzeldemir-Akcakanat, E., & Marakoğlu. (2017). High levels of heavy metal accumulation in dental calculus of smokers: a pilot inductively coupled plasma mass spectrometry study. *Journal of Periodontal Research*, *52*(1), 83–88. https://doi.org/10.1111/jre.12371

Zhang, N., Dong, G., Yang, X., Zuo, X., Kang, L., Ren, L., … Chen, F. (2017). Diet reconstructed from an analysis of plant microfossils in human dental calculus from the Bronze Age site of Shilinggang, southwestern China. *Journal of Archaeological Science*, *83*, 41–48. https://doi.org/10.1016/j.jas.2017.06.010

Appendix I

1. Human dental calculi

Sample code	Sample number	
T1	14.388	
Sex	**Age**	
Male	Mature	

Sample code	Sample number	
T2	14.420	
Sex	**Age**	
Unknown	Unknown	

Sample code	Sample number	
T3	14.72	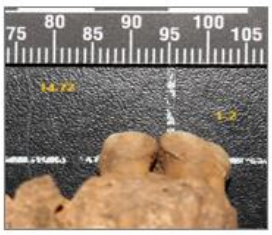
Sex	**Age**	
Female	Old	

Sample code	Sample number	
T4	14.271	
Sex	**Age**	
Unknown	Unknown	

Sample code	Sample number
T5	16.113

Sex	Age
Unknown	Unknown

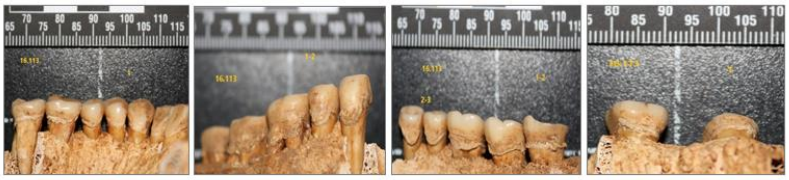

Sample code	Sample number
T6	16.255

Sex	Age
Male	Mature

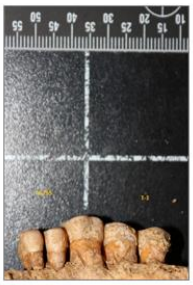

Sample code	Sample number
T7	18.100

Sex	Age
Male	Mature

Sample code	Sample number
T8	18.212

Sex	Age
Unknown	Unknown

Sample code	Sample number	
T9	18.3	
Sex	Age	
Female	Unknown	

Sample code	Sample number	
T10	19.19	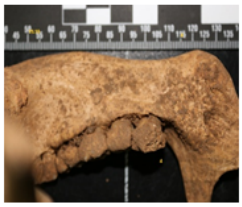
Sex	Age	
Male	Mature	

Sample code	Sample number	
T11	19.23	
Sex	Age	
Male	Unknown	

Sample code	Sample number	
T12	20.144	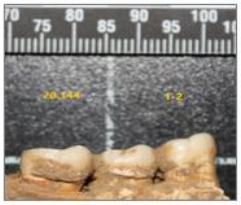
Sex	Age	
Female	Young	

2. Fauna dental calculi

Sample code	Sample number	
A1	14.1004F	

Species: Bos

Sample code	Sample number	
A2	14.1348F	

Species: Equus

Sample code	Sample number	
A3	14.1498F	

Species: Bos

Sample code	Sample number	
A4	14.252F	

Species: Bos

Sample code

A5

Sample number

14.324F

Species

Ovis/Capra

Sample code

A6

Sample number

20.1194F

Species

Bos

C:\HERCULES\Roshan\Fauna SMOL.1 03-05-2018 11:43:21

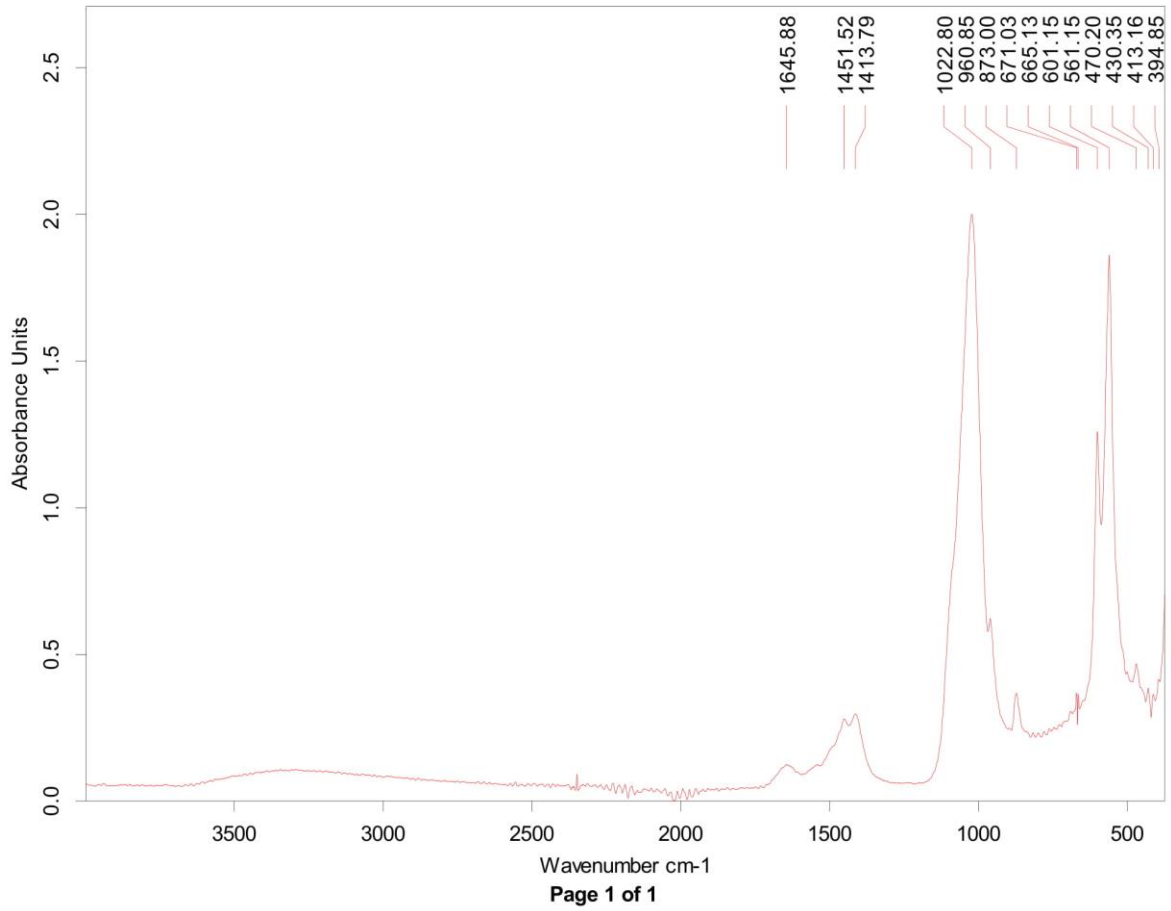

Page 1 of 1

Appendix II

Sample ENT2

	POSSIBLE SOURCE OF ORIGIN
PROTEINS	Pyridine, Pyrrole, 3-methyl-1H-Pyrrole, 1-methyl-1H-Pyrrole, 2-Aminopyridine, 2-Acetylpyrrole, Indole, Indene
FATTY ACIDS	Acrylonitrile, 1-Nonanol, 1-Decene, Decane, 1-Undecene, Octane, Dodecane, Nonane, 1-Nonene, 1-Octene, ? 1-Heptene, 1-Dodecene, Undecane, Nonanenitrile, Benzenepropanenitrile,
CHAR	1,4-Dihydronaphthalene, Naphthalene, 2-methyl-Naphthalene, 1-Naphthalenamine, 2-Naphthalenamine, Fluorene, Phenanthrene, Phenol, 3-methyl-Phenol, 3,4-dimethyl-Phenol, 2-propyl-Phenol,
CARBOHYDRATES	Benzene, cyclopropyl-
UNKNOWN	Toluene, Ethyl benzene, propyl-Benzene, Benzyl nitrile, Benzonitrile, 2,5-Dimethylbenzonitrile, Biphenyl

Sample T10

	POSSIBLE SOURCE OF ORIGIN
PROTEINS	Pyridine, Pyrrole, 3-methyl-1H-Pyrrole, 2-Aminopyridine, ? 2-Acetylpyrrole, 1-methyl-1H-Indene, Indole, 1,3-dimethyl-1H-Indole,
FATTY ACIDS	1-Heptene, Heptane, Octane, 1-Octene, 1-Decenecyclopropyl-Benzene, 1-Undecene, 1-Nonene, Nonane, 1-Nonanol, 1-Hexene, 1-Dodecene, Hexadecanal, Nonanenitrile
CHAR	1,3-dimethyl-Benzene, Styrene, (1-methylethyl)-Benzene, 3-methyl-Phenol, 2-methyl-Phenol, 1,4-Dihydronaphthalene, Naphthalene, 2-methyl-Naphthalene, 1-Naphthalenamine, 2-Naphthalenamine, Fluorene, Phenanthrene
CARBOHYDRATES	2,3-Butanedione, Cyclopentanone, 1-Hydroxy-2-butanone, 2-methyl-2-Cyclopenten-1-one, 3-methyl-2-Cyclopenten-1-one, 2-Cyclohexen-1-one, Furfural, 2,3-dimethyl-2-Cyclopenten-1-one,
UNKNOWN	Benzene, Toluene, Ethyl benzene, o-Xylene, isocyanato-Methane, 3 methyl-Benzenamine, propyl-Benzene, Benzaldehyde, Benzonitrile,

	Sample T9 unclean	Sample T9 clean01	Sample T9 clean02
PROTEINS	Pyridine, Pyrrole, 3-methyl- 1H-Pyrrole, 2-Aminopyridine, Indene, 2-Acetylpyrrole, 1-methyl-1H-Indene,	3-formylpyrrole, 2,5-dimethyl-Pyrazine, 2,2-dimethyl-Aziridine, 2-Pyrrolidinone, 2-Aminopyridine, N-Cyclohexyl-N'-(pyrazin-2-yl)urea, 6,7-dihydro-5H-1-Pyrindine, 1H-Pyrrole-2-carbonitrile, Indole,	Pyridine, 3-methyl-1H-Pyrrole, Indole
FATTY ACIDS	1-Pentanol, Octane, 1-Nonene, Nonane, 1-Decene, Decane, 1-Undecene, 1-Nonanol, Dodecane, Benzenepropanenitrile, ? 1-Dodecene, (E)-2-Octenal, Tridecane, 1-Tridecene, 1-Tetradecene, 1-Pentadecene, Pentadecane, 1-Hexadecene, Hexadecanal, Cyclododecane, Nonanenitrile	3,8-dioxatricyclo[6.3.0.0[1,5]] undecan-2,9-diol, Heptane, 3,3,5-trimethyl-(CAS), 5-methyl-Undecane, Nonanenitrile, Pentadecanal	Acetonitrile, HCN, 1-PHENYL-2-PROPANOL, 4-[N-(Cyanmethyl)imino]butan enitrile, [illegible] [illegible] *SOURCE OF ORIGIN* (Cyanmethyl)imino]butan enitrile, 3-Nitro-2-pentanol
CHAR	Styrene, 2-methyl-Phenol, 3-methyl-Phenol, 1,4-Dihydronaphthalene, Naphthalene, 2-methyl-Naphthalene, 2-Naphthalenamine, Fluorene, Phenanthrene	2-Naphthalenamine,	N-(tert-Butyloxycarbonyl)-N-(2-propynyl)-4-(benzyloxy)-1-bromo-2-naphthylamine, Styrene,
CARBOHYDRATES	2-methyl-2-Cyclopenten-1-one, cyclopropyl-Benzene,	6-(Dimethylamino)-3-methyl-3,5-hexadien-2-one, (R)-2-(2'-oxo-1"-propyl)-2,5-dihydrofuran, 2-isobutyl-4-methyl-5,6-dihydro-4H-pyran,	2-amino-2-decoxy-4-C-methyl-á-L-erythro-2-Pentulofuranosonamide,
UNKNOWN	Toluene, Ethyl benzene, 1,3-dimethyl-Benzene, o-Xylene, Butyrolactone, 1-propenyl-Benzene, Benzonitrile, Phenol, 3 methyl-Benzenamine, Bibenzyl,	Phenol, 3-methyl-Phenol, 2-methyl-Phenol,	Toluene

	Sample T5.1b	**Sample T5.TMAH**	**Sample T5.1l**	**Sample T5.1m**	**Sample T5.1d**	**Sample T5.2**
PROTEINS	Pyridine, Pyrrole, 3-methyl-1H-Pyrrole, o-Xylene, Styrene, Phenol, 2-Aminopyridine, 1H-Pyrrole-2-carbonitrile, Indene, o-Toluidine, 3 methyl-Benzenamine, 3-methyl-Phenol, 1-methyl-1H-Indene, 2,5-dimethyl-Phenol, 1-methylene-1H-Indene, Indole, 1,3-dimethyl-1H-Indole, Phthalimide.	1,2-diethyldiborane-D4, Guanidine, 2-methyl-Pyridine, 1-methyl-1H-Pyrrole, 3-methyl-1H-Pyrrole, 2,4-dimethyl-1H-Pyrrole, 3,4-Dimethyl-1H-pyrrole, N-(2-(2-Furyl)ethyl)-2,6-piperidinedione, o-Toluidine, 2,3-dimethyl-Pyridine, 1-ethyl-1H-Pyrrole, Pyrrole, 2-ethyl-4-methyl-1H-Pyrrole, 2-ethyl-6-methyl-Pyridine, 2,3,5-trimethyl-1H-Pyrrole, Indene, 2-methyl-Phenol, 4-methyl-Phenol, 3-methyl-Phenol, 2,3,4,5-tetramethyl-1H-Pyrrole, Indole, 2,5-dimethyl-Phenol, Azulene.	Pyridine, Pyrrole, Toluene, 3-methyl-1H-Pyrrole, 1H-Pyrrole-2-carbonitrile, 2-Aminopyridine, Indene, 2-methyl-Phenol, Acetophenone, o-Toluidine, 3 methyl-Benzenamine,, 1-methyl-1H-Indene, 1-methylene-1H-Indene, Indole, 1,3-dimethyl-1H-Indole.	1-methyl-1H-Pyrrole, Pyridine, Pyrrole, 3-methyl-1H-Pyrrole, Phenol, 2-Aminopyridine, o-Toluidine, Indene, 2-methyl-Phenol, Acetophenone, 3 methyl-Benzenamine, 3-methyl-Phenol, 1-methyl-1H-Indene, 1-methylene-1H-Indene, Indole.	Pyridine, Pyrrole, 3-methyl-1H-Pyrrole, 2-Aminopyridine, Indene, 1-methyl- 1H-Indene, Indole, 1,3-dimethyl- 1H-Indole,	Pyridine, Pyrrole, 3-methyl-1H-Pyrrole, Phenol, 2-Aminopyridine, Indene, 2-methyl-Phenol, Acetophenone, o-Toluidine, 3-methyl-Phenol, 1-methyl-1H-Indene, 1-methylene-1H-Indene, Indole.

	Sample T5.1b	Sample T5.TMAH	Sample T5.1l	Sample T5.1m	Sample T5.1d	Sample T5.2
FATTY ACIDS	1-Decene, Decane, cyclopropyl-Benzene, butyl-Benzene, 1-Nonanol, Dodecane, Benzenepropanenitrile, (E)-2-Hexenal, (E)-2-Octenal, 2-methyl-1H-Isoindole-1,3(2H)-dione, Nonanenitrile.	N,N-dimethyl-Methylamine, Spiro[3.3]hepta-1,5-diene, 2,5-Norbornadiene, 1,3,5,7-Cyclooctatetraene, 3-Pyridinecarbonitrile, 3 methyl-Benzenamine, 3,5-dimethyl-1-Hexene, 1-Decene, 1-Undecene, 4-methyl-Benzenamine hydrochloride, (R*,S*)-1,2-Cyclohexanedimethanol, Tetracyclo[4.3.0(2,4).0(3,5)]nona-7-ene, 2,3-dimethyl-2-Cyclopenten-1-one, 3-phenyl-1-Propyne, 1-Hexene, Undecane, Heptane, 1-Nonene, exo-3,6,7-Trimethyl-7-propylbicyclo[4.2.0]oct-2-en-8-one, 1-(1,1-dimethylethoxy)-3-methyl-Benzene, 1,1-difluoro-Dodecane, Dodecane, 9-methyl-1-Decene, 1-methyl-1H-Indene, 4,4-Dideuterio-6,6-dimethylcyclohexanone, 1,1-difluoro-dodecane.	Nonane, 1-Pentanol, Decane, cyclopropyl-Benzene, 1-isocyano-3-methyl-Benzene, 1-Undecene, Undecane, (1-methylenepropyl)-Benzene, pentyl-Benzene, 1-Nonanol, Dodecane, Benzenepropanenitrile, (E)-2-Octenal.	Octane, acrylonitrile, 1-Nonene, 1-Decene, Decane, cyclopropyl-Benzene, 1-propenyl-Benzene, 2,3-dimethyl-2-Cyclopenten-1-one, 1-Undecene, Undecane, 1-Nonanol, Dodecane, Benzenepropanenitrile, (E)-2-Octenal, Nonanenitrile.	1-Heptene, 1-Pentanol, Octane, 5,6-dimethyl-1,3-Cyclohexadiene, 1-Nonene, Nonane, 1-Decene, Decane, 1-Dodecene, 1-Nonanol, Dodecane, 2-Nonenal, 1-Tridecene, 2-Octenal, Tetradecane, 1-Tetradecene, 1-Pentadecene, 1-Hexadecene, Nonanenitrile, Hexadecanal	3-methyl-2-Cyclopenten-1-one, 1-Decene, cyclopropyl-Benzene, 2,3-dimethyl-2-Cyclopenten-1-one, 1-isocyano-3-methyl-Benzene, 1-Pentanol, 1-Nonanol, Benzenepropanenitrile, (E)-2-Octenal.

	Sample T5.1b	Sample T5.TMAH	Sample T5.1l	Sample T5.1m	Sample T5.1d	Sample T5.2
CHAR	1,4-Dihydronaphthalene, 2-methyl-Naphthalene, Fluorene, Phenanthrene. Styrene,	Styrene, Phenol, 1,4-Dihydronaphthalene, 1,2-dihydro-Naphthalene.	Styrene, 1,4-Dihydronaphthalene, Naphthalene, 2-methyl-Naphthalene, Fluorene, Phenanthrene, Fluoranthene, Pyrene.	Styrene, 1,4-Dihydronaphthalene, Naphthalene, 2-methyl-Naphthalene, Fluorene, Phenanthrene.	1,3-dimethyl-Benzene, Styrene, 2-methyl-Phenol, 3-methyl-Phenol, 1,4-Dihydronaphthalene, 3,4-dimethyl-Phenol, 2,5-dimethyl-Phenol, Naphthalene, 2-methyl-Naphthalene, Fluorene, Phenanthrene	Styrene, 1,4-Dihydronaphthalene, 2-methyl—Naphthalene, Fluorene, Phenanthrene.

	Sample T5.1b	Sample T5.TMAH	Sample T5.1l	Sample T5.1m	Sample T5.1d	Sample T5.2
CARBOHYDRATES	Furfural	2,3-dihydro-Benzofuran,		2-methyl-Cyclopentanone, 2-methyl-2-Cyclopenten-1-one, 3-methyl-2-Cyclopenten-1-one,	2-methyl-2-Cyclopenten-1-one, 2-Cyclohexen-1-one, 2,3-dimethyl-2-Cyclopenten-1-one,	

	Sample T5.1b	**Sample T5.TMAH**	**Sample T5.1l**	**Sample T5.1m**	**Sample T5.1d**	**Sample T5.2**
UNKNOWN	Toluene, Ethyl benzene, 1,3-dimethyl-Benzene, Benzonitrile, 2-methyl-Phenol, 1-isocyano-3-methyl-Benzene, Benzyl nitrile, 3,4-dimethyl-Phenol, 2,5-Dimethylbenzonitrile, Biphenyl.	trimethyl-Borane, Toluene, trans-3-chloroallyl benzyl ether, Benzenamine, p-Xylene, o-Xylene, 1-ethynyl-3-methylenecyclobutane, Acetic acid, trifluoro-, 2-cyclohexen-1-yl ester, rel-(5R,6S,10S)-6-[2-((methylsulfonyl)oxy)ethyl]-6,10-dimethylspiro[4.5]deca-3,7-dien-2-one, Benzonitrile, (1-methylethyl)-Benzene, 1-propenyl-Benzene, cyclopropyl-Benzene, 1-isocyano-3-methyl-Benzene, 3-methyl-Benzonitrile, 2-Methylanisole, 2,6-dimethyl-Phenol, (1-methylenepropyl)-Benzene, Benzyl nitrile, 1-Methylbutyl nitrite, 2-Ethyl phenol.	Benzene, Ethyl benzene, 1,3-dimethyl-Benzene, o-Xylene, Benzaldehyde, propyl-Benzene, Benzonitrile, Phenol, 3-methyl-Phenol, Benzyl nitrile, 2,5-Dimethylbenzonitrile, Biphenyl.	Toluene, Ethyl benzene, o-Xylene, Benzonitrile, 1-isocyano-3-methyl-Benzene, Benzyl nitrile, Biphenyl.	Toluene, o-Xylene, Phenol,	Benzene, Toluene, Ethyl benzene, Benzonitrile, Benzyl nitrile, Biphenyl.

Ion Extract Chromatograms (m/z = 55, 57)

E2

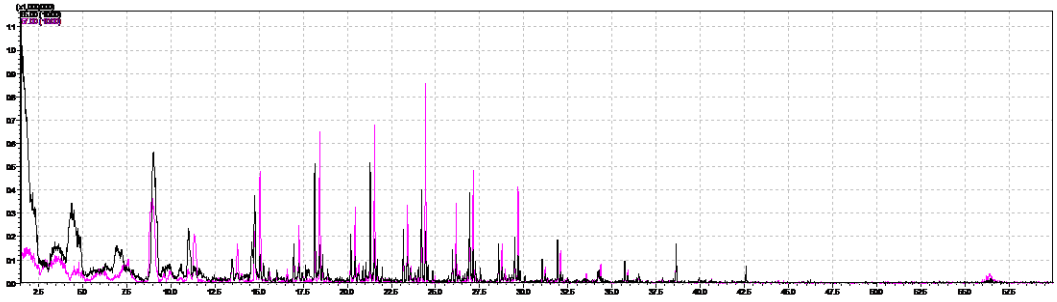

T5.TMAH

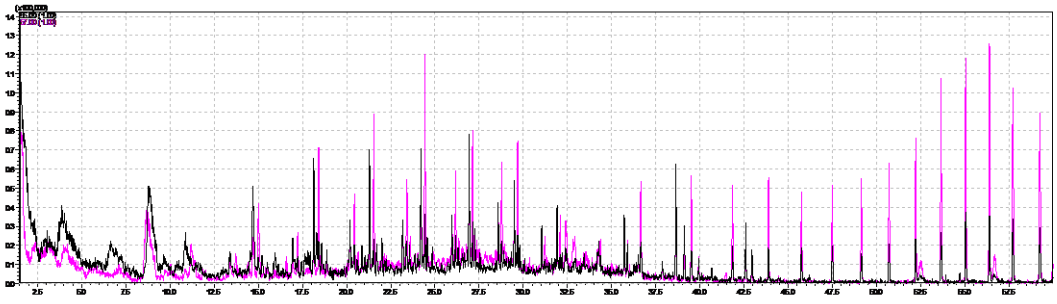

T5.1b

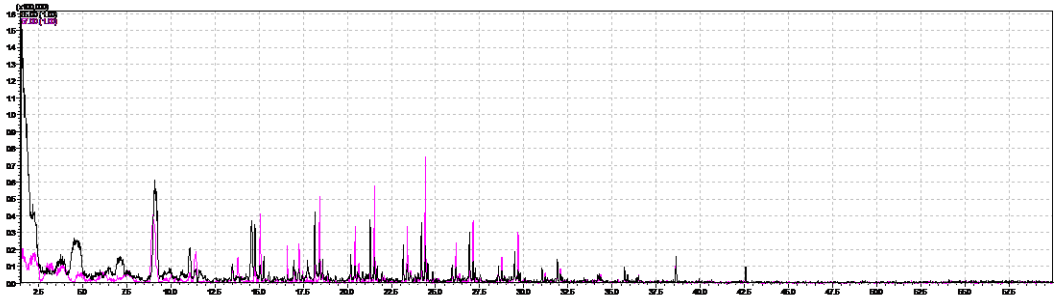

T5.1d

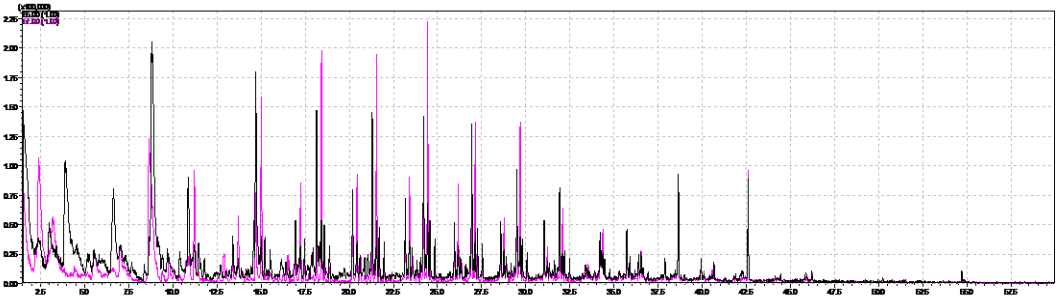

T5.1l

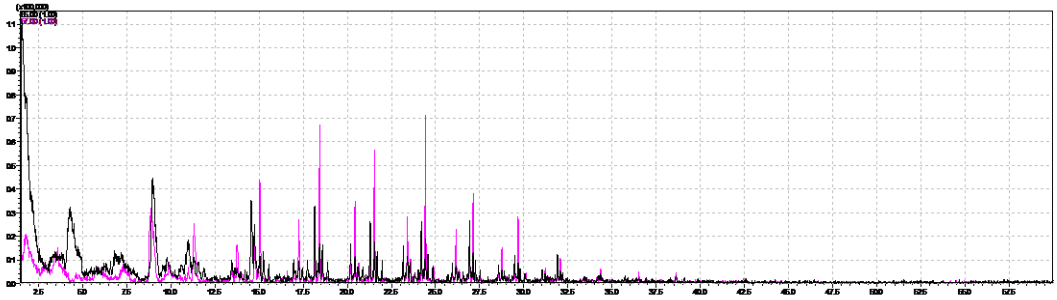

T5.1m

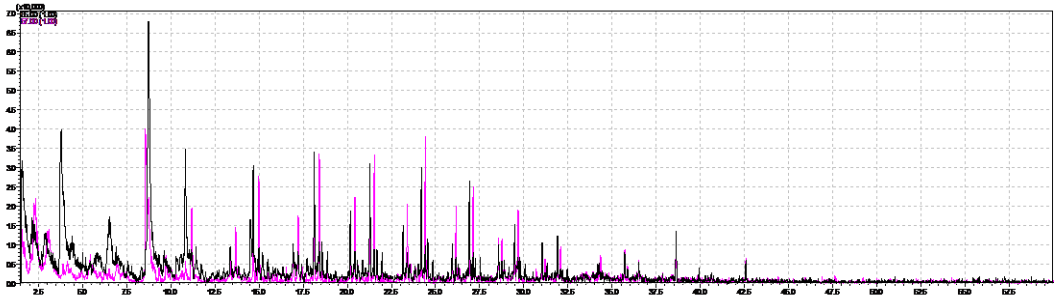

T9.1

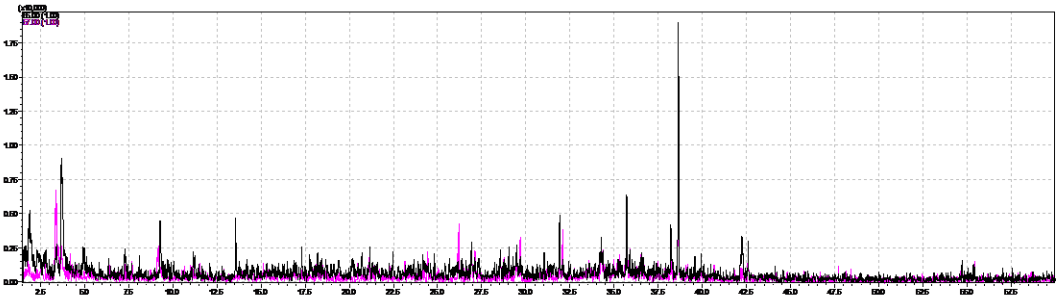

T9.2

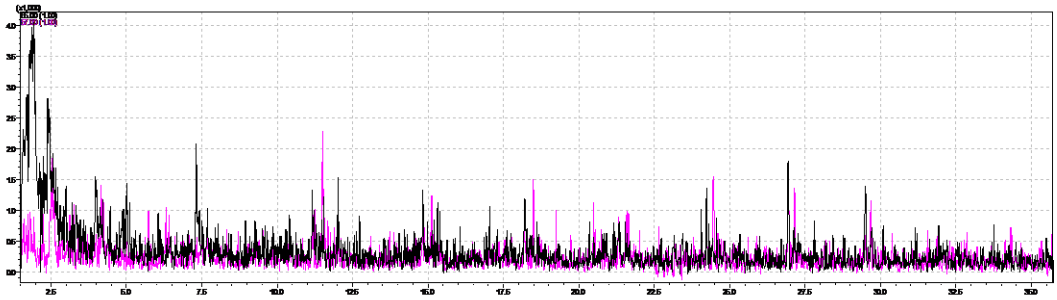

T9.1.Unclean

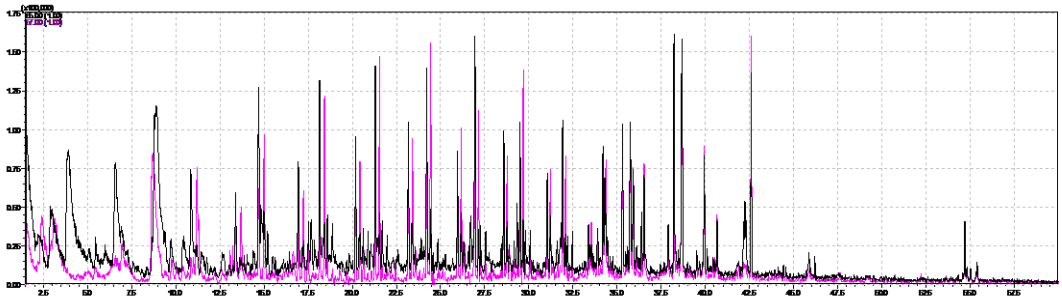

T10.1

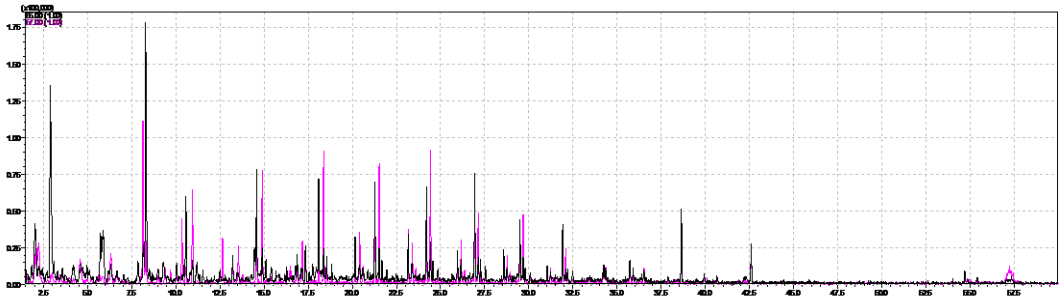

Standard Alkane Mix